Mechanism of the translocon

Taufik, Intan

DOI:
10.33612/diss.102814953

Mechanism of The Translocon: Events at The Gate

Intan Taufik

Mechanism of The Translocon: Events at The Gate

Intan Taufik
PhD thesis
University of Groningen

ISBN: 978-94-034-2226-8 (printed version)
ISBN: 978-94-034-2225-1 (electronic version)

The research presented in the thesis was performed in the Molecular Microbiology research group, which is part of the Groningen Biomolecular Sciences and Biotechnology institute (GBB) of the Universtity of Groningen, the Netherlands.

university of groningen

Cover design and layout by: Firman Mustari
Printed by: Ipskamp Printing

university of groningen

Mechanism of The Translocon: Events at The Gate

PhD thesis

to obtain the degree of PhD at the
University of Groningen
on the authority of the
Rector Magnificus Prof. Cisca Wijmenga
and in accordance with
the decision by the College of Deans.

This thesis will be defended in public on

Friday 6 December 2019 at 12.45 hours

by

Intan Taufik

born on 28 February 1975
in Bandung, Indonesia

Supervisor
Prof. A.J.M. Driessen

Assessment Committee
Prof. J.M. van Dijk
Prof. O.P. Kuipers
Prof. W. Bitter

For my wife ***Enci***,
daughter ***Bianglala*** &
son ***Azzam***

Table of Contents

Chapter 1

The Working Translocon - Structure and Mechanism

Intan Taufik and Arnold J.M. Driessen

CHAPTER ONE

The Working Translocon - Structure and Mechanism

1. Introduction

Most of the genetic information of living organisms is localized in the nucleoid in prokaryotes or nucleus in eukaryotes. DNA provides the blueprint and instructions to direct life and is via the intermediate messenger RNA, translated into proteins that serve as the functional entities of the cell. Cells are embordered by a hydrophobic cytoplasmic membrane that insulates the interior or cytosol from the environment, and protects cells against toxic substances. The cytoplasmic membrane is also the site where enzymes convert energy sources into electrochemical energy and where energy requiring processes such as nutrient uptake and motility occur. It is imperative to cells to also be able to perform enzymatic functions outside of the cell either as constituents of the extracellular cell envelop that provides rigidity and protection, or function as enzymes to convert macronutrients into smaller molecules that can enter the cell via uptake processes. Extracellular proteins are synthesized in the cytosol and thus must be translocated across the cytoplasmic membrane before reaching their final destination. In bacteria, approximately one third of the cellular proteins are membrane proteins[1,2], and extracellular proteins[3,4], and these need to be inserted or translocated into or across the cytoplasmic membrane. These processes are essential for life and involve an evolutionary conserved proteinaceous complex found in all domains of life[5].

The Sec translocase is the major and universally conserved route for protein transport into and across the membrane, found in the endoplasmic reticulum of eukaryotes, the cytoplasmic membrane of bacteria and archaea and then thylakoid membrane of chloroplasts[6]. It consists of a protein-conducting channel embedded in the lipid bilayer, and peripherally associated components. The protein-conducting channel is formed by a heterotrimeric membrane protein known as Sec61[7] in eukaryotes, SecYEG[8] in bacteria and SecYEβ[9] in archaea. The first high resolution crystal structure was of the archaeal pore complex from *Methanocaldococcus jannaschii*[10]. The channel is formed by SecY (or Sec61α) subunit. SecY consists of ten transmembrane segments (TMSs) which are arranged as two sets of 5 TMSs that are connected by a hinge region. These two sets of TMSs are organized as a clam-shell encompassing a central hydrophilic

interior[11] that subcentral is closed by a hydrophobic constriction (pore ring) and a periplasmic re-entrance loop (plug). Opening of the pore requires that the constriction ring widens and the plug vacates its position to form a vectorial channel that allows unfolded polypeptides to cross the lipid bilayer. Because of the clam-shell opening mechanism, pore opening also results in the formation of lateral opening into the membrane where hydrophobic transmembrane segments may be released into the lipid bilayer. Various components can associate with the translocon but this differs among the domains of life[5,6,12,13]. These components can be classified as cytosolic chaperones or regulators that are involved in the targeting of substrates to the pore, energy transducing ATPases which powers translocation, and integral membrane complexes which stimulate translocation. Furthermore, translating ribosomes can associate with the translocon allowing co-translational translocation or insertion of nascent membrane proteins into the lipid bilayer concomitantly with chain elongation at the ribosome.

The pathway that involves the Sec translocase was the first secretion route discovered in bacteria. The initial discoveries, from the genetics to the biochemical characterization of the components, culminating into a reconstituted protein translocation reaction using purified components was extensively reviewed [14,15]. In short, initial genetic screening for conditional lethal mutants for protein secretion in the era of 1980-1988 resulted in the identification of the majority of the *sec* genes. This was followed by a biochemical analysis that involved protein overexpression, purification and functional characterization, and the reconstitution to faithfully mimic protein translocation *in vitro*[16] in 1990. These advances lead to the elucidation of many of the enzymatic and mechanistic features of protein translocation in the pre-structure era. The first high-resolution of Sec translocase subunits was in 2003[10]. Structural information allowed a better definition of the translocation mechanism and in recent years this was followed by advanced biophysical approaches including single molecule and molecular dynamic studies to detail the mechanism further. A simplified time line of the various milestones in elucidating the many salient features of the canonical bacterial protein translocation is provided in Figure 1. Here, I will discuss the primary components of the Sec translocase in bacteria, including the structure and its working mechanism. Other more specific translocases of the bacterial membrane are discussed elsewhere[13].

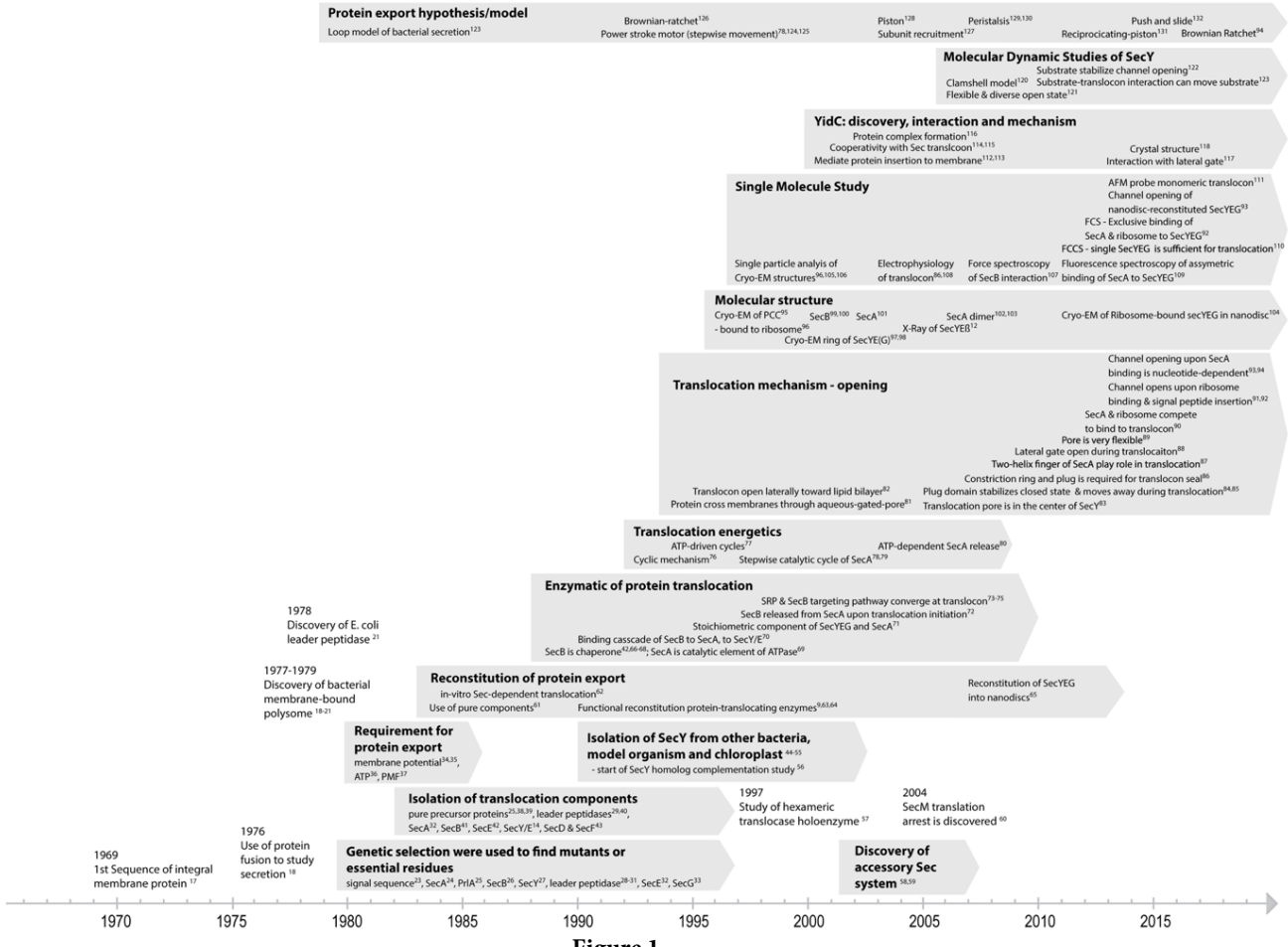

Figure 1
Timeline of important findings/progression in bacterial protein export

2. Translocation of secretory proteins in bacteria

Signal sequence

Proteins that functions outside the cytosol of bacteria are synthesized by ribosomes with an N-terminal extension termed the signal sequence. Signal sequences share a tripartite organization but differ in amino acid sequence. These signals consist of a positively charged N-terminus (N-region), a hydrophobic α-helix forming core domain of 10-15 residues (H-region) with carboxyl-terminal polar domain (C-region) that contains the signal sequence cleavage site (for review see[133]). The signal sequence affects folding of the mature protein domain, promotes interaction between the unfolded protein with cytosolic chaperones and motor protein SecA[134–136], and guides secretory proteins to the translocon. The signal sequence is important for channel opening as will be outlined below. During translocation, the signal sequence is removed by a universally conserved membrane bound peptidase[137,138], and the mature region of the secretory protein is released at the outer face of the cytoplasmic membrane for folding or further targeting to the outer membrane[139–141]. The structure and mechanism of signal peptidases is discussed elsewhere[137,138,142,143].

Targeting routes

Bacterial secretory proteins can follow two major targeting routes to reach the Sec translocase. Typically, the signal sequence and mature protein region is bound by the peptidyl-prolyl isomerase trigger factor whereupon the protein is transferred to the molecular chaperone SecB[75] for posttranslational targeting to the Sec-translocase (Fig. 2, step A). On the other hand, with nascent membrane proteins that carry hydrophobic TMSs and a subset of secretory proteins with high hydrophobicity of its signal sequence are recognized by signal recognition particle (SRP) (Fig. 2, step B)[74] and co-translationally targeted as a ribosome:nascent chain (RNC):SRP complex to the Sec-translocase. SRP and trigger factor compete for nascent chain binding, but because of the preference of SRP for hydrophobic signal sequences, early binding of trigger factor is prevented, and the protein is directed into the co-translational targeting pathway.

While the secretory protein emerges from the ribosome tunnel and enter the reducing environment of cytosol, it is kept in unfolded conformation[144,145] which is stabilized by SecB that bind to the mature domain[146] (for review see reference[147]). Other chaperones such as DnaK, trigger factor, and GroEL[67], may also assist in this process while CsaA[148] is a chaperone only present in Gram-positive bacteria. Upon completion of translation, SecB transfers the completely synthesized secretory protein to SecA. Next, SecA binds with high affinity to translocon and releases SecB upon the binding of ATP[72], whereupon the secretory protein enters the translocation pore formed by SecYEG[70]. The secretory protein is then translocated through the pore by means of process that requires multiple

cycles of ATP binding and hydrolysis by SecA and protein motive force (PMF)[124,149,150].

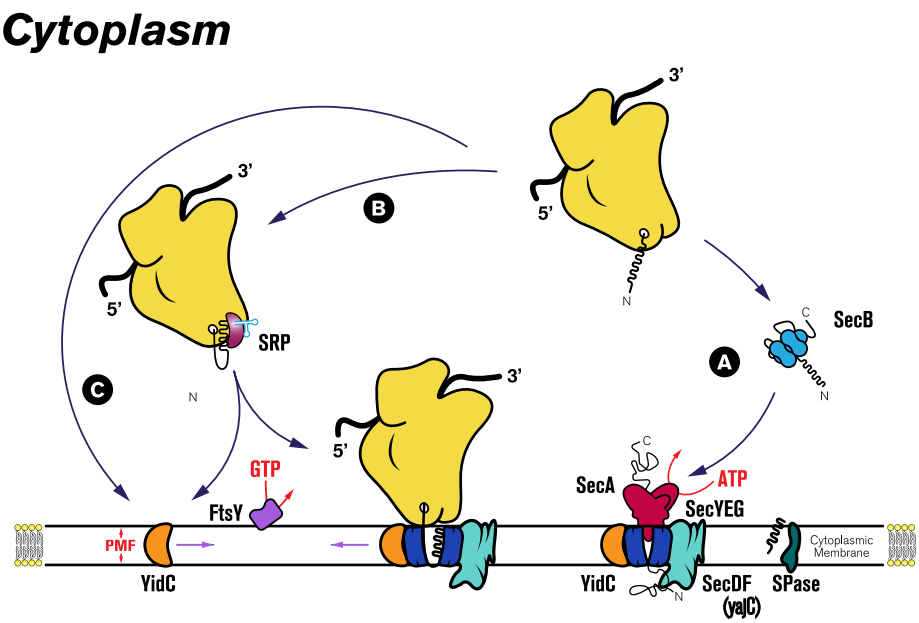

Figure 2. Different routes for protein targeting to the bacterial Sec translocase at the cytoplasmic membrane. The translocase complex consists of the peripheral membrane bound motor protein SecA, the protein-conducting channel SecYEG or translocon, and the associated membrane proteins SecDF(yajC) and YidC. **(A)** Secretory proteins are posttranslationally recognized by the molecular chaperone SecB and stabilized in an unfolded state. Next, the protein is targeted to translocon-bound SecA, and subsequently translocated at the expense of ATP hydrolysis in a process that is stimulated by the proton motive force (PMF) by SecA. Signal peptidase (SPase) cleaves the signal sequence from the secretory protein at the periplasmic face of the membrane. **(B)** Membrane proteins and some secretory proteins are targeted cotranslationally by signal recognition particle (SRP) to the translocon. SRP binds its receptor FtsY, which results in GTP hydrolysis and a release of the nascent membrane protein from SRP and subsequent transfer to the translocon. **(C)** Some membrane proteins are inserted to the cytoplasmic membrane with the assistance of YidC, but YidC can also assist in the translocon-mediated insertion of membrane proteins.

In the co-translational targeting pathway, SRP specifically interact with the signal sequence or hydrophobic TMS of a nascent proteins while it exits the ribosome[151,152] (for detailed review see[153,154]). The ternary ribosome:nascent chain (RNC):SRP complex then interact with FtsY[155] that is bound to the cytoplasmic membrane to form an SRP:FtsY heterodimer. This process activates SRP for GTP hydrolysis whereupon it releases the nascent chain to SecYEG[73,156]. Next, the growing nascent membrane protein inserts into the membrane in a process that is driven by translation and hydrophobic partitioning into the phospholipid bilayer.

Newly synthesized TMSs escape the SecYEG pore laterally into the lipid bilayer. Co-translationally targeted secretory proteins, however, still require SecA for translocation[157], and thus their translocation is post-translational. A detailed discussion on how the translocon recognizes TMSs, and how membrane proteins are inserted into the membrane and fold is described elsewhere[158,159]. Membrane proteins not only insert into the lipid bilayer through the translocon, but insertion of a subset of smaller membrane proteins occurs through the insertase YidC[112]. YidC also cooperates with SecYEG[113,115] in membrane insertion (for reviews see[160,161]).

Although the main Sec translocase components are omnipresent in bacteria, some Gram-positive bacteria contain additional copies of SecA and/or SecY. These non-canonical translocase components are involved in the translocation of a subset of specific proteins, including virulence factors[162].

3. Structure of the Sec-translocase

SecB and SRP – Cytosolic chaperones and targeting factors

During post-translational targeting, secretory proteins are kept in unfolded state by the molecular chaperone SecB. SecB is a homotetrameric protein, organized as dimer of dimers, as evidenced from its crystal structure[99,100,163] (Fig. 3A). The tetrameric structure contains two grooves on each side that, on each side, fuse into a long groove to form a ~70Å long peptide-binding channel. Likely, the polypeptide substrate is wrapped around the SecB tetramer explaining why the bound substrates lack stable tertiary structure. The solvent exposed negatively charged surface on each side are involved in SecA binding[164]. This region interacts with the positively charged zinc-binding domain at the carboxyl-terminus of SecA. Since SecA is dimeric, the two carboxyl-termini capture SecB on both of its sides. All of these features provide the functionality to SecB to bind polypeptide substrates, to maintain them in a translocation competent unfolded state and to deliver them to the SecYEG channel-bound SecA protein[70].

During the co-translational targeting of nascent membrane proteins, SRP binds to the hydrophobic TMSs once they emerge from ribosome. SRP of E. coli is a riboprotein and composed of 4.5S RNA and a 48-kDA GTPase P48 or Ffh (fifty-four homolog)[165]. The crystal structures of several intermediate states of SRP have been solved[166,167], and detailed information on co-translational-targeting pathway intermediates in complex with the Sec translocon[168] have been obtained by cryo-EM (Fig. 3B). SRP interact with the nascent chain at the tunnel exit of the ribosome. TMS or signal sequence recognition by SRP promotes the dimerization of SRP with the SRP receptor, which is termed FtsY in E. coli. The 'closed' state of SRP-SR- heterodimeric targeting complex allows binding to the translocon, and results in a re-localization of the GTPase complex to the opposite end of the RNA

providing a mechanism for coupling GTP hydrolysis to the handover of cargo to the translocon.

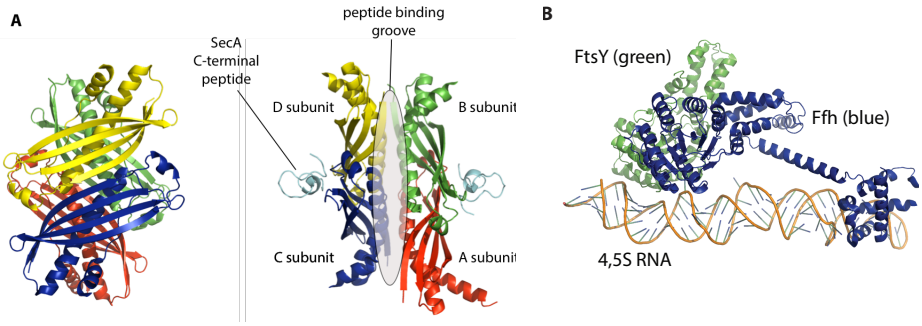

Figure 3. Structures of the cytosolic chaperones SecB and SRP. (A) SecB is shown as a homotetrameric protein (PDB: 1OZB) of subunit A, B, C and D, in two orthogonal views. Front view on the left shows one side of the ß-sheet of two monomers that are packed into a dimer. The side view on the right, shows the peptide binding groove on the dimer-dimer interface. Two SecA C-terminal peptides are shown on the side view to bind to the flat anionic surface. **(B)** Structure of SRP in complex with FtsY (PDB: 2XXA). The *E. coli* SRP consists of a 4.5S RNA and 48-kDA GTPase P48 or Ffh which is shown in blue, whereas FtsY or SR is shown in green. This complex binds to hydrophobic transmembrane segment of nascent membrane proteins once they emerge from the ribosome.

SecA – a multidomain motor protein

SecB transfers the unfolded secretory protein to SecA. Since SecB does not interact with the signal sequence, this region is available for SecA binding. ATP binding to SecA triggers a conformational change to the SecA-SecB complex whereupon SecB releases the unfolded polypeptide for transfer to SecA. Next, SecA delivers the secretory protein to SecYEG and further directs translocation. In bacteria, SecA is an essential component of the Sec-translocase and fulfils multiple roles (Fig. 2). Its predominant role is to energize the post-translational translocation of the secretory protein through the translocon pore, but it is also required for the translocation of large extracytoplasmic hydrophilic loops of integral membrane protein during their co-translational insertion. SecA exist both in a soluble form in the cytosol and peripherally membrane bound[169], where it associates with SecYEG[69,70] and anionic phospholipids[170]. The membrane bound SecA reflects an intermediate in the targeting cycle where binding of SecA to anionic phospholipids triggers a conformational change in SecA whereby it can bind SecYEG with high affinity[171].

The structure of SecA has been resolved in different conformational states and from different bacterial species[101–103,128,172–177]. Based on these mostly dimeric structures and further biochemical work, a series of subdomains have been identified in SecA. The SecA protomer is composed of several subdomains with specific functions in either energy generating motor/regulator and

ligand/substrate binding (Fig. 4). Preprotein binding occurs at the preprotein crosslinking domain (PPXD) or preprotein binding domain (PBD)[178–180].

The C-terminal linker (CTL) and α-helical scaffold domain (HSD)[181], together with the α-helical wing domain (HWD) and IRA1 localize to the C-terminal region of SecA. The CTL interacts with SecB[72,182] and phospholipids[183]. The HWD, together with PPXD and HSD, is proposed to provide peptide-binding groove[173]. It is proposed that the energy from ATP binding and hydrolysis is converted into conformational movement by the DEAD motor – domain with conserved motifs of DNA/RNA helicases[184]. The motor comprises nucleotide binding folds 1 and 2 (NBF-1 and NBF-2). NBF-2 is also known as intramolecular regulator for ATP hydrolysis 2 (IRA2) which controls the hydrolysis of ATP[173,176,185]. Movement of motor domain are induced by ATP binding and ADP release[180,186]. Another structure called intramolecular regulator of ATP hydrolysis (IRA1) is responsible for inhibiting the ATPase activity of cytosolic and unliganded SecA[187].

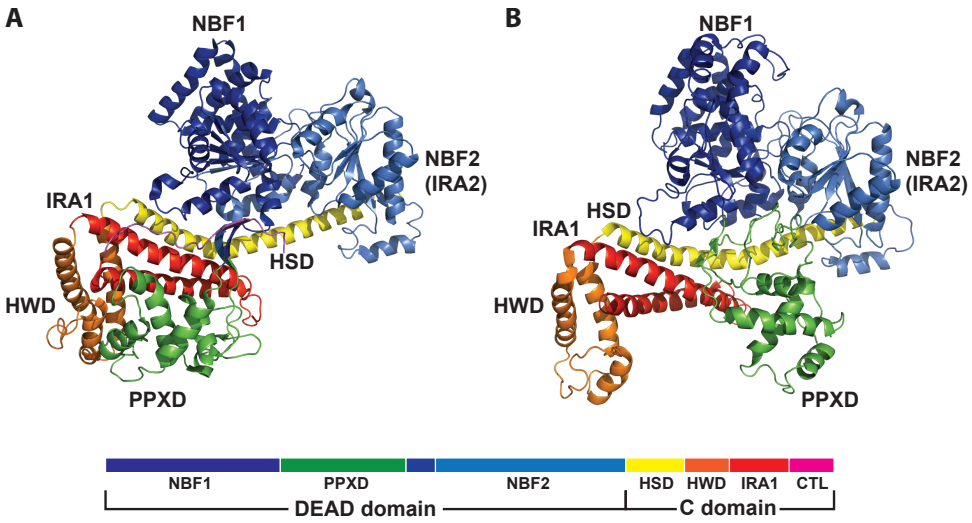

Figure 4. Proposed conformational changes of SecA based on crystal structures. (A) SecA protomer of *B. subtilis* (1M6N), **(B)** SecA protomer of *T. maritima* (3DIN) bound to SecYEG (not shown).

The HSD connects all the domains, and mediates the conversion of mechanical work to protein translocation[101,188]. Both the HWD and HSD have been implicated in the interaction with SecYEG, and this part of SecA becomes highly resistant to protease treatment when bound to SecYEG in the presence of a nonhydrolysable ATP analog[77,189,190]. The *B. subtilis* SecA structure (Fig. 4a) is considered to reflect a closed state, whereas *T. maritima* SecA structure (Fig. 4b) exhibits movement of PPXD toward NDF2 and is considered to be in an open

transition state that can bind the preprotein. In the structure of SecA bound to SecYEG, the rotation of PPXD toward NBF2 may align the preprotein to the lateral gate of SecYEG[175,191]. Another structure of *B. subtilis* SecA bound to *Geobacillus thermodenitrificans* SecYE and signal sequence indicate similar conformational changes, suggesting that SecA does not undergo further significant conformational changes when binding the preprotein[177]. The preprotein is suggested to trail through the clamp formed by the PPXD, HSD and NDF2, and then contacts the two-helix finger (2HF) of SecA, guiding it into the SecY channel[87,176,192]. Structural and molecular dynamic studies suggest that clamp closure occurs in distinct phases where the PPXD, HSD and HWD act as a unit[191]. A SecA mutant with a defective clamp is inactive for translocation.

The 2HF of the HSD has been suggested to interact with the polypeptide chain at the entrance of the SecYEG pore[87]. The finger consisting of two helices connected by a loo that moves into the cytoplasmic opening of SecY[176,177]. At the tip of the 2HF there is a conserved tyrosine residue that may contact the translocating polypeptide[87,132]. It is thought that in the ATP hydrolysis cycle, the movement of the 2HF would push translocating peptide into the channel. Translocation activity is still maintained when the 2HF is crosslinked to the most flexible cytosolic loop of SecY[193]. On the other hand, crosslinking of the 2HF to a more rigid region in the translocon cavity eliminate translocation activity[193], suggesting that its interaction with the polypeptide is not the only means for providing directionality in translocation. The 2HF might act as a guide to align polypeptide for translocation[194], and work in concert with the clamp[94,195]. Binding of ATP to SecA would result in a conformational change of 2HF that directs polypeptide into the translocon, whereas a subsequent positional reset occurs upon ATP hydrolysis which is then coupled to the tightening of the interaction between the clamp and the polypeptide, thereby maintaining progression of translocation. Opening of the clamp would allow the polypeptide to diffuse or slide passively through the pore until a next round of ATP binding and hydrolysis.

SecYEG – a proteinaceous membrane-embedded channel

The *E. coli* protein conducting channel comprises of three integral membrane protein, SecY, SecE and SecG[16] that form a stable heterotrimeric complex in the membrane. This complex has been purified to homogeneity, and functionally reconstituted into proteoliposomes to faithfully mimic the SecA and ATP-dependent translocation of preproteins[8,63]. In early 2000, the translocon has extensively been studied by electron microscopy both in eukaryotes[95,96] and bacteria[97,98,196]. These studies provided insight regarding its shape. It is resolved from the EM-resolved structure that *E. coli* translocon comprises of 15 TMS; 10 TMS of SecY, 3 TMS of SecE, and 2 TMS of SeG[196], consistent with its polypeptide hydropathy profile. These studies, provided insight regarding shapes, interacting domain and oligomerization but resolution was insufficient to resolve mechanistic aspects of the translocation. In 2004, van den Berg and coworkers

resolved the first high resolution crystal structure of SecYEβ from *Methanocaldococcus jannaschii*[10] providing architectural detail of the channel organization (Fig. 5A). The structure presented a channel in a closed state and corresponds to a pseudo symmetrically aligned assembly molding an hourglass clamshell structure formed by ten α-helical transmembrane segments (TMS) of SecY. TMS 1-5 and TMS 6-10 forming two halves of the clamshell structure. SecE, in its minimal form, consists of two TMS that partially enwrap SecY with the N-terminal amphipathic helix oriented on the cytoplasmic surface, and tilted on the outside of TM6 and TM7 of SecY, connected via a hinge region, while the C-terminal TMS is highly titled and positions at the "back" of the translocon. Secβ only comprises one TMS which is localized close to the C-terminus of SecE and almost perpendicular to the membrane.

The overall structure of the *M. jannaschii* SecYEβ matched the cryo-EM density map[196] of the *E. coli* SecYEG, with slight structural differences in the long cytoplasmic loops and other conformational differences related to the evolutionary lineage. Through cryoEM[104,197–199] and X-ray[175–177,200–202], further high resolution structures were reported. The structures of SecYEG from *T. maritima*[175] (Fig. 5C, TmSecYEG) and *T. thermophilus*[202] (TtSecYEG) provided insight in the position of the 2 TMS of SecG, whereas a nanodisc-reconstituted cryo-EM reconstruction of *E.coli* SecYEG[104] provided further positional information on the 2 distal TMS of the *E. coli* SecE which are not needed for activity *per se* (Fig. 5E) (See below). The various structures provided further insights in the structural basis of channel opening, but also signify some discrepancies.

In *E. coli*, SecE consists of three TMSs unlike the SecE in most other eubacteria that entail only one TMS[203]. In the absence of SecE, SecY is unstable and readily degraded by the membrane protease FtsH[204]. SecE is essential for cell viability and protein translocation [205,206], while the conserved region of cytoplasmic amphipathic helix and the consecutive TMS suffice to support the SecE function[203,205,207]. The structural data suggests that SecE is important for the stability of the translocon[208], and also for functionality as in coordinating channel opening with ligand (SecA or ribosome) binding[209].

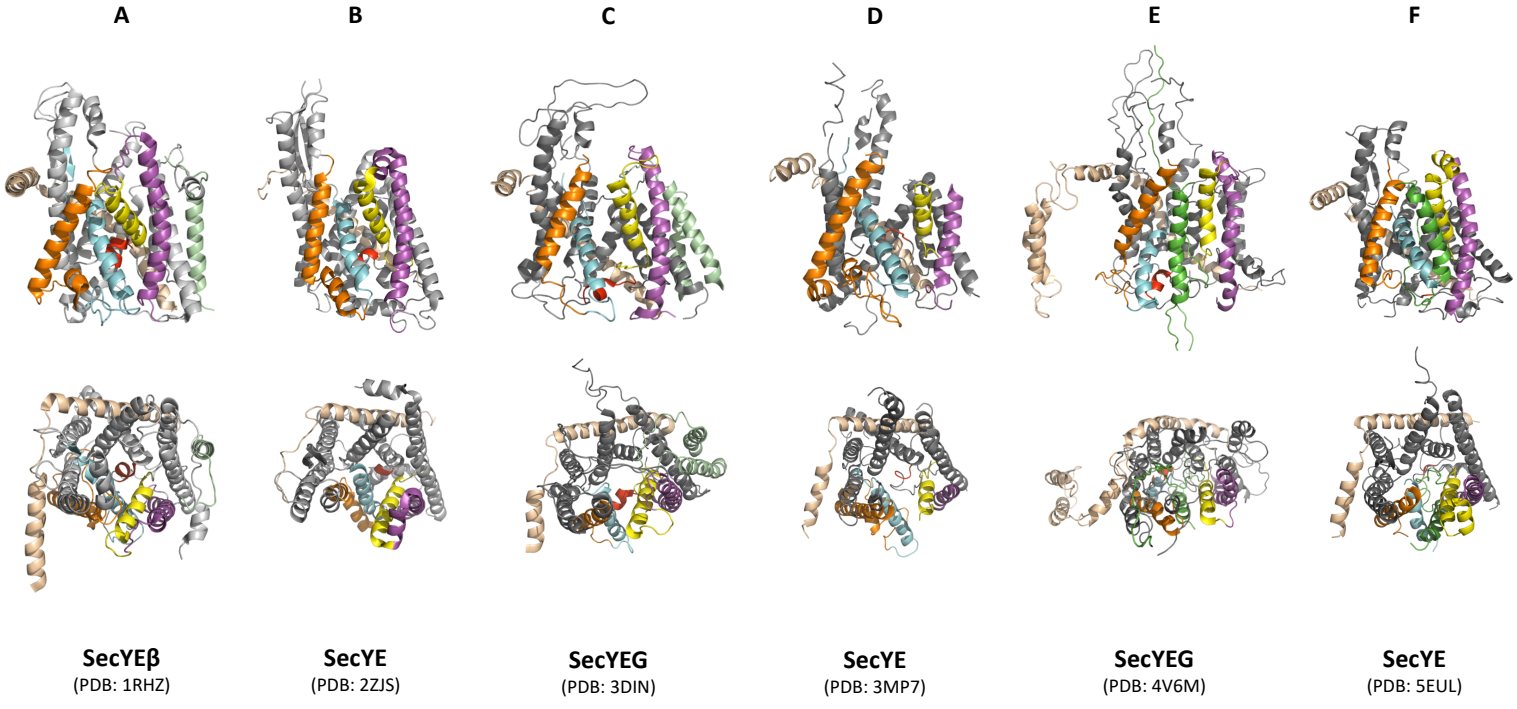

Figure 5. Cartoon representations of various SecYE(G/ß) complexes. SecY (grey), indicated with lateral gate helices TMS 2b (yellow), TMS 3 (magenta), TMS 7 (cyan) and TMS 8 (orange), and plug (red); SecE (light yellow/cream); SecG (pale green). **(A)** SecYEß of *Methanocaldococcus jannaschii* (PDB: 1RHZ); **(B)** SecYE of *Thermus thermophilus* (PDB: 2ZJS); **(C)** SecYEG of *Thermotoga maritima* (PDB: 3DIN); **(D)** SecYE form *Pyrococcus furiosus* (PDB: 3MP7); **(E)** SecYEG of *Escherichia coli* (PDB: 4V6M), with polypeptide (green); **(F)** SecYE of *Geobacillus thermodenitrificans* (PDB: 5EUL), with signal sequence (green). See text for more details.

Secß present in the *M. jannaschii* structure (Fig. 5A) is remotely homologous to the bacterial SecG. Like Secß, SecG is not essential for viability or translocation, but only promote translocation efficiency[8,210,211]. SecG is required for translocation at low temperatures[211] or at low PMF[212]. It also localizes peripherally from SecY as demonstrated in the TmSecYEG and TtSecYEG (Fig. 5B and D) structures and further biochemical data[213–215]. At this position, SecG might be able to interact with the accessory protein complex SecDF[57,216], and also with SecA[217–219]. Additionally, the structure of TtSecYEG shows that the cytoplasmic SecG loop covers the pore ring, while crosslinking at this position inhibits translocation[202]. Various studies suggested an SecA dependent topology inversion of the two SecG TMSs during translocation[220–223], but crosslinking approaches that fixed the topology of SecG did not inactivate translocation[224]. Both SecG and SecE maintain their interactions with SecY during translocation[225], and currently there is no plausible mechanism on the basis of these structures that would support the idea of topology inversion.

SecY is the central unit of the conducting channel with all characteristics of a gated channel. The pseudo symmetrical arrangement of the two sets of five TMSs of SecY forms an hourglass shape pore with a cytoplasmic and periplasmic entry and exit funnel, respectively. Uncharged amino acid dominates the walls of the internal cytoplasmic funnel, whereas the rim contains both positive and negative residues. In closed or resting state, six hydrophobic residues forming a central constrictions project their side chains radially inward to form a tights seal preventing leakage of water or ions[226,227]. The constriction ring provides a hydrophobic gasket around the translocating polypeptide thus prevent undesired ion leakage[228]. At the periplasmic funnel, or trans side of the constriction ring, a small α-helix TM2a or reentrance loop forms a plug domain that obstructs the exit path of the pore[227,229]. The two halves of the SecY clamshell structure are connected by an external loop between TM5 and TM6, which act as a hinge. Viewed from the cytoplasmic side, termed 'front' (Fig. 5), the structure would open with TM2b, TM3, TM7 and TM8 as main elements of a lateral gate. Upon opening, this gate provides access to the lipid bilayer[175]. These lateral gate are tiled in the membrane and connected to protruding cytoplasmic loops between TM6 and TM7 and between TM8 and TM9 that extend ~20Å above the membrane plane[10]. These loops provide the binding sites for the cytosolic partners, SecA[200] or ribosome[104,175,230] as established by crosslinking and mutagenesis studies[200,231,232].

The available structures of SecYEG/ß and its eukaryote homolog Sec61 complex, display different conformational states; Figure 5 (A-F) represent presumptive subreactions in the channel opening mechanism. The *M. jannaschii* SecYEß structure (Fig. 5A) is in a closed state indicated by a compact structure, the narrow constriction of the hydrophobic ring and the position of the plug domain obstructing the channel. In the 'closed' state, the lateral gate, is also closed. The structure of TtSecYE (Fig. 5B), which was crystallized with Fab fragment bound to one of the cytoplasmic loop that interacts with SecA, exhibit a partial

displacement of helices at the cytoplasmic side of the lateral gate. This suggest that binding of cytosolic partners to the cytoplasmic loops already triggers a conformational change of the translocon, partially cracking open the lateral gate. In this structure, the interaction between SecY and SecG is also weakened[202]. The binding of cytosolic partner introduces a hydrophobic crack or crevice as confirmed by a FRET study, that disrupts three polar interactions between TM2 and TM7 which play a role in stabilizing the idle complex. The crack at the lateral gate, termed 'primed' state, would then be available for the binding of signal sequence[233], where it is also become exposed to the lipid[82] in order to induce α-helicity to the signal sequence.

In the structure of TtSecYEG (Fig. 5C) bound to a SecA monomer stabilized by an ATP hydrolysis intermediate, the C-terminal half of SecY is notably shifted outward thereby opening a window in the lateral gate to the lipid bilayer. Such displacement caused a gap between side chains of TM2 and TM7 of about 5 Å. The displacement of the TMSs and its interactions would consequently change the conformation of the complex, including exposing hydrophilic surface of the pore interior to the hydrophobic lipid bilayer, a widening of the hydrophobic constriction ring and a destabilization of plug domain at the periplasmic funnel. These changes of translocon conformation resulted in formation of a vectorial translocation path and is also referred to as 'pre-open' state. The crystal structure of the *Pyrococcus furiosus* SecYE was resolved with partial insertion of TMS10 from neighboring SecY into the channel, as such mimicking a polypeptide within the channel (Fig. 5D). The structure showed a larger opening of the lateral gate and a further widening of hydrophobic ring, albeit in that particular structure the plug domain still blocked the vectorial passage. Since the inserting polypeptide is hydrophobic, this structure may resemble an intermediate in the membrane protein insertion process where hydrophobic TMS may slide into the lipid bilayer from the lateral gate without the formation of a vectorial aqueous path. The structure of SecYEG reconstituted in nanodiscs bound to a ribosome-nascent-chain (RNC) of a membrane protein showed an even wider opening of lateral gate (Fig. 5E). Such opening was caused by residing of substrate polypeptide near to the lateral gate prying open the N- and C-terminal halves of SecY. The structure also displays a displacement of plug domain, but the periplasmic end of the vectorial pathway in this structure is hindered by a periplasmic loop. This 'unlocking' of the translocon by binding of signal sequence is also shown by previous FRET study[234], where it also showed that the signal sequence binding alone is not sufficient for plug displacement for full vectorial channel opening.

The structure of *G. thermodenitrificans* SecYE (Fig. 5F) was resolved in a bound state with SecA and with a covalently linked OmpA signal sequence and a short polypeptide linked to the SecA 2HF[177]. The structure also showed a large opening of the lateral gate, and a further widening of the hydrophobic ring. The ß-stranded plug structure moves to the periplasmic side towards the back of the channel, away from lateral gate. *T. maritima* SecY (Fig. 5C) and *P. furiosus* SecY

(Fig. 5D) show a wider opening of the lateral gate at the periplasmic side, as compared to the structure of *G. thermodenitrificans* SecY. This is mainly caused by a re-positioning of TM7 which is now closer to TM3, and also from the tilt of TM7. This conformation in turn, however, provides a wider opening of the hydrophobic ring, allowing a signal sequence to intercalate into the channel. The C-terminal region of the signal sequence replaces the 'closed' state of periplasmic end of TM7 in the *M. jannaschii* structure, where its side chains point into the periplasmic cavity previously occupied by the plug, thus sealing it from the surrounding lipid molecules. This is in agreement with a recent study that showed that full opening of the complex, including a complete displacement of the plug, is only achieved in the presence of a polypeptide and upon the binding of ATP to SecA[234].

Specific crosslinking experiments have been conducted to probe the interactions between and within the translocon subunits during protein translocation. Crosslinking of the hydrophobic ring residues abolishes translocation supporting the notion that polypeptides moves through the center of the SecY[83]. Crosslinking of TM2 to TM7 at the mid of the lateral gate reveal that the gate need to open to at least 5 Å to allow translocation[88]. The lateral opening mechanism is also supported by a FRET study[92]. This opening must occur along the lipid bilayer interface, from the cytoplasmic surface[92, this thesis (chapter 2)] to the periplasmic surface[93], although crosslinking of the gate at periplasmic interface of the membrane is less inhibitory for translocation[this thesis (chapter 2 and 3)] as compared to that at cytosolic interface or mid of the lateral gate. The conformational changes that occur during channel opening also includes a movement of the plug domain. Although plug domain is not essential[235,236], it is required to seal the channel[86]. Crosslinking studies have shown that the plug is able to move and interact with SecE[84,237], but the movement is rather small and does not need to occur all the way up to the SecE C-tail[229,238]. However, in the *G. thermodenitrificans* SecYEG structure with a covalently bound signal sequence in the lateral gate, the plug domain moved all the way close to the C-tail of SecE[177].

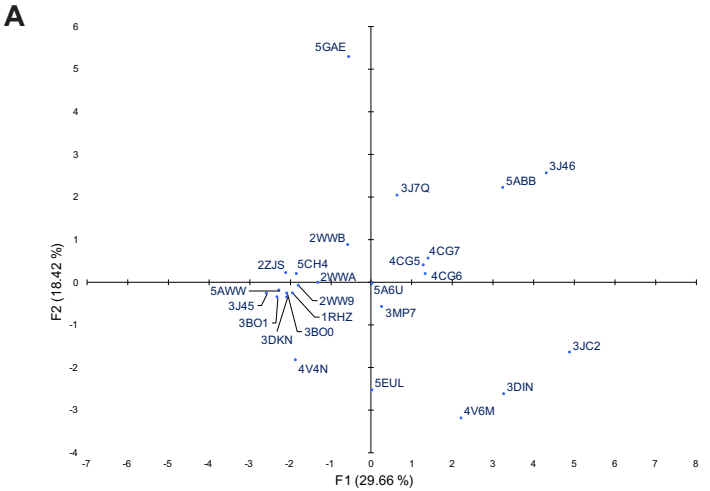
A
5GAE
3J46
3J7Q
5ABB
2WWB
4CG7
4CG5
2ZJS
5CH4
4CG6
2WWA
5AWW
5A6U
3J45
2WW9
3MP7
1RHZ
3BO1
3BO0
3DKN
3JC2
4V4N
5EUL
3DIN
4V6M
F2 (18.42 %)
F1 (29.66 %)

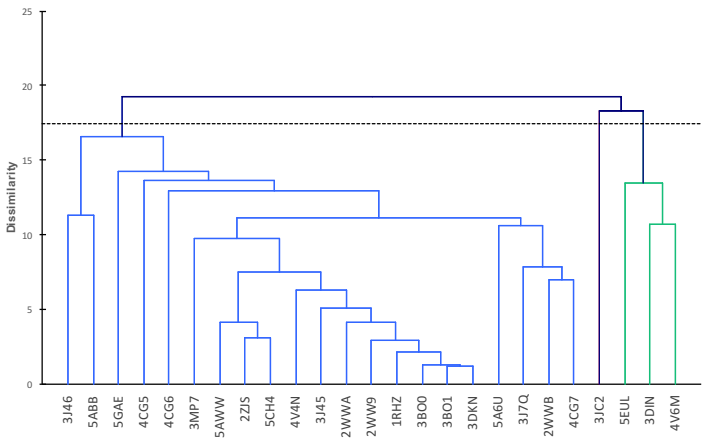
B
Dissimilarity
3J46
5ABB
5GAE
4CG5
4CG6
3MP7
5AWW
2ZJS
5CH4
4V4N
3J45
2WWA
2WW9
1RHZ
3BO0
3BO1
3DKN
5A6U
3J7Q
2WWB
4CG7
3JC2
5EUL
3DIN
4V6M

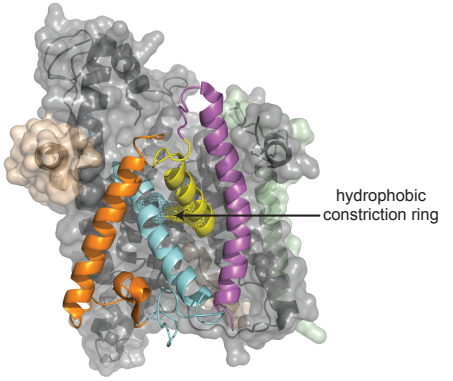
C
hydrophobic
constriction ring

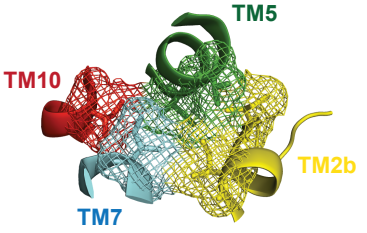
D
TM5
TM10
TM2b
TM7

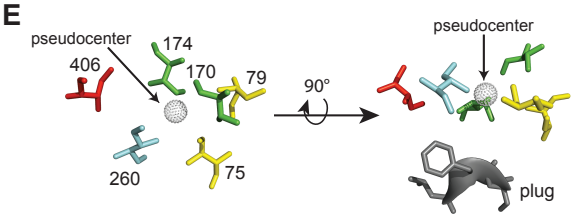
E
pseudocenter
406
174
170
79
260
75
90°
pseudocenter
plug

Figure 6. Analysis of translocon conformation. (A) Scatter plot of Principal Component Analysis (PCA) visualizing the variance of available Sec translocon structures characteristics based on distances of amino acid residues between various points making up the lateral gate, hydrophobic ring and plug domain. **(B)** Dendogram of Agglomerative Hierarchical Clustering (AHC) of the structures. **(C)** Crystal structure of SecYEß (PDB: 1RHZ). SecY (grey), indicated with lateral gate helices TMS 2b (yellow), TMS 3 (magenta), TMS 7 (cyan) and TMS 8 (orange), SecE (light yellow/cream), SecG (pale green). Hydrophobic ring is indicated with arrow. Lateral gate opening is measured by the distances of the nearest residues at the cis- (TM2b-TM8), mid- (TM2b-TM7) and trans- (TM3-TM7) side. **(D)** Hydrophobic ring is composed of six hydrophobic residues that are part of TM2b, TM5, TM7 and TM10, and are represented in the sticks and mesh configuration. **(E)** Constriction ring residues of SecYEß. A pseudoatom is generated to generate a pseudocenter to calculate the distance of plug domain to center of hydrophobic ring. Note: In the 3JC2 structure, the plug domain is missing, and a pseudoplug was generated by averaging the distance from all other available structures.

The large number of translocon structures in different conformations allows a detailed analysis of distances between relevant amino acids that are part of the lateral gate, constriction ring, and plug domain. By performing ordination analysis of these distances, the various structures can be clustered in related conformational states. Based on standardized distance value (Supplementary Table 1), there are some extreme or outlier positions suggesting large movements with the lateral gate, hydrophobic ring and plug domain. Extreme cis-side lateral gate opening is observed in the openings exhibited by structure 5ABB and 5CH4, whereas mid-side opening is seen in 3J46, while trans-side opening is observed in 3DIN and 4V6M. Extreme plug-domain displacement is seen in 5EUL. Not all of these are reflected on the scatter plot of PCA, presumably due to effect of incorporation of distance values between hydrophobic ring residues. However, these measurement and analysis could provide basis for further exploration of the translocon passage structure. From the clustering analysis, most of the structures are more or less related to 1RHZ, representing the 'closed' state conformation (Fig. 6A and B). However, the grouping/clustering does not illustrate/represent the previously described processes from closed state to the wide opening of lateral gate and plug displacement. Based on correlation data (Supplementary Table 2, numbers in bold), there is a strong correlation between the partitioning of lateral gate at different positions. Movements of the lateral gate at the cis-side correlate with movements of the mid-part of lateral gate, while later movements further correlate with movements of hydrophobic ring residues that are between TM2b-TM7 and TM5-TM7. The opening of the mid part of the lateral gate is indeed due to movements of SecY halves. Opening of the trans-side of the lateral gate significantly correlates with movement of hydrophobic ring residues that of TM5-TM7, each belonging to different halves of the SecY translocon, and also correlates with movement of hydrophobic ring residues that of TM2 and TM5. Partitioning of the trans-side of lateral gate also correlates with a movement of the plug domain away from the hydrophobic ring. Also, the widening of the trans-side funnel perturbs the interaction of the plug with hydrophobic residues in the channel. All features of the channel opening are all structurally interconnected.

Associating membrane protein complexes

To catalyze its activities, the translocon also interacts with a number of accessory membrane proteins. One of these complexes is the membrane-embedded SecDFyajC complex[57,239]. SecD and SecF are both integral membrane proteins with six TMS and a large periplasmic domain[240,241] (Fig. 7A). YajC is a small, non-essential membrane protein found to associate with SecF and SecYEG[57,116]. While translocation *in vitro* does not require SecDFyajC[16], translocation *in vivo* is greatly reduced without SecD and SecF[242]. It is proposed that SecDF utilizes the PMF to complete protein translocation after ATP-dependent initiation of translocation by SecA[241]. In this mechanism, the periplasmic "head" domain of SecDF would function as kind of PMF-driven lever to pull the translocating protein into the periplasm.

YidC is a member of YidC/Oxa1/Alb3 family[243] and is essential for cell viability[112]. It plays role in inserting various Sec-independent protein[244–247], but also assist Sec-dependent protein[248–254] or its proper folding[255–257]. YidC co-purifies with SecDF[116] or SecYEG[113]. It localizes at the lateral gate of SecY, where it contacts all four TMS of lateral gate[117]. However, these contacts are lost when a ribosome nascent chain binds to SecYEG. YidC consists of conserved core domain of five TMSs, with a hydrophilic cavity to localizes to the hydrophobic lipid bilayer region and that is open towards the cytoplasm[118] (Fig. 7B). It has been suggested that the hydrophobic cavity locally disrupts the phospholipid bilayer structure and that this might be the site where TMS of membrane proteins slide into the membrane. For detail review of YidC, please refer to references[258,259]

Several other factors might interact with the translocon, i.e. FtsY[260], Syd[261–264], Ppid[265] and YidD[266-chapter 4] and fulfil functions in targeting and folding.

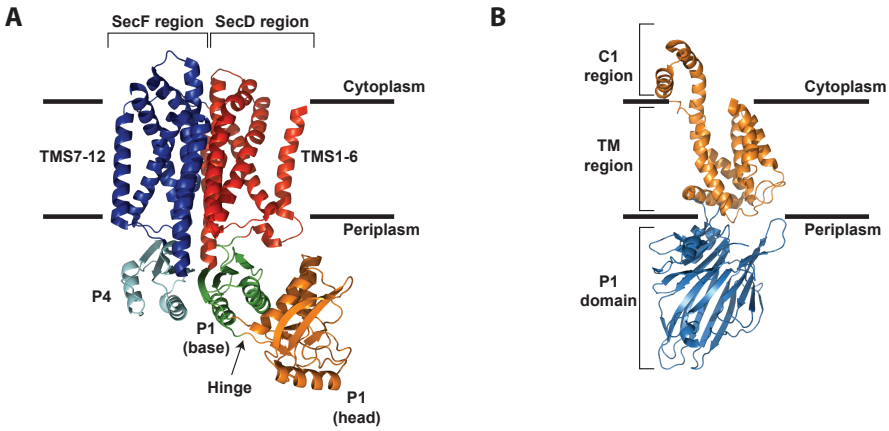

Figure 7. Structure of SecDF and YidC, viewed from the membrane side. (A) Structure of *T. thermophilus* SecDF (PDB: 3AQP) composed of periplasmic domain (P1 – head an base, and P4), and 12 TMSs of SecD (TM1-6) and SecF (TM7-12). **(B)** Structure of *E. coli* YidC (PDB: 3WVF) with the periplasmic P1 domain, TM region and C1 region.

4. Mechanism of translocation through the pore

Several models for the protein translocation mechanism have been suggested, namely: Brownian ratchet, power stroke, subunit recruitment, piston, peristalsis and reciprocating piston. As the name implies, the Brownian ratchet model suggests that translocation occurs through a random Brownian movement of the polypeptide, where the unfolded polypeptide moves freely in the translocation pore but its movements is directed by chaperones on the cis and/or trans-side of the channel[126]. SecA function may be to open the channel through its interactions with the SecY pore, and then allow the polypeptide to diffuse through the channel. By binding the polypeptide at the cis-side, SecA would also prevent

backsliding of the protein. By repeated binding and release events, a stepwise translocation can occur although in such mechanism the step-size will not be uniform. A recent study based on MD simulation and single molecule FRET suggests a regulation of SecA nucleotide exchange by the substrate-SecY channel interaction[94]. However, this model does not explain a near to uniform size step translocation[78,124,125].

In vitro studies have shown that translocation is a stepwise process where binding of ATP to SecA induces a translocation progress of 20-25 amino acid [78,124,125], followed by ATP hydrolysis, that by an unknown mechanism causes a further translocation progress with a similar step size. These observations suggest a power stroke mechanism where SecA would push polypeptide segments into the channel. This pushing mechanism would depend on multiple contacts between preprotein and SecA[178,180,267]. It has been proposed that the 2HF in SecA functions in the mechanism[87] as suggested from its apparent 'movement' in different SecA structures (Fig. 4). The hydrophobic tip with its conserved tryptophan would interact with the translocating protein through side-chain interactions. Considering that the 2HF conformational change is relatively small, it remains difficult to relate a power stoke movement of this region as it would fall short in translocating the step size observed *in vitro*. Comparison of various SecA structures, including that of SecA bound to SecYE with a signal sequence[177], indicate the extent of conformational change of within SecA in particular the clamp closure[191] and the protrusion of 2HF[176,177]. It is evident that the 2HF works in concert with clamp[94,195] during the ATP binding-hydrolysis cycle. Binding of ATP would result in a conformational change of the 2HF guiding the polypeptide into the translocon, where subsequent ATP hydrolysis is coupled with a clamp action that captures the polypeptide to prevent back-sliding. Release of the polypeptide by the clamp, would allow the polypeptide to traverse passively until a next round of ATP binding-hydrolysis. This suggest a process in which ATP hydrolysis generates a power stroke on the polypeptide, and allow it to slide through the opening of the channel[132]. In the presence of a PMF, translocation occurs very fast without the apparent accumulation of translocation intermediates. In this process, SecDF may pull large segments of the polypeptide across the pore whereupon the secretory protein will fold at the trans-side (or periplasm).

Studies on the reconstituted translocation components have shown that SecA cycles between the cytosol and cytoplasmic membrane[268]. While SecA binds to lipids with low affinity, binding is enhanced when negatively charged lipids are present[170,269]. Without the negatively-charged phosphatidylglycerol, SecA does not bind to the membrane[170]. The N-terminus of SecA is highly amphipathic. Its positively charge characteristic plays a critical role in membrane binding[270,271]. Also, the positively charged N-terminus of the signal sequence interacts with negatively charged phospholipids[272–275]. In its membrane-bound state, SecA exhibits a higher affinity to SecB/preprotein complex[70] most likely because of

binding of the unfolded secretory protein[170]. SecA next binds to membrane embedded SecYEG complex with high affinity in nanomolar range[90]. It was previously shown that anionic membrane phospholipids are important for protein translocation[276]. Experiments with a defined distribution of phospholipids in nanodiscs show that this require the presence of large lipid surface[171]. SecA gains access to the translocon via this lipid-bound intermediate state[171].

An intriguing aspect of the SecA structure is its ability to dimerize (see reference[131]). Various lines of evidence demonstrate that SecA is active as a dimer. The two SecA protomers have a high binding affinity, i.e., a K_d in the subnanomolar range. To imply the SecA dimer in the translocation mechanism, a subunit recruiting mechanism has been proposed in which SecA undergoes dimerization or monomerization at the translocation site. This model was inspired by *in vitro* observations that the acidic phospholipids induce monomerization of SecA whereas, primarily based on physiological interaction findings that long-chain phospholipid monomerize SecA while adding signal peptide binding would cause dimerization[127]. The model requires that dimerization of SecA is a dynamic process where the SecYEG bound SecA monomer would recruit a second SecA protomer.

Based on the crystal structure of an antiparallel SecA dimer with a central opening at the dimer interface, a piston model was proposed[128]. According to this model, the SecA-bound preprotein is pushed through the pore by means of an ATP dependent power stroke[128]. A further extension of this model is the peristalsis model, which built upon docking of the dimeric SecA onto SecYEG, framing a large vestibule between the protein complexes[129,130]. After binding of ATP, the central opening of dimeric SecA would trap the polypeptide and a subsequent change in conformation of SecA would shrink the dimensions of this vestibule dimension concomitantly with the opening SecYEG channel. This would direct polypeptide segments to translocate to the trans-side, whereas backsliding is hindered by the trapping of the polypeptide with the SecA dimer central opening. ATP hydrolysis would reverse the SecA dimer conformation and close the SecYEG channel. Following polypeptide segments are then translocated by repeated cycles of the aforementioned ATP-dependent steps.

A further refinement of this model involves an asymmetrical association of the dimeric SecA with SecYEG and takes into account a ligand dependent equilibrium of SecA monomer-dimer. It also integrates the findings that translocation occurs in at least two distinct steps involving SecA-preprotein binding and ATP-binding, whereas SecA releases the preprotein upon ATP hydrolysis. The reciprocating piston model[131] includes SecA membrane cycling via a monomeric intermediate. In this model, the SecA dimer binds to SecYEG with high affinity[277,278], where one protomer bind directly to SecYEG while the other SecA protomer is bound to the SecYEG-bound protomer[109]. These reactions prime SecA for ATP binding and hydrolysis[170,279]. Next, the SecA dimer accepts

the preprotein from SecB[280], and upon ATP binding, SecA would cause a partial opening of the SecYEG channel[281], insert a hairpin-like structure of signal sequence and adjacent mature domain of preprotein[282,283], and release SecB[72]. ATP hydrolysis would cause the release of one of the SecA protomer from the complex, that can rebind in a following translocation step. It is unclear if the dissociation of the SecA protomer is complete as previous data on PrlA mutants of SecY have been shown to bind SecA more tightly while also causing increased translocation rates. However, cycling of SecA is supported observations that SecA mediated translocation occurs at concentrations that are far in excess to the concentrations needed to saturate binding to SecYEG. Rebinding of the SecA protomer to the SecYEG-bound SecA might also be responsible for the nucleotide independent translocation step similar to that of peristalsis and subunit recruitment models[77,284]. Repeated cycles of ATP binding and hydrolysis, and SecA dissociation and re-binding will result in stepwise preprotein translocation. In the absence of a SecA interaction, translocation may occur through passive sliding of the polypeptide through the channel. Retrograde movement of polypeptide is prevented by trapping the preprotein at the cis-side of the membrane, but also by SecDF that likely binds the preprotein at the trans-side of the membrane.

5. Scope of this thesis

Our understanding of the mechanism of protein secretion has advanced significantly after proceeded for more than three decades of experimental. Following the identification of its genes, proteinaceous components were purified, overexpressed and reconstituted into in-vitro reconstituted system to interpret intimate details of the enzymatic and mechanism underlying the translocation processes. The result of various studies in regard to translocation mechanism and its apparatus are discussed in **Chapter 1**. The availability of high-resolution structures enabled detailed mechanistic interpretations of the various components during translocation processes and how it relates to conformational changes within the Sec-translocase. In this thesis, the role of the lateral gate of SecY and its opening mechanism is further investigated in relation to the translocon plasticity and its interaction with the associating motor protein, SecA. **Chapter 2** describes the use of variable-length chemical crosslinkers to probe the dynamics of lateral gate opening on the cis-, mid- and trans- side of the translocon providing further insights in the degree of the lateral gate opening. In **Chapter 3**, the lateral gate was probed with an optical switch to examine its plasticity. The result further supports the fact that lateral gate opening at its trans-side is less restrictive, showing the lateral gate is flexible and dynamic with different degree of opening throughout its lining which opens like a wedge. **Chapter 4** examines the interaction of translocon with its associating protein, SecA, by investigating the activity of a single translocon reconstituted into nanodiscs. The result showed that SecA binding cause partitioning of lateral gate

and is nucleotide-dependent process. It also verifies that monomers of SecYEG are sufficient for protein translocation. **Chapter 5** aimed to monitor the dynamics of the 2HF of SecA by means of measuring FRET signals of fluorophores conjugated to the 2HF domain and the *cis*-side of SecYEG. Our findings demonstrate strong FRET signal upon establishment of interaction between the two proteins. Nevertheless, our experimental setup was unable to measure further dynamics upon the addition of either nucleotide or substrate. These findings suggest further explorations are needed to elucidate the intricate details of the translocation mechanism.

Supplementary information

S1. Standardized value of amino acid residues distances

Protein Structure (PDB ID)	lateral gate			hydrophobic ring residue													Ring - plug
	cis	mid	trans	1-3	1-4	1-5	1-6	2-3	2-4	2-5	2-6	3-5	3-6	4-5	4-6	5-6	
1RHZ	-0.41	-0.20	-0.64	-0.76	0.17	-0.85	-0.57	-0.15	-0.16	-0.82	-0.53	-0.80	-0.22	-0.65	-0.38	-0.33	-0.19
2WW9	-0.67	-0.48	-0.51	-0.82	-0.28	-0.66	-0.38	0.91	0.06	-0.86	-0.58	-0.45	0.31	-0.92	0.01	-0.59	-0.46
2WWA	-0.63	-0.26	-0.45	-0.82	-0.21	-0.72	-0.52	0.86	0.74	-0.60	0.45	-0.54	-0.16	-0.65	-0.90	0.27	-0.40
2WWB	-0.48	-0.53	-0.61	0.98	0.69	0.44	1.32	-0.43	-0.93	-0.46	-0.67	-0.45	0.78	-0.44	0.08	-0.26	-0.27
2ZJS	**1.57**	-0.53	-0.59	-0.76	-0.86	-0.63	-0.43	-1.10	-0.63	-0.86	-0.18	-0.54	-0.51	-0.58	-0.57	-0.26	-0.06
3BO0	-0.71	-0.59	-0.64	-0.76	0.17	-0.53	-0.57	-0.15	-0.16	-0.82	-0.49	-0.80	-0.22	-0.65	-0.31	-0.86	-0.59
3BO1	-0.82	-0.86	-0.64	-0.76	-0.02	-0.85	-0.57	-0.15	-0.16	-0.82	-0.53	-0.80	-0.22	-0.65	-0.38	-0.86	-0.59
3DIN	-0.71	1.46	**2.33**	0.65	-0.99	0.66	-0.99	1.47	0.74	0.48	-1.47	**1.80**	0.43	**2.14**	**2.15**	-0.72	**1.82**
3DKN	-0.67	-0.59	-0.45	-0.76	-0.02	-0.85	-0.57	-0.15	-0.16	-0.67	-0.53	-0.80	-0.22	-0.65	-0.38	-0.59	-0.48
3J45	-0.56	-0.53	-0.45	-0.49	-0.67	-0.59	-0.38	-0.99	-0.72	-0.67	-0.18	-1.48	-0.80	-0.85	-1.03	-0.13	0.09
3J46	1.28	**3.12**	**-0.32**	-0.38	0.30	**1.82**	1.28	-0.43	1.04	**2.98**	**2.40**	**1.55**	1.07	0.82	0.27	-0.20	-0.30
3J7Q	-0.44	-0.53	-0.61	0.05	-1.05	0.76	0.38	-0.88	-0.59	0.70	1.29	0.55	**1.89**	0.65	1.24	-0.59	-0.17
3JC2	-0.44	-0.53	1.19	0.32	**2.24**	**1.95**	-0.14	0.46	**1.86**	**1.89**	-0.49	**2.27**	**-1.50**	**3.03**	-0.12	**3.17**	**-1.55**
3MP7	0.83	1.46	-0.03	-0.44	-0.73	-0.05	-1.18	-0.10	0.36	0.27	-0.09	0.71	-0.16	0.48	-0.90	-0.26	-0.93
4CG5	-0.63	-0.42	-0.35	-0.33	0.17	-1.17	-0.57	**2.70**	**3.02**	0.52	1.20	0.55	1.42	0.44	0.79	-0.46	0.09
4CG6	0.90	0.30	0.79	**2.61**	**2.17**	1.40	**1.51**	0.02	-0.50	0.63	0.09	-1.05	-0.45	-0.61	-0.83	-0.13	-0.33
4CG7	-0.63	-0.53	-0.51	1.09	0.95	**1.72**	0.85	-0.26	-0.16	0.70	-0.62	0.49	1.13	0.54	0.01	0.14	-0.25
4V4N	-0.71	-0.59	-0.35	1.14	-0.60	-1.21	-1.37	**1.75**	-0.16	-0.93	-0.44	-0.45	-1.33	-0.71	-0.51	-0.72	-0.40
4V6M	-0.26	1.30	**3.05**	**2.12**	1.40	-0.79	-0.85	0.07	0.14	0.52	-0.53	0.90	-0.80	0.51	-0.31	-0.20	**1.87**
5A6U	-0.44	-1.09	1.14	-1.15	-1.44	0.63	0.14	**-1.55**	-0.93	0.77	-0.58	0.99	-0.57	0.24	0.59	1.19	-0.59
5ABB	**2.66**	1.46	-0.64	1.14	1.33	0.92	**1.94**	1.13	1.26	0.74	1.65	0.11	-0.04	0.71	1.18	0.60	0.33
5AWW	0.83	0.52	-0.61	-0.66	-0.73	-0.76	-0.38	-0.77	-1.23	-0.96	-0.58	-0.61	-0.80	-0.88	-0.90	-0.06	-0.12
5CH4	**2.13**	-0.53	-0.48	-0.55	0.04	-0.50	0.19	-0.38	-0.85	-0.86	-0.35	-0.76	-0.74	-0.78	-0.90	-0.13	-0.09
5EUL	-0.48	-0.48	0.90	0.00	-0.99	0.69	-0.57	-0.82	-1.15	-0.02	-0.67	0.80	-0.92	0.44	-0.83	-0.72	**3.41**
5GAE	-0.52	-0.37	-0.53	-0.66	-1.05	-0.82	**2.41**	-1.05	-0.72	-0.86	**2.40**	-1.20	**2.59**	-0.99	**2.92**	**2.71**	0.15

Values of standardized measurement. Lateral gate partitioning, hydrophobic ring opening and plug domain displacement are measured based on shortest distances between representing amino acid, of each Sec translocon structure. Each measurement is then standardized, prior to subsequent analysis. Those in bold in bold-cell-borders are considered extreme position or condition, as values is x<-1.96 or x>1.96. Those in bold with regular cell-borders are distances with value of -1.95<x<-1.5 or 1.5<x<1.96, indicating distances that rather significantly differ compared to 'closed' state. Lateral gate openings are measured at three position, cis-side, mid-side and trans-side. Hydrophobic ring residue are measured among those located in different transmembrane helices; TM2b – residue 1 (75/Ile) and 2 (79/Val), TM5 – residue 3 (170/Ile) and 4 (174/Ile), TM7 – residue 5 (206/Ile), TM10 – residue 6 (406/Leu); numbers refers to amino acid sequence number in structure 1RHZ.

Table S2. Correlation matrix of residue distances (Pearson (n-1))

Variables	cis	mid	trans	1-3	1-4	1-5	1-6	2-3	2-4	2-5	2-6	3-5	3-6	4-5	4-6	5-6	Ring - plug
cis	**1**	**0.477**	-0.155	0.120	0.200	0.215	0.366	-0.116	-0.001	0.188	0.329	-0.025	-0.141	-0.014	-0.125	0.044	-0.074
mid	**0.477**	**1**	0.290	0.287	0.189	0.331	0.154	0.163	0.331	**0.571**	0.352	**0.430**	0.109	0.366	0.151	-0.083	0.188
trans	-0.155	0.290	**1**	**0.474**	0.192	0.259	-0.233	0.097	0.126	0.391	-0.342	**0.602**	-0.295	**0.573**	0.122	0.136	**0.603**
1-3	0.120	0.287	**0.474**	**1**	**0.638**	**0.400**	0.247	0.278	0.089	0.321	-0.066	0.191	-0.090	0.287	0.030	-0.026	0.302
1-4	0.200	0.189	0.192	**0.638**	**1**	**0.416**	0.309	0.283	**0.400**	**0.399**	0.017	0.135	-0.185	0.294	-0.182	0.231	-0.084
1-5	0.215	0.331	0.259	**0.400**	**0.416**	**1**	**0.476**	-0.161	0.131	**0.802**	0.123	**0.610**	0.089	**0.666**	0.159	0.312	0.100
1-6	0.366	0.154	-0.233	0.247	0.309	**0.476**	**1**	-0.272	-0.085	0.300	**0.627**	-0.118	**0.534**	-0.037	**0.462**	**0.463**	-0.125
2-3	-0.116	0.163	0.097	0.278	0.283	-0.161	-0.272	**1**	**0.764**	0.079	0.011	0.205	0.002	0.257	0.138	-0.176	0.032
2-4	-0.001	0.331	0.126	0.089	**0.400**	0.131	-0.085	**0.764**	**1**	**0.510**	0.315	**0.495**	0.142	**0.563**	0.237	0.165	-0.065
2-5	0.188	**0.571**	0.391	0.321	**0.399**	**0.802**	0.300	0.079	**0.510**	**1**	0.367	**0.799**	0.157	**0.769**	0.239	0.292	0.094
2-6	0.329	0.352	-0.342	-0.066	0.017	0.123	**0.627**	0.011	0.315	0.367	**1**	-0.010	**0.619**	-0.016	**0.462**	0.313	-0.163
3-5	-0.025	**0.430**	**0.602**	0.191	0.135	**0.610**	-0.118	0.205	**0.495**	**0.799**	-0.010	**1**	0.001	**0.925**	0.272	0.225	0.338
3-6	-0.141	0.109	-0.295	-0.090	-0.185	0.089	**0.534**	0.002	0.142	0.157	**0.619**	0.001	**1**	-0.016	**0.720**	0.076	-0.110
4-5	-0.014	0.366	**0.573**	0.287	0.294	**0.666**	-0.037	0.257	**0.563**	**0.769**	-0.016	**0.925**	-0.016	**1**	0.325	0.336	0.320
4-6	-0.125	0.151	0.122	0.030	-0.182	0.159	**0.462**	0.138	0.237	0.239	**0.462**	0.272	**0.720**	0.325	**1**	0.365	0.140
5-6	0.044	-0.083	0.136	-0.026	0.231	0.312	**0.463**	-0.176	0.165	0.292	0.313	0.225	0.076	0.336	0.365	**1**	-0.122
Ring - plug	-0.074	0.188	**0.603**	0.302	-0.084	0.100	-0.125	0.032	-0.065	0.094	-0.163	0.338	-0.110	0.320	0.140	-0.122	**1**

Values in bold are different from 0 with a significance level alpha=0.05

Distances between various measurement of lateral gate partitioning, hydrophobic ring opening, and plug domain displacement are analyzed to see its correlation. Those in bold indicate strong correlation between the measurement.

Table S2. Principal Component Analysis

Eigenvalues:

	F1	F2	F3	F4	F5	F6	F7	F8	F9	F10	F11	F12	F13	F14	F15	F16	F17
Eigenvalue	5.042	3.132	2.019	1.829	1.371	1.292	0.802	0.432	0.407	0.219	0.167	0.120	0.082	0.051	0.020	0.009	0.006
Variability (%	29.658	18.422	11.875	10.760	8.063	7.602	4.719	2.542	2.392	1.287	0.983	0.708	0.485	0.299	0.119	0.050	0.036
Cumulative %	29.658	48.080	59.955	70.715	78.779	86.380	91.100	93.642	96.033	97.320	98.303	99.011	99.496	99.795	99.913	99.964	100.000

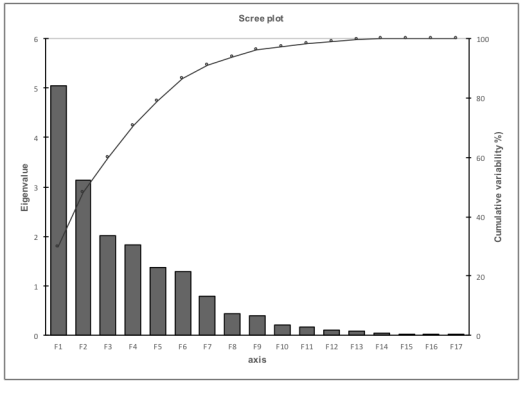

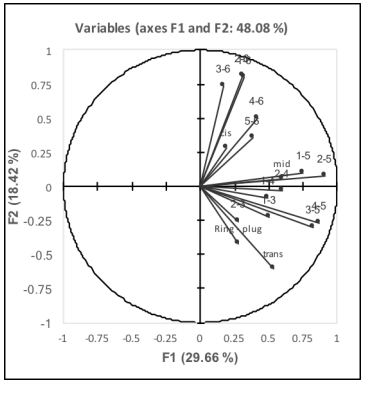

Chapter 2

The Lateral Gate of SecYEG Opens to its Full Length to Facilitate Protein Translocation

Intan Taufik and Arnold J.M. Driessen

CHAPTER TWO

The Lateral Gate of SecYEG Opens to its Full Length to Facilitate Protein Translocation

Abstract – The SecYEG translocon forms an aqueous pore for the transfer of unfolded preproteins across the cytoplasmic membrane. Opening of a lipid exposed lateral gate appears to be an important step in the pore opening mechanism. Upon SecA-dependent initiation of preprotein translocation, the distance between the central positions in contacting lateral gate transmembrane segments 2 and 7 needs to expand by at least 8 Å. Here we further examined the dynamics of lateral gate opening at the cytoplasmic (*cis*) and periplasmic (*trans*) face of transmembrane segments 2/8 and 3/7, respectively, to determine if lateral gate opening needs to occur across its full length. Oxidation of introduced cysteine residues that fixed the gate at the *cis* and *trans* sides abolished translocation but allowed for SecA-SecYEG binding and SecA translocation ATPase. While all long space length crosslinkers introduced at the *cis* side of the lateral gate obstructed translocation, a flexible longer spacer length of ~13.3 Å was allowed at the *trans* side suggesting a greater promiscuity for opening at the periplasmic interface. These data suggest that the lateral gate needs to open for its full length to support preprotein translocation.

1. Introduction

In bacteria such as the Gram-negative model bacterium *Escherichia coli*, protein are sorted to specific locations to support life processes. After synthesis on ribosomes in the cytosol, the majority of the protein that function in the periplasm and outer membrane pass the inner membrane through the activity of the Sec translocase [130,285]. Preproteins are targeted to the translocase by the molecular chaperone SecB [147], bind to the molecular motor SecA and then are passed on to the SecYEG protein conducting channel [70]. SecA utilizes cycles of ATP binding and hydrolysis to direct unfolded preproteins through the channel, allowing them to cross the membrane [124,149].

The translocase consists of a heterotrimeric complex termed SecYEG [16] that is conserved among the three domain of life [5]. SecY is the major component of the translocon and harbors 10 transmembrane segments (TMS) organized into N-terminal domain of TMS1-5 and C-terminal domain of TMS6-10 [10]. These domain halves form a clamshell-like structure that encompasses an hourglass shape pore with a hydrophobic constriction ring in the middle, which prevent leakage of ions when the channel is closed [227]. Another element that seals the channel is a plug domain, which is a small helical re-entrance loop on the periplasmic face of the channel.

In the *Thermotoga maritima* SecYEG structure, SecA binding induces changes in the SecY conformation, primarily at the lateral gate which is formed by TM2b, TM3, TM7 and TM8 [175]. The movement of two halves creates a lateral opening to the lipid bilayer perpendicular of the channel axis. Also, the crystal structure of *Geobacillus thermodenitrificans* indicates similar shifts, with tilting of the TM7 helix and the formation of a lipid exposed smaller gap at the periplasmic interface of the lateral gate [177]. The structure of the *Thermus thermophilus* SecYE with an anti-SecY Fab fragment showed a 'pre-open' state of the translocon, providing a hydrophobic crevice at only the cytoplasm face [200]. It has been proposed that an opening between TM2b and TM7 is used for signal sequence to further open the channel, and to act as a passage to release cleaved signal sequences and to insert transmembrane segments into the lipid bilayer [10]. Other resolved structures provided different extends of lateral gate opening, of full length opening from *cis* to *trans* interface [201,286], to a periplasmic crevice [199] – all of which are obtained with different ligand binding partner and translocation states.

The mechanism of lateral gate opening upon translocation is poorly understood. We have previously shown that translocation requires a lateral gate opening by at least 8Å at its membrane central position [88,287]. Molecular dynamics simulations [119–121,288–291] suggest that the lateral gate needs to open throughout its full length from *cis* to *trans* interface. Here we have investigated the opening of the lateral gate at the *cis* interface TMS 2/8 and *trans* interface TM 3/7 using a crosslinking approach. The results demonstrate that the lateral gate needs to open along its full length for SecA-mediated preprotein translocation.

2. Materials and Methods

Materials

Inner membrane vesicles (IMVs) containing overexpressed SecYEG [292], proOmpA [293], SecB [182], SecA [109] and OmpT [88] were purified as described. ProOmpA (245C) were labeled with fluorescein-5-maleimiede (Invitrogen) as described [292] . Sodium tetrathionate (NaTT) was from Sigma-Aldrich and reducing agent 1,4-dithiothreitol (DTT) was from Roche Applied Science. Crosslinking reagent dibromobimane (bBBr) was from Invitrogen, whereas bismaleimidoethane (BMOE), bismaleimidohexane (BMH) and dithiobismaleimidoethane (DTME) were obtained from ThermoFisher Scientific. DNA manipulation enzymes were obtained from Fermentas and other chemicals were from Sigma-Aldrich.

Bacterial strains and plasmid

E. coli strains and plasmids are listed in Table 1. DNA manipulations were performed using *E. coli* DH5α cells. Double cysteine mutants were constructed by first introducing single cysteine residue into a cysteine-less SecY template vector pEK1 according to Stratagene QuickChange® site-directed mutagenesis kit and subsequently using the resulting construct to introduce the second cysteine. The *NcoI-ClaI* SecY fragment containing unique cysteines was then used to substitute the same fragment of SecY in the expression vector pEK20. Proteins were overexpressed in either *E. coli* strain SF100 or NN100. Substitutions were confirmed by sequence analysis.

Table 1 Strains and plasmids used in this study

Strains/plasmids	Relevant characteristics	Source
E. coli DH5α	*supE44, ΔlacU169(Δ80lacZ_M15) hsdR17, recA1, endA1, gyrA96 thi-1, relA1*	[294]
E. coli SF100	*F⁻, ΔlacX74, galE, galK, thi, rpsL, strA 4, ΔphoA*(pvuII), *ΔompT*	[295]
E. coli NN100	SF100, *unc⁻*	[296]
pND9	OmpT	[297]
pMKL18	SecA	[298]
pHKSB366	SecB	[182]
pET36	proOmpA (245C)	[287]
pEK1	Cysteine-less SecY	[213]
pEK20	Cysteine-less SecYEG	[213]
pFE-SecY16	$SecY_{87C-286C}EG$	[88]
pEK20-97C-335C	$SecY_{97C-335C}EG$	This study
pEK20-97C-374C	$SecY_{97C-374C}EG$	This study
pEK20-138C-293C	$SecY_{138C-293C}EG$	This study

Chemical crosslinking and OmpT assay

To oxidize or crosslink cysteine residues within the overexpressed $SecY_{97C\text{-}335C}EG$, $SecY_{97C\text{-}374C}EG$, $SecY_{87C\text{-}286C}EG$ and $SecY_{138C\text{-}293C}EG$ complexes, IMVs were diluted to 2 mg/ml and treated with NaTT (2 mM), bBBr (2 mM), BMOE (0.6 mM), BMH (0.6 mM) or DTME (0.2; 0.05 mM), respectively. Incubation with NaTT and bBBr were carried out for 30 minutes at 37°C, whereas for BMOE, BMH and DTME crosslinking, incubation was for 1 hour at room temperature. For the control, DTT was used at a final concentration of 10 mM. The crosslinking efficiency was analyzed by means of the OmpT assay as described [88] . Typically,10 μg of IMVs were incubated with 5 μg of purified OmpT for 30 minutes at 37°C, and SecY was visualized by means of SDS-PAGE and Coomassie Brilliant Blue R250 staining.

In vitro translocation of proOmpA

In vitro translocation of proOmpA was assayed by accessibility to proteinase K as described [69] employing fluorescein-labeled proOmpA [80]. Translocation reactions were started by adding ATP to the translocation buffer containing SecA, SecB and 10 μg SecYEG IMVs, and incubated at 37°C. Translocation reactions were terminated after 10 minutes on ice by proteinase K treatment, analyzed by SDS-PAGE and visualized with Fujifilm LAS-4000 image analyzer.

Surface Plasmon Resonance

Binding of SecA to SecYEG was monitored in real time using Surface Plasmon Resonance as described [299] using the Biacore 2000. IMVs were diluted to 1 mg/ml and subjected to sucrose cushion centrifugation, collected as a pellet and resuspended in Buffer A containing 50 mM Tris HCl pH 8, 50 mM KCl, 5 mM MgCl2 and 1 mM DTT. The IMVs were passed 13 times through a 100-nm polycarbonate membrane (Avestin, Ottawa, Ontario, Canada) and immobilized on a L1 sensor chip (GE Healthcare Life Sciences). Binding experiments of SecA was performed in buffer B (50 mM Tris-HCl pH 8.0, 150 mM KCl, 5 mM MgCl2, 0.5 mg/ml BSA, and 1 mM ATP) at 25°C. Regeneration of the SecA binding sites was obtained by injection of 100 mM Na_2CO_3, pH 10. Data analysis was done by fitting binding curves from injections of multiple ligand concentrations using BIAevaluation from Biacore AB.

Other techniques

SecA ATPase activity was determined by measuring released free phosphate by means of malachite green assay [69]. Protein concentrations were determined with the Bio-Rad RC DC protein assay kit using bovine serum albumin as standard.

3. Results

Introduction of cysteine in the cis and trans interface of SecYEG lateral gate

The lateral gate of SecY has been suggested to play an important role in the opening of SecYEG channel and to provide an exit path for transmembrane segments of newly synthesized proteins into the lipid bilayer [10]. The lateral gate is formed by TM2b, TM3, TM7 and TM8[175]. Previous studies, employing a crosslinking approach to immobilize the lateral gate at its central position of TM2b and TM7, and these analyses suggest that lateral gate opening is a critical step during SecA-dependent protein translocation [88]. To explore the extent of lateral gate movement during translocation, we introduced unique cysteine pairs in SecY to probe the movement of the lateral gate at the cytoplasmic and periplasmic face. Based on *M. jannaschii* SecYEß crystal structure [10], three residues at the cytoplasmic interface (V97 in TM2, L335 in TM8, T374 in TM 9) and two residues at the periplasmic interface (G138 in TM3, W293 in TM7) were chosen for cysteine substitution in *E. coli* SecY (Fig. 1). The indicated amino acid were step wise replaced by cysteines via site-directed mutagenesis using the cysteine-less SecY template vector, resulting cysteines pair of $SecY_{97C\text{-}335C}EG$, $SecY_{97C\text{-}374C}EG$, and $SecY_{138C\text{-}293C}EG$. Resulted mutants (Table 1) were cloned into expression vector, and expressed in *E. coli* strain SF100 or NN100.

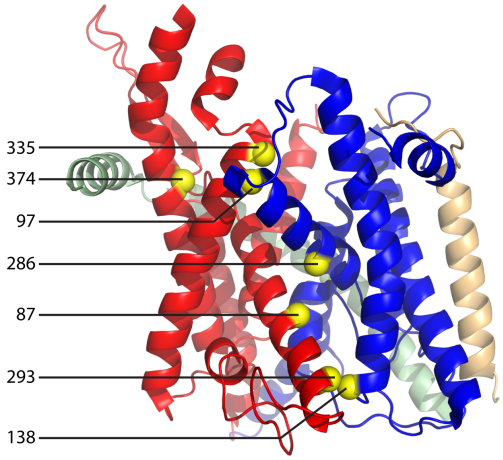

Figure 1. Position of cysteine mutations introduced into the *E. coli* SecY as mapped on the *M. jannaschii* SecYEß structure. Image showing two halves of SecY colored in blue and red, and shown as yellow balls, amino acid 97, 335 and 374 of TM2, TM8 and TM9, respectively at the *cis* side, and 138 and 293 of TM3 and TM7, respectively at *trans* side of the membrane.

Crosslinking the lateral gate at the cis and trans interface

In order to immobilize the lateral gate, IMVs with overexpressed level SecYEG mutants were oxidized with sodium tetrathionate (NaTT). Crosslinks were visualized by means of the OmpT assay [88]. OmpT cleaves at the two arginine residues in the cytoplasmic loop connecting TMS 6 and TMS 7 which results in N- and C-terminal SecY fragment that migrate at 25 and 18 kDa, respectively (Fig. 2). Upon crosslinked, crosslinked SecY protein would migrate as a full length protein on SDS PAGE. OmpT treatment of the double cysteine mutant resulted in appearance of the N- and C-terminal SecY fragments, and a disappearance of full length SecY. When oxidized by NaTT, the majority of the $SecY_{97C\text{-}335C}$ and $SecY_{138C\text{-}293C}$ migrated as a full length protein with high crosslinking efficiencies (>75%) (Fig. 2A). When the oxidized SecY proteins were treated with DTT prior or after OmpT treatment, SecY was cleaved into two fragments. From the SecYEG structure it follows that the cysteine pair located at the *cis* interface of the lateral gate of TM 2/8 and the *trans* interface of TM 3/7 are in close proximity in the closed state, i.e., approximately 3.3 - 3.9 Å and 3.2 – 4.2 Å, respectively [10,286].

Treating of IMVs containing $SecY_{97C\text{-}374C}EG$ with NaTT did not result in crosslinks, and all SecY was cleaved by OmpT (Fig 2C). The distance between these two cysteines is >12Å and separated by TM8, and this likely prevents the formation of a disulfide bridge. However, addition of DTT resulted in the appearance of full length SecY upon OmpT treatment. The amount of full length SecY correlated with the concentration of DTT added after NaTT-treatment. Although unexpected, DTT[300,301] and other reducing agents[302] have been reported to create covalent bonds with the thiols, and acting similarly to bifunctional crosslinkers thus preventing the cleaved SecY to migrate as two separate fragments on SDS-PAGE.

IMVs were also treated with various covalent chemical crosslinkers with different spacer length, namely bBBr (5Å), BMOE (~8Å) and BMH (~13Å). Incubating with bBBr resulted a reduced crosslinking efficiency of ± 60% for $SecY_{97C\text{-}335C}$ and $SecY_{138C\text{-}293C}$. With BMOE and BMH, the efficiency varied between 70-80% (Fig. 2A). As previously mentioned, the distance between the cysteines in the aforementioned SecY mutants would be compatible with chemical crosslinker to form covalent bonds. As for $SecY_{97C\text{-}374C}$, all covalent crosslinkers yielded only low efficiencies (<50%) (Fig. 2D), which is reasonable due its distant position.

We also tested the cleavable chemical crosslinker DTME (~13.3Å) with a disulfide bridge in the center that can be reduced. We use this crosslinker to immobilize the lateral gate at *cis* ($SecY_{97C\text{-}335C}$), *trans* ($SecY_{138C\text{-}293C}$), and mid ($SecY_{87C\text{-}286C}$) positions. This yielded a crosslinking efficiency of about 70%. Treating the DTME-crosslinked species with DTT before the OmpT addition, resulted in complete cleavage of SecY (Fig. 2B). The data suggests that the *cis, trans* and mid

positions of the lateral gate are relatively flexible allowing formation of covalent bonds with different spacer length chemical crosslinkers.

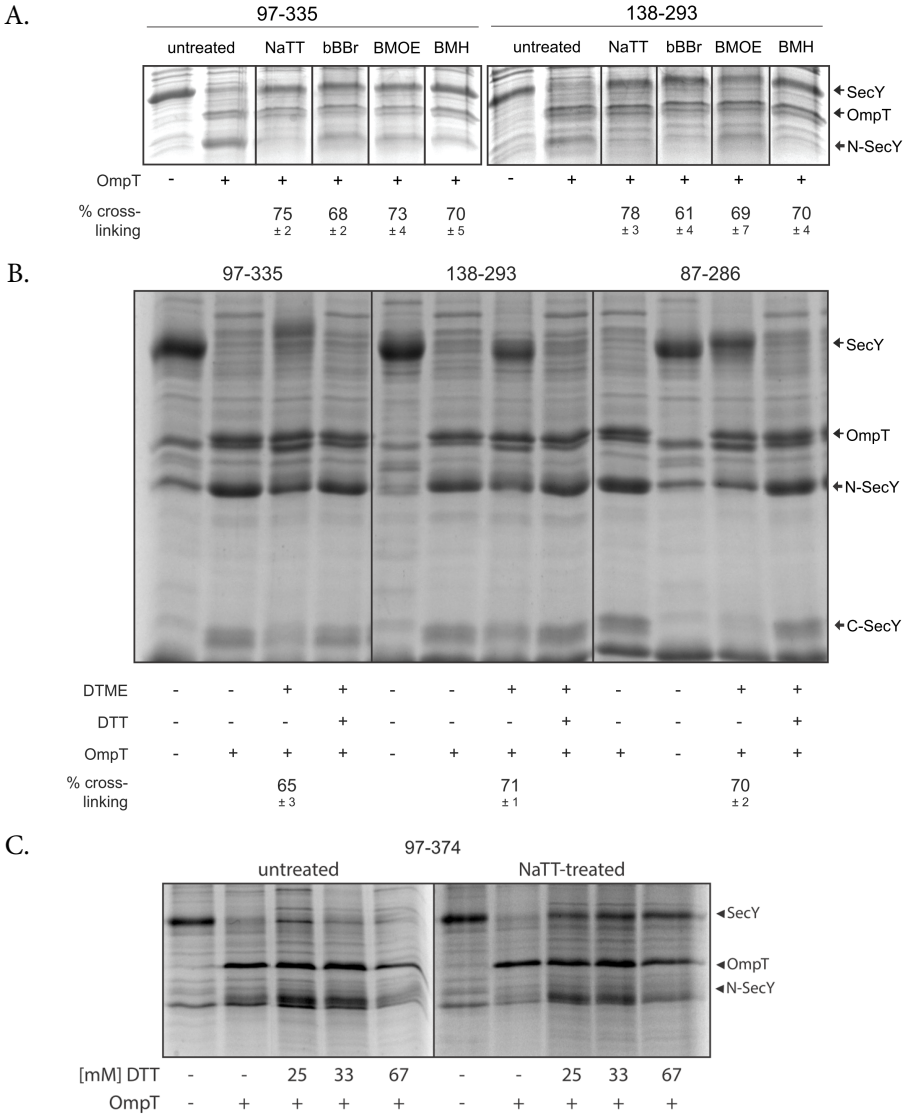

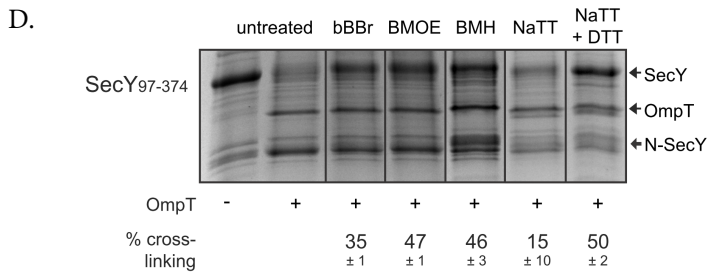

Figure 2. SecY cysteine intra crosslinking efficiency determination using OmpT treatment. (A) IMVs containing the $SecY_{97C\text{-}335C}$ and $SecY_{138C\text{-}293C}$ mutants were treated with NaTT, bBBR, BMOE and BMH and subsequently cleaved with OmpT to assess the crosslinking efficiency which is indicated as percentage of full length SecY remaining relative to the untreated sample. **(B)** IMVs containing $SecY_{97C\text{-}335C}$, $SecY_{138C\text{-}293C}$ and $SecY_{87C\text{-}286C}$ mutants were treated with DTME. DTME was cleaved by the addition of 50 mM DTT resulting N- and C-terminal fragment of SecY. **(C)** $SecY_{97C\text{-}374C}$ cannot be oxidized by NaTT. However, a DTT adduct is formed covalently after NaTT treatment yielding full length SecY upon OmpT treatment. **(D)** IMVs containing the $SecY_{97C\text{-}374C}$ mutants were treated with NaTT, bBBR, BMOE and BMH and subsequently cleaved with OmpT to assess the crosslinking efficiency.

Protein translocation activity of crosslinked SecYEG mutants

To determine the impact of lateral gate immobilization, the activity of translocon was assayed using *in vitro* translocation reactions with fluorescently labeled proOmpA (Fig. 3A). Restricting the movement via oxidation of $SecY_{97C\text{-}335C}$ and $SecY_{138C9\text{-}293C}$ nearly completely inhibited translocation. Whereas for $SecY_{97C\text{-}374C}$, the same level of inhibition occurred after the formation of DTT adduct. Restricting the mobility of the lateral gate at *cis* side of TM 2/8 with bBBR also resulted in a near to complete inhibition, whereas crosslinking with the longer and more flexible BMOE and BMH shows some residual activity. Likewise, restricting the lateral gate at *trans* side of TM 4/7 with bBBr, BMOE and BMH also caused inhibition of translocation activity. Also, treatment of $SecY_{97C\text{-}374C}$ with various crosslinkers resulted in reduced activities showing that immobilization of the lateral gate could be achieved by arresting the movement of the clamshell.

We further tested the DTME-immobilized double cysteine mutants at the *cis*, *trans* and middle of the membrane (Fig. 3B). Restricting the movement of the lateral gate at the *cis* interface greatly reduced translocation, whereas at the middle of the lateral gate, translocation was only partially inhibited. On the other hand, the DTME-restriction on *trans* interface showed full translocation activity. The DTME crosslink was revered by adding DTT. Full activity restoration was observed at the middle position, whereas the activity of the crosslinked *cis* interface was only partially restored.

We also performed SecA ATPase assays using the mutants oxidized with NaTT or treated with various crosslinkers. Compared to cysteine-less mutant, the

introduction of double cysteine mutant at the *cis* ($SecY_{97C\text{-}335C}EG$) and mid ($SecY_{97C\text{-}335C}EG$) positions of the translocon caused a somewhat reduced activity (Fig. 4A); whereas the *trans* ($SecY_{138C\text{-}293C}$) mutant showed similar SecA ATPase activity. Immobilization the *cis* interface at a short distance by NaTT slightly promote ATPase activity, whereas the longer distance crosslinkers bBBr, BMOE and BMH all lowered the activity. Fixing the middle part of the lateral gate had little effect, except for the NaTT-induced oxidation which lowered SecA ATPase activity significantly confirming our earlier report [88]. Formation of a disulfide bridge at the *trans* interface of the translocon did not impact the SecA ATPase activity, while the longer crosslinkers including DTME even increased the activity (Fig 6B). On the other hand, DTME decreased the SecA ATPase activity when conjugated to the cysteines at *cis* interface, similar to BMH. Reversal of the DTME crosslinked gate by addition of DTT only slightly increased ATPase activity for the mutants at the *cis* interface.

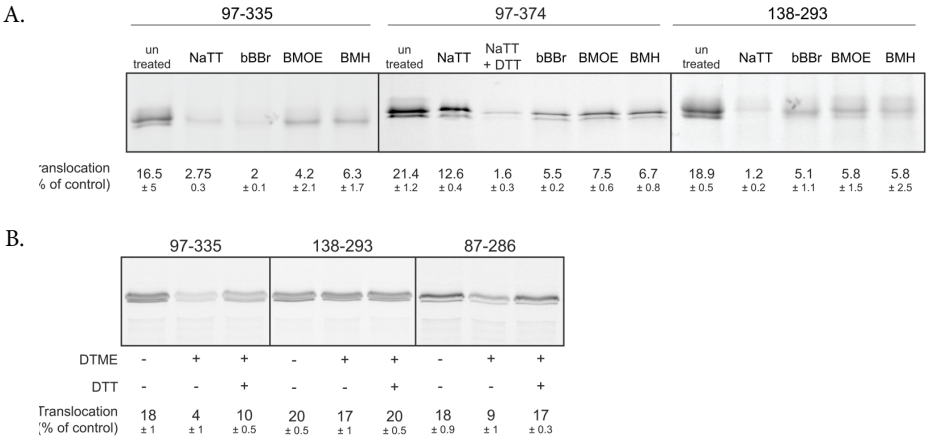

Figure 3. ProOmpA translocation by IMVs oxidized by NaTT and crosslinked with various crosslinker (A) ProOmpA translocation by the indicated SecYEG IMVs oxidized with NaTT, os crosslinked with bBBr, BMOE and BMH. **(B)** ProOmpA translocation by SecYEG IMVs crosslinked with the cleavable crosslinker DTME, with and without treatment of DTT. Quantification of the translocation activity is provided by the numbers under each lane.

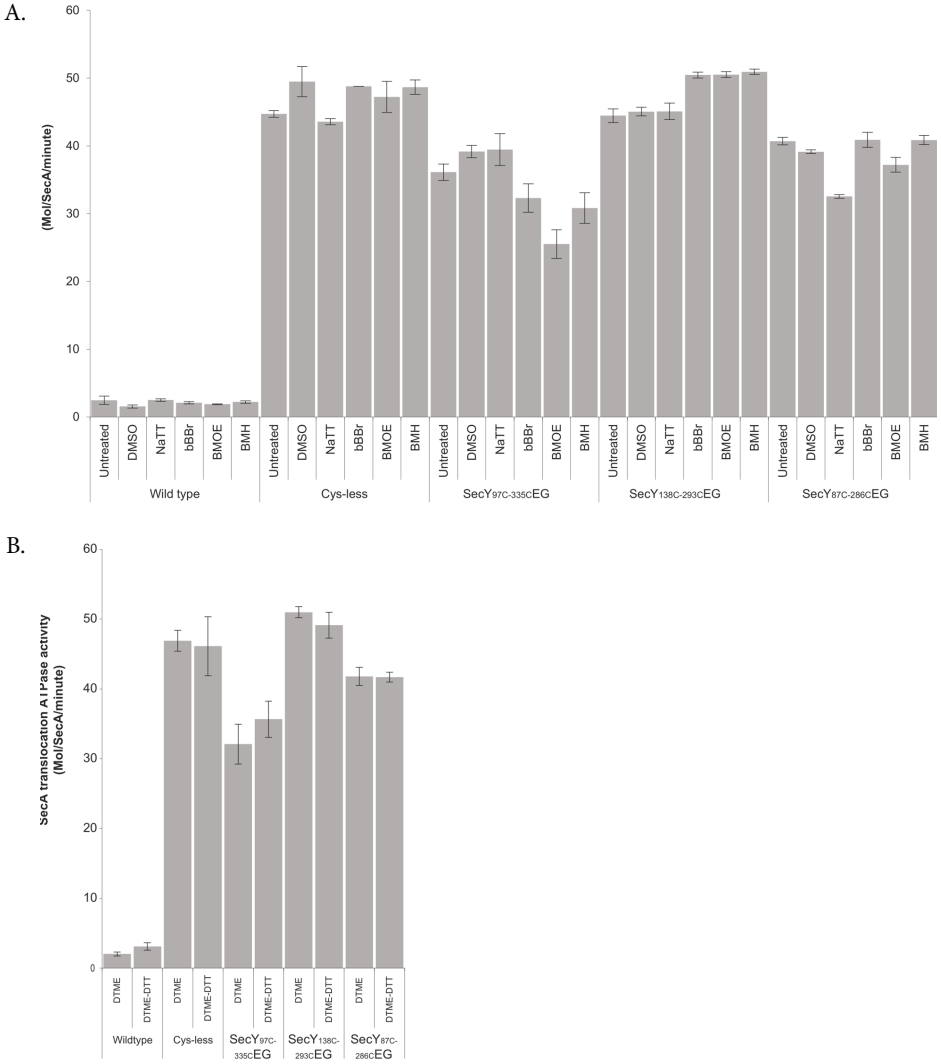

Figure 4. SecA Translocation ATPase activity in the presence of vesicles containing SecYEG treated with different crosslinkers. Values were corrected for ATP hydrolysis in absence of preprotein. **(A)** SecA translocation ATPase activity in the presence of SecYEG overexpression IMVs oxidized with NaTT or treated with bBBr, BMOE and BMH. **(B)** SecA translocation ATPase activity in the presence of SecYEG IMVs treated with the cleavable crosslinker DTME, and DTT. Wild type indicates the SecA ATPase activity supported by the endogenous levels of SecYEG present in the IMVs.

Binding of SecA to SecYEG

The interaction between SecA and SecYEG was studied by Surface Plasmon Resonance. IMVs bearing overexpressed levels of SecYEG were either left untreated or oxidized with NaTT. After removal of the oxidizer, the IMVs were immobilized to the L1 chip for Biacore recordings. Binding of SecA to SecYEG IMVs was followed in time by injecting buffer and subsequently different concentrations of SecA (0.5 - 100 nM). In between the injections with SecA, binding sites were recovered by a carbonate wash. Kinetic data were fitted using a 1:1 binding mass transfer model (Fig. 5). Immobilization of the lateral gate through oxidation of the introduced cysteine residues at the *cis*, mid or *trans* site, barely affected the binding of SecA to SecYEG, with affinity (K_d) constants (Table 2) comparable with those reported previously [80,303,304]. This result indicate that immobilization of the lateral gate does not affect the SecA-SecY binding, indicating that SecA binds with high affinity to the closed state of the SecYEG complex.

A.

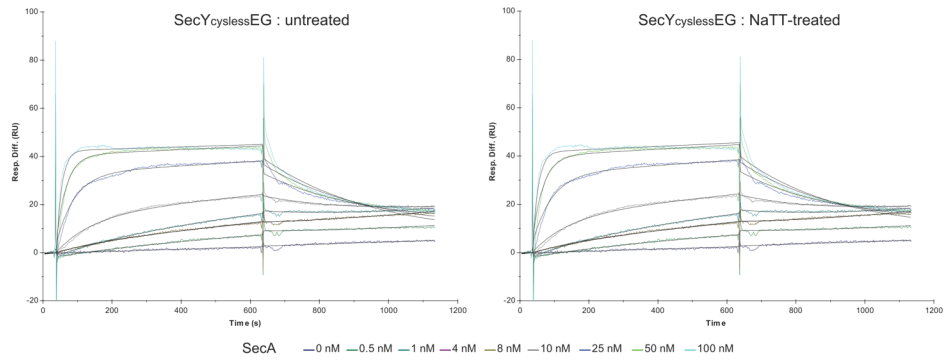

B.

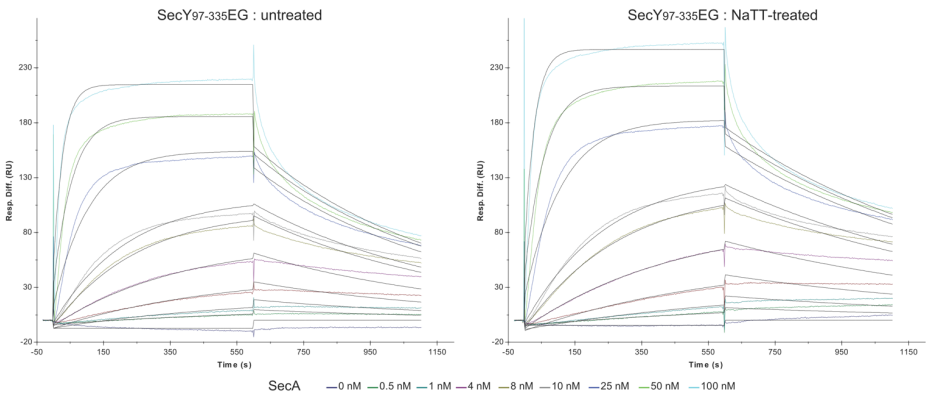

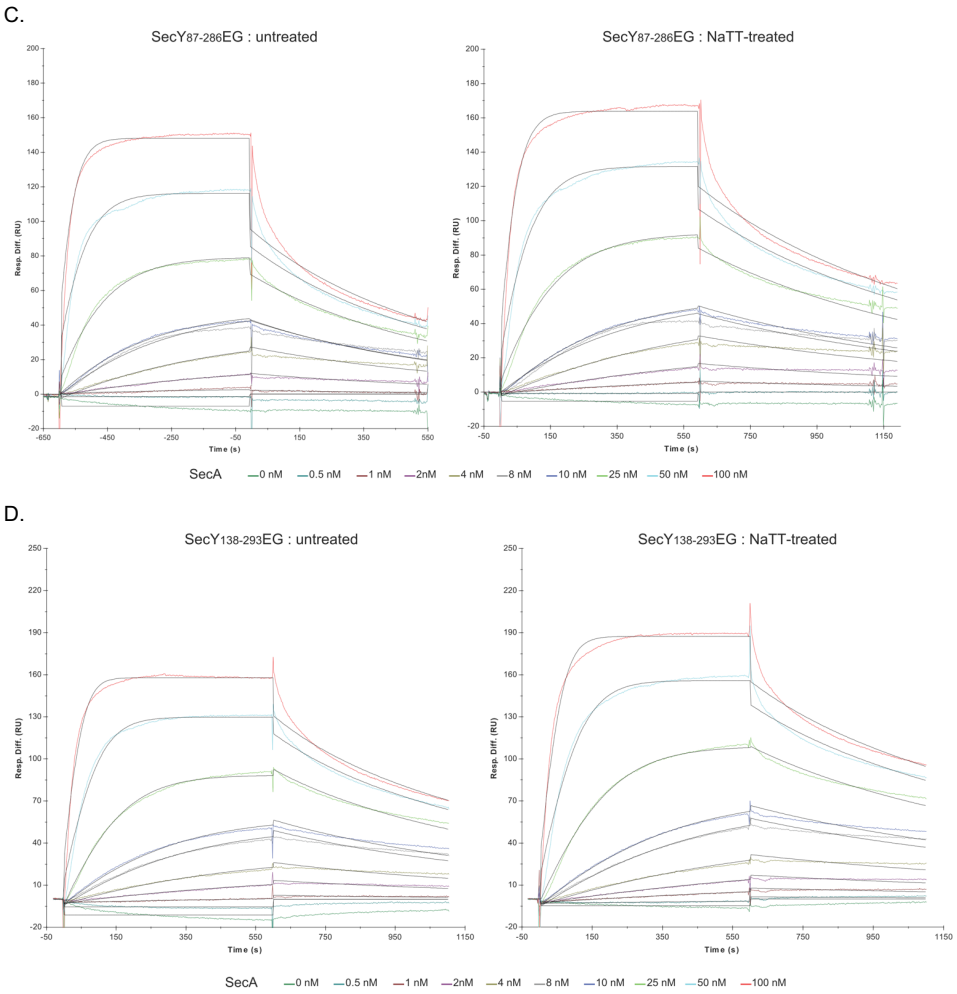

Figure 5. SecA binding to inner membrane vesicles harboring overexpressed levels of SecYEG mutant complex. Simultaneously fitted sensograms of multiple SecA injections to untreated and NaTT-treated mutant SecYEG IMVs immobilized on a Biacore chip. Sensograms were corrected by the response of control channel containing IMVs bearing wild type levels of SecYEG. Binding experiments were performed at a flow rate of 20 µl/min. Fitting binding curves of multiple injections of various ligand concentration was done using BIAevaluation following a simple 1:1 binding model with mass transfer. For simplicity, the multicomponent character of the release curve is not taken into account.

Table 2 Calculated Affinity constants of the SecA-SecYEG interaction

SecYEG mutants	KD (x 10-9 M)	
	Untreated	NaTT-treated
Cys-less	4.5 (± 1.0)	5.3 (± 2.0)
SecY97C-335CEG	4.8 (± 2.5)	3.6 (± 0.6)
SecY87C-286CEG	5.5 (± 0.3)	4.8 (± 0.7)
SecY138C-293CEG	4.0 (± 1.4)	3.6 (± 1.1)

4. Results

Here, we have further investigated the role of the lateral gate of SecY in preprotein translocation across the cytoplasmic membrane. Based on the structure and sequence homology with the *M. jannaschii* SecY [10], we have engineered three pairs of cysteines into the lateral gate of the *E. coli* SecY protein, two set at the cytoplasmic face (cis) and a pair at periplasmic face (trans) of the membrane. Previous structural studies suggest that the lateral gate can be opened to different extents. In the structure of the SecYE of *T. thermophillus* [200] stabilized by a Fab fragment attached to a cytosolic loop, a crack or partial opening of the lateral gate at the cytoplasmic face of the membrane was observed. In the structure of the *P. furiosus* SecYEß bearing a substrate mimic corresponding to a SecY cytosolic loop that entered into the central pore region, an opening of the lateral gate all the way from *cis* to *trans* interface was observed [201]; a similar opening is also seen in the cryo-EM structure of Sec61 with signal peptide traversing the translocon [286], as well as in a recent crystal structure of the *T. maritima* SecA-SecYEG with a fused signal peptide that latches into the lateral gate (REF).

In the *T. maritima* SecA-SecYEG co-structure [175] without the signal peptide, the opening of the lateral gate is not uniform and a larger opening occurred at the periplasmic interface. Likewise, extensive *trans* side opening is observed in a cryo-EM structure of SecYEG reconstituted into nanodisc [104]. These structural data thus suggest a great plasticity of the lateral gate but also indicate that opening is modulated by ligand of translocation most notably the signal peptide and SecA. The crosslinking data of *E. coli* SecYEG presented in this study support this flexibility of the lateral gate, and the notion that it needs to open to its full length to allow preprotein translocation.

Previously, it was reported that a cysteine pair introduced in the middle region of TM2 and TM7 could readily be crosslinked by oxidation [88], and that this blocks translocation. In this study, double cysteines were introduced in TM 2/8 at the position of 97 and 335 as well as TM2/9 at the position of 97-374 corresponding to the *cis* side, and in TM3/7 at position 138 and 292 at the *trans* side of the translocon. With the TM2/9 pair, oxidation of the thiols did not result in crosslinking consistent with the two helices being far apart, but addition of DTT

resulted in crosslinking. The latter is likely due to adduct formation and covalent interaction between DTT and the thiol as reported previously for other enzyme [300,301]. Because of this unexpected behavior, this mutant was not further studied.

For the double cysteine mutants of TM 2/8 at *cis* and TM 3/7 at *trans* interface, our observations confirm that immobilization of the lateral gate by disulfide bonding abolishes the translocation activity. This further supports previous findings that the lateral gate needs to open for its full length to allow translocation [88]. Translocation was, however, also inhibited when different spacer-length chemical crosslinkers of bBBr, BMOE and BMH were introduced to both *cis* and *trans* side of the translocon. This result appears contradictive with previous studies, where crosslinking was no longer disruptive with spacer length beyond 8Å, with the use of BMOE [88]. However, unlike the central position, immobilization of the lateral gate at the *cis* and *trans* interface may provide to much of a structural constraint that propagates to the remainder of the lateral gate. The incorporation of cleavable crosslinker DTME at the *cis* and middle positions of the lateral gate also inhibited translocation but was restored after reduction with DTT in case of the middle position. On the other hand, crosslinking with DTME at the *trans* interface had not impact on translocation suggesting a greater promiscuity of the trans versus the cis positions. The *cis* interface covers the contact site between SecA and SecY [175] and likely needs to be an unobstructed path for the signal sequence to insert into the lateral gate [10]. This may explain why crosslinking at this site is more obstructive than the middle and *trans* regions. Importantly, the crosslinking did not significantly affect the high affinity binding of SecA to SecYEG, which is also in accordance with the SecA translocation ATPase activities. This suggests that SecA initially binds he closed state of the SecYEG channel, but because of the immobilization of the lateral gate by the crosslinking reagents used, this binding event no longer propagates into a conformational change of SecYEG which results in partial opening of the channel.

In conclusion, our data indicate that full lateral gate opening is needed for SecA-dependent protein translocation. Furthermore, the lateral gate appears as a flexible and dynamic entity that needs to undergo different degrees of opening.

5. Acknowledgements

This work was supported by Ministry of National Education of the Republic of Indonesia scholarship to I.T.

Chapter 3

Introduction of a Long Spanning Optical Switch into the SecYEG Lateral Gate

Intan Taufik, Gábor London, Ben L. Feringa and Arnold J.M. Driessen

CHAPTER THREE

Introduction of a Long Spanning Optical Switch into the SecYEG Lateral Gate

Abstract – Opening of the lipid-exposed lateral gate of the SecYEG translocon is an important step in channel opening and SecA-dependent protein translocation. Previous studies have shown that the lateral gate transmembrane segments 2 and 7 are in contact at the middle of the membrane. At that site, the lateral gate needs to open by at least 8 Å for channel activation. At the periplasmic and cytosolic face of the membrane, the lateral gate helices are further apart, and constriction of the gate to distances of 13 Å and less inhibits translocation. Here, we have introduced an optical switch based on bismaleimidoazobenzene that spans a distance of 10 Å (cis) to 19 Å (trans) into the periplasmic region of the lateral gate and examined the effect of switching on protein translocation.

1. Introduction

Cellular processes rely on a set of protein machineries that define the functioning of the cell. Progress in the field of molecular biology, synthetic chemistry and nanotechnology have allowed us to venture into these cellular machineries. Studies on light modulation of biological activities has been conducted for long time. During the late 1960s, azo-based chemistry have been studied in inhibition-photoregulation of chymotrypsin [305], acetylcholinesterase [306,307], acetylcholine receptor [308], and membrane potential modulation [309,310]. These early studies amongst others exploited different affinity of the cis and trans isomeric state of the photoisomerizable compounds to a protein receptor at the membrane. It took more than two decades for the field to directly modify protein by covalent linkage of photoisomerizable component, that is by anchoring photochromic azo groups to papain backbone [311], insecticides [312], photoresponsive drugs [313,314], G-protein potassium channel [315], cell signaling molecules [308,316], biomolecular motors [317,318], and mechanically control nanovalves [319]. The use of light in controlling protein machineries is especially of interest since it does not tamper the biological systems and can be used in a timely and spatially non-invasive manner [320].

The SecYEG complex of *E. coli* functions as a protein conducting pore in the cytoplasmic membrane [130]. After being synthesized at ribosome, secretory proteins (preproteins) designated to be transported across the cytoplasmic membrane are targeted by the molecular chaperone SecB to the SecYEG-bound SecA protein [41,147]. SecA is a molecular motor and uses the energy from ATP hydrolysis to bind and release the secretory protein, and guide it across the SecYEG channel in a stepwise manner [78,124]. SecA induces changes in the SecY channel structure, causing the widening of the pore and simultaneously opens the lateral gate to lipid bilayer perpendicular of the channel axis [175]. The lateral gate is formed by transmembrane segments (TMS) 2b, 3, 7 and 8 [175]. Previous studies have shown that in order for a preprotein to pass the channel, the interface of segments 2 and 7 at the middle of the lateral gate, needs to expand to at least 8 Å [88,287]. Here we further investigated the lateral gate opening mechanism focusing on the spatial constrains at the membrane interface, i.e., at the *cis* side between TMS 2/8, and the *trans* side between TMS 3/7. At those sites, the lateral gate helices are much further apart and constriction by chemical crosslinking results in inactivation of protein translocation [this thesis]. However, although crosslinking the interface at the *trans* side with bismaleimidohexane (BMH - ~13 Å) partially inhibited translocation, the slightly longer dithiobismaleimidoethane (DTME - ~13.3 Å) does not affect translocation. This suggests a critical transition at these longer length scales in the lateral gate at the periplasmic face of the membrane. On the other hand, crosslinking the lateral gate at the cytosolic face of the membrane in all cases resulted in a reduced activity. Likely this region is also critical for a proper positioning of the signal sequence into the lateral gate while it is also actively engaged in SecA binding. Hence, the crosslinking may be more

obstructive. Here we have used an azobenzene-based optical switch spanning a long range to control the opening and closing of the translocon channel.

2. Experimental Procedure

Materials

Inner membrane vesicles (IMVs) containing overexpressed $SecY_{97C-335C}EG$, $SecY_{138C-293C}EG$, proOmpA [293], SecB [182], SecA [109] and OmpT [88] were purified as described. *E. coli* strains and plasmids are listed in Table 1. *E. coli* SF100 were transformed with designated expression vectors and was used for overproduction of different double-cysteine SecYEG mutants complexes. ProOmpA were labeled with fluorescein-5-maleimide (Invitrogen) as described [292]. Dibromoazobenzene (dBAB) and bismaleimidoazobenzene (bMAB) was obtained from Prof. Ben L. Feringa, Synthetic Organic Chemistry, University of Groningen.

Table 3 Strains and plasmids used in this study

Strains / plasmid	Relevant characteristics	Source
E. coli SF100	*F⁻, ΔlacX74, galE, galK, thi, rpsL, strA 4, ΔphoA*(pvuII), *ΔompT*	[295]
pET36	proOmpA (245C)	[182]
pHKSB366	SecB	[182]
pMKL18	SecA	[298]
pND9	OmpT	[321]
pEK20-97C-335C	$SecY_{97C-335C}EG$	This thesis
pEK20-138C-293C	$SecY_{138C-293C}EG$	This thesis

Chemical crosslinking, purification and reconstitution of SecYEG

Crosslinking of SecYEG cysteine mutant was conducted with either IMVs or purified SecYEG in the presence of detergent. Crosslinking in IMVs were conducted by incubating 2 mg/ml of IMVs with either DBAB or BMAB (10 mM stock in DMSO or DMF, 50 mM Tris-HCl pH 7) to a final concentration of 0.1 to 1 mM for 1-2 hours at 37°C. Where stated, mixtures were then subjected to sucrose cushion and the IMVs were resuspended in buffer. Crosslinking efficiency was analyzed by means of OmpT assay as described [88]. Typically, 10 μg of IMVs are incubated with 5 μg of purified OmpT for 30 minutes at 37°C and SecY was visualized by means of SDS-PAGE and Coomassie Brilliant Blue R250 staining.

Crosslinking of solubilized membrane proteins was conducted by incubating 400 μg of IMVs in 50 mM Tris-HCl pH 8.0, 20% (v/v) glycerol, 100 mM NaCl, 2% (w/v) β-D-dodecylmaltoside (DDM) for 30 minutes at 4°C. Non-solubilized materials were removed by tabletop centrifugation at maximum speed for 10

minutes. Solubilized proteins were incubated with 50 µl Ni-NTA agarose beads (Qiagen) for 1 hour. Beads were pelleted and washed four times with 50 mM Tris-HCl pH 8, 20% (v/v) glycerol, 100 mM NaCl, 0.05% DDM, and 10 mM Imidazole; last wash done by substituting Imidazole with 2 mM TCEP and adjusting of buffer pH to 7. Crosslinking were conducted by incubating the beads in 0.2 mM either DBAB or BMAB in the buffer for 2 hours, either in room temperature or in 37°C, followed by pelleting and washing with wash buffer for three times. Prior to crosslinking, chemical crosslinkers were sonicated for 30 minutes at 37°C and rendered to cis or trans isomer by exposing it to UV light (λ_{max}=365nm) using SelectTMXLE-1000 UV Crosslinker (Spectroline Corporation) or visible light using white light box for 10 minutes, as previously described [287]. Crosslinked SecYEG complexes were eluted with similar buffer which substitute TCEP with 400 mM Imidazole. Eluate was analyzed by 15% SDS PAGE. Crosslinking efficiencies were analyzed as previously described [88]

SecYEG was reconstituted by incubating 100 µl of 5 µM purified SecYEG with equal volume of 4 mg/ml acetone/ether washed *E. coli* phospholipids (Avanti) in 0.5 (v/v) Triton X100 for 30 minutes on ice. Biobeads (Biorad) were prepared by washing twice in each solution of methanol, followed by demi water and lastly with buffer A (50 mM Tris HCl pH 8, 50 mM KCl). Liposome/SecYEG mixture were incubated overnight at 4°C with 100 mg of washed biobeads. Proteoliposomes were subsequently separated and collected by ultracentrifugation using TLA 100.4 (Beckman) at 100k rpm. Recovered pellets were resuspended in 100 µl buffer A and analyzed by 15% SDS PAGE.

In vitro translocation of proOmpA

In vitro translocation of proOmpA was assayed by accessibility to proteinase K as described [268] employing fluorescein-labeled proOmpA [322]. Translocation reactions were started by adding ATP to the translocation buffer containing SecA, SecB and 10 µg SecYEG IMVs or proteoliposomes, and incubated at 37°C. Translocation reactions were terminated after 10 minutes on ice by proteinase K treatment, analyzed by SDS-PAGE and visualized with Fujifilm LAS-4000 image analyzer. To induce cis-trans isomerization of the azobenzene unit prior to translocation, IMVs were irradiated with UV light (λ_{max}=365nm) for 1 minutes using SelectTMXLE-1000 UV Crosslinker (Spectroline Corporation) or with visible light using white light box for equal length of time as previously described [287].

3. Results

Crosslinking of the SecYEG lateral gate with DBAB and bMAB

SecY forms a transmembrane channel encompassing an hourglass pore that opens up to the lipid membrane by a lateral gate composed of TM2b, TM3, TM7 and TM8 [175]. Based on the *M. jannaschii* SecYEß structure [10] and a model of the *E.*

coli SecYEG, two pairs of residues, i.e., V97-L335 in TM2b and TM8, and G138-W293 in TM3 and TM7 (Fig. 1), were chosen at the lateral gate region at the interface of *cis* and *trans* side of the membrane, respectively. Each residue in each pair localizes to a different halve of the SecY clamshell structure. V97 and G138 are located in the N-terminal halve, whereas W293 and L335 are located in C-terminal halve. Based on the assumed resting state provided by the crystal structure of SecYEß, the distance between these residues are ~9Å on the *cis* side, and ~4Å on the *trans* side of the membrane. The selected residues were substituted with cysteine via site directed mutagenesis using the cysteine-less SecY as template. Resulted mutants were expressed in *E. coli* SF100 strain, inner membrane vesicles (IMVs) were isolated and when indicated purified and liposome-reconstituted SecYEG was used in this study.

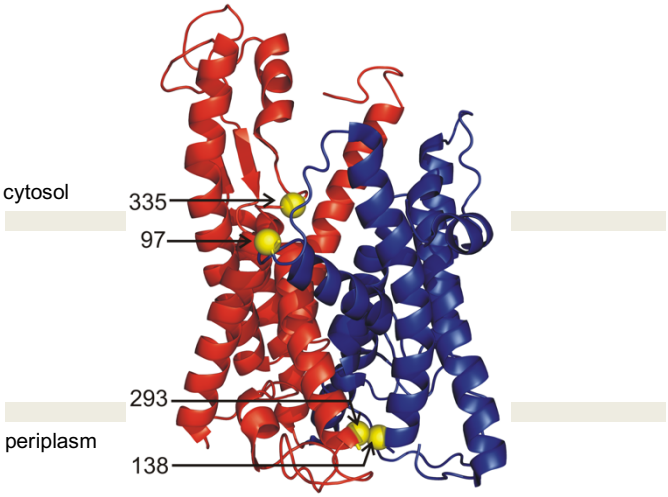

Figure 1. Position of introduced cysteine mutations mapped on *M. jannaschii* SecY structure (1RHZ). Scheme showing the SecY channel composed of two halves of N-terminal in blue and C-terminal in red, with the lateral gate facing forward. The four yellow balls representing the introduced cysteine mutation into SecY, with one pair at the interface of *cis* and one pair at the *trans* of the lipid bilayer. Each pair constitute of a cysteine located on N-terminal halves, and another cysteine on C-terminal halves.

IMVs with overexpressed levels of the double-cysteine SecYEG mutants were treated with the homobifunctional optical switchable crosslinkers Dibromoazobenzene (dBAB) and bismaleimidoazobenzene (bMAB) (Fig. 2). These optical switching molecules can be reversibly converted from their trans to cis isomerization state by means of exposing to UV light or white light, respectively. The azobenzene switch undergoes a structural change which alters its dimensional length approximately from 9.3Å to 13Å for dBAB (~4Å) and from 10Å to 19Å for bMAB (~9Å). To demonstrate successful conjugation to the pair cysteine residues, the previously developed OmpT assay was used [88]. OmpT

protease cleaves two arginine residues in the fourth cytoplasmic loop of SecY connecting TM 6 and TM 7 that would result in specific N- and C-terminal protein fragments at 25 and 18 kDa, respectively.

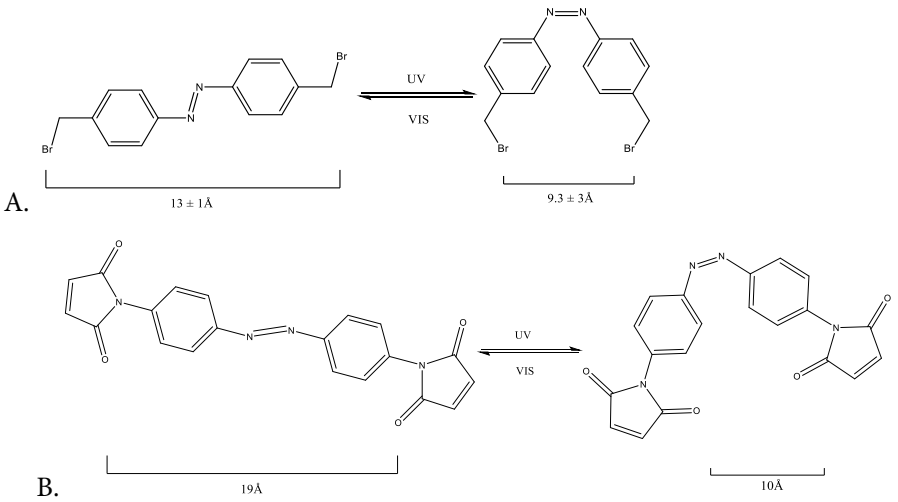

Figure 2. Optical switches dibromoazobenzene (dBAB) and bismaleimidoazobenzene (bMAB). Light dependent isomerization structural scheme of (A) trans isomer of dBAB with stretching to 13±1Å, and upon UV irradiation shortening to 9.2±3Å. (B) bMAB spans a greater distance and alters from its trans state of 19Å to its cis state of 10Å, upon UV irradiation. Irradiation with white light render the molecules back into their trans state.

Crosslinking was attempted in a range of concentrations of the optical switch. By means of OmpT protease which cleaves in between two arginine residues at the fourth cytoplasmic domain (C4), crosslinking efficiencies can be determined by the amount of full length SecY protein remaining upon OmpT treatment as visualized by SDS-PAGE. The OmpT assay indicated that with increasing concentration of the polar aprotic solvent DMSO, less SecY gets cleaved by OmpT (Fig 3A). This is likely due to an inactivation of the OmpT protease.

Increasing concentrations of DMSO are known to progressively destabilize secondary structure and unfold proteins[323], as it strip water from protein surfaces and compete strongly for hydrogen bonding between amino acids[324–326]. Molecular dynamics simulations show that it readily diffuses across the bilayer membrane, expanding the membrane at higher concentration[327]. Although the mechanism of its interference is not clear, it can be assumed that polar aprotic solvents destabilizes the OmpT by collapsing its structure[328]; whereas high concentrations may also disturb the bilayer membrane of the IMVs and the

structure of embedded SecYEG structure rendering the C4 loop inaccessible for OmpT.

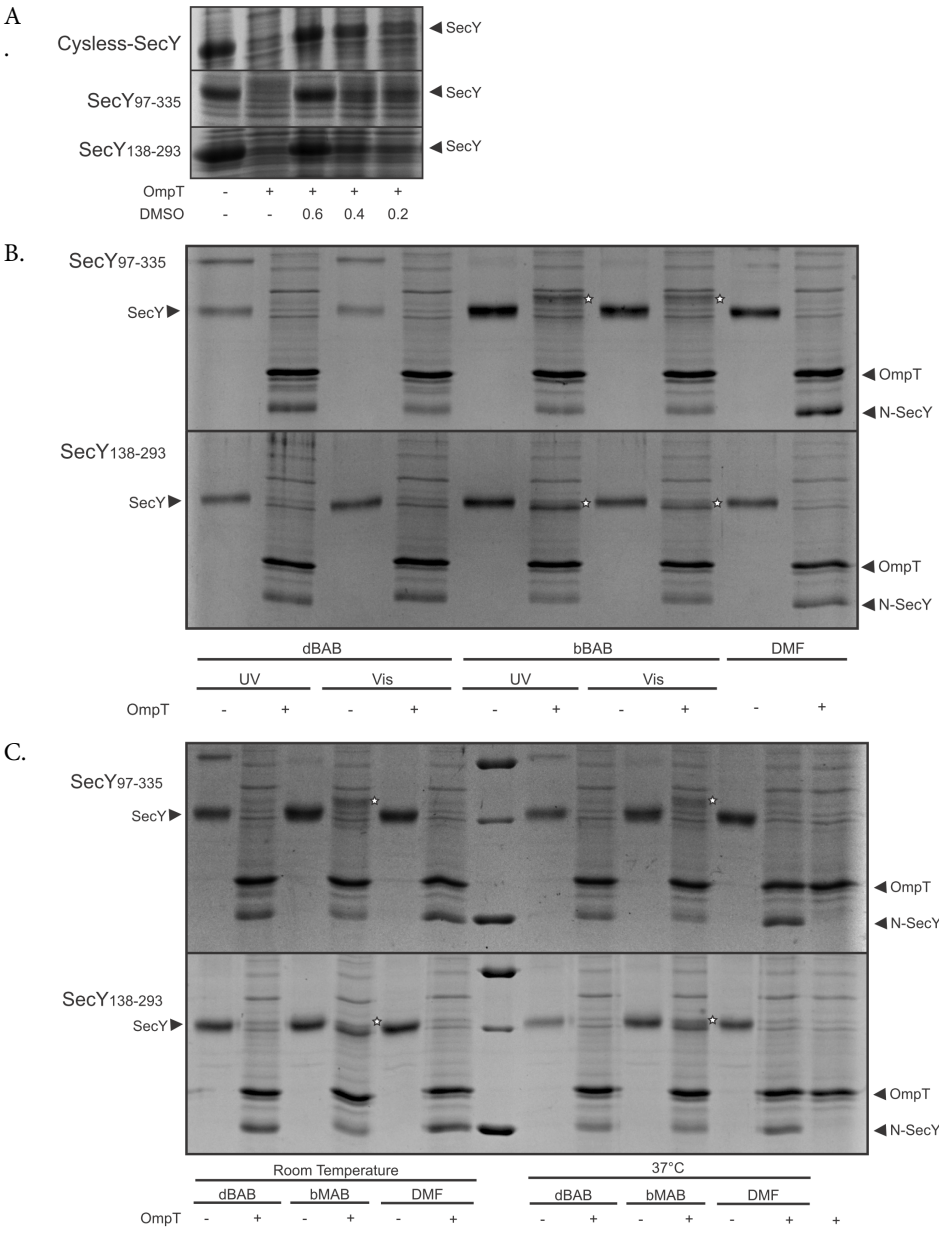

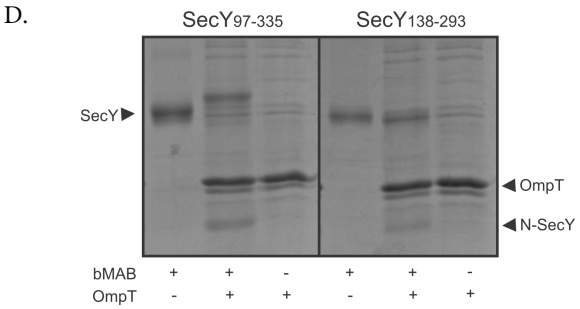

Figure 3. OmpT assay on conjugation reaction of cysteine-pair at different position of SecYEG lateral gate. (A) High concentration on the polar aprotic solvent DMSO impaired the OmpT assay. In the presence of increasing concentration of DMSO, OmpT protease was unable to cleave SecY. **(B)** Proteoliposome containing SecYEG mutants were incubated with the indicated crosslinker of different isomeric state dissolved in DMF, and at **(C)** different temperature. The different isomeric states did not significantly influence the crosslinking efficiency, nor did temperature. **(D)** bMAB crosslinking of $SecY_{138C\text{-}293C}EG$ (± 80%) and $SecY_{97C\text{-}335C}EG$ (<50%). The aberrant upshift in migration of the crosslinked $SecY_{97C\text{-}335C}$ upon OmpT treatment was also observed with other chemical crosslinkers and is likely due to the imposed structural constraint which prevents complete unfolding of the protein in SDS.

To resolve these issues, DMF was used that appeared less inhibitory than DMSO and also provided a better solubility (not shown). Attempts to remove the polar aprotic solvent via sucrose cushion centrifugation resulted in significant loss of sample. Therefore, crosslinking was conducted with the solubilized SecYEG complex bound to Ni-NTA, where polar aprotic solvent was eliminated in the following wash steps. We tested whether the efficiency of cysteine-pair crosslinking with the azobenzene compounds varied for the different isomeric state by pre-irradiating the crosslinker with UV or white light prior to incubation with the Ni-NTA- bound SecYEG complexes. We also tested whether different incubation temperature yielded different crosslinking efficiency. The use of the UV-irradiated shorter isomeric state of both crosslinkers did not show any significant improvement, nor did the different incubation temperatures (Fig. 3B). Although UV-irradiation of crosslinker prior to incubation with the SecYEG complex would render it into cis form, extended reaction times would inherently render the compound to re-isomerize to its stable trans isomer [305,329]. This may explain the lack of a difference in crosslinking efficiency when comparing the two isomeric states. For consistency of treatment, the azobenzene crosslinkers used in their trans isomeric state. The crosslinking is dependent on the type of crosslinker used and the location of the cysteine pair. Crosslinking was more efficient using the longer spanning bMAB compared to dBAB (Fig. 3C) which is unexpected as this bMAB would be expected to be a less efficient match to the distance between the two cysteines of $SecY_{138C\text{-}293C}EG$ than dBAB.

Protein translocation activity of the bMAB-crosslinked SecYEG Mutants

Protein translocation activity was assessed *in vitro* by monitoring the translocation of fluorescent-labeled proOmpA into the proteoliposomes by SDS-PAGE. As shown on Figure 4, the $SecY_{138C\text{-}293C}EG$ crosslinked with bMAB was able to translocate significant amount of substrate across the membrane, while the bMAB-crosslinked $SecY_{97C\text{-}335C}EG$ showed no activity. When the bMAB-crosslinked $SecY_{138C\text{-}293C}EG$ complex was switched from the trans isomeric form (~10Å) to the cis form (~19Å) by irradiation with UV light, no significant change in activity was observed suggesting that the spatial constraint on the lateral gate at interface of *trans* side of the membrane of SecY does not impact lateral gate opening.

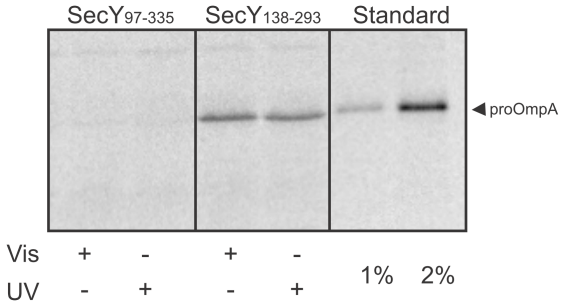

Figure 4. proOmpA translocation by bMAB treated SecYEG. ProOmpA translocation of proteoliposome-reconstituted $SecY_{97C\text{-}335C}EG$ and $SecY_{138C\text{-}293C}EG$ and treated with UV or visible light.

4. Discussion

Previously, the azo-based compound, dibromoazobenzene or dBAB was successfully conjugated to the Sec translocon of *E. coli* [287]. Two cysteine at the mid of the lateral gate of SecYEG were engineered to allow crosslinking by dBAB in order to modulate the channel opening by light and study its plasticity. Due to the geometry of transmembrane helices that constitute the lateral gate, TM2 and TM7 are in contact at the mid of the membrane but separated further away at the *cis* and *trans* side interface of the membrane. At the periplasmic interface, TM7 is in proximity to TM3, whereas TM2 is vicinity of TM8 (Fig. 1). A recent study, observed that the opening of the lateral gate at the membrane-water interface, either at *cis* or *trans* side, are dictated by different structural constrains [this thesis]. We used the homobifunctional crosslinkers BMH and DTME to restrict the opening of the lateral gate at the *cis* and *trans* side of the membrane. Crosslinking the lateral gate at the periplasmic interface with BMH which span ~13Å partially inhibited translocation, while DTME which span ~13.3Å was without effect. On the other hand, crosslinking the lateral gate at *cis* side of the membrane in all cases resulted in a reduced activity suggested a high need for flexibility. We further explored the characteristics and the opening of the lateral

gate at the *cis* and *trans* of SecYEG by utilizing a longer optical switch which switch its isomeric state from ~10Å cis state, to ~19Å trans state. We also included the previously used dBAB which spans a shorter distance. Both azobenzene-based photoisomerizable crosslinkers can be switched from the cis to trans state, and vice versa by means of light or UV-light irradiation. Crosslinking of SecY protein within IMVs and quantification of the crosslinking efficiency using OmpT was hindered by the polar aprotic solvent used to dissolve the azobenzene-based compounds likely because of the solvent's ability to destabilize the membrane [328] caused significant loss of the samples. As an alternative, the crosslinking was performed with the detergent solubilized purified SecYEG complex which was less prone to inactivation.

When comparing the purified $SecY_{97C\text{-}335C}EG$ and $SecY_{138C\text{-}293C}EG$, crosslinking of the later, i.e., which is the lateral gate at *trans* side of the membrane was found to be more efficient. Although crosslinking was conducted in presence of detergent, where presumably induces some structural flexibility, crosslinking of the translocon at the *cis* side of the membrane resulted in complete inactivation irrespective of cis and trans isomeric state of bMAB. Likely, immobilization at the *cis* side of the translocon may interfere with the binding of cytosolic partners, such as SecA, or prevent proper docking of the signal sequence in the lateral gate.

The cysteine pair position at the *trans* side is about ~4Å apart [10]. Remarkably, bMAB was still successfully introduced into the $SecY_{138C\text{-}293C}EG$ mutant. As bMAB spans ~10Å up to ~19Å, the result implies that the lateral gate helices at the trans side are relatively flexible and possibly the structure breaths and thereby accommodates this longer spaced crosslinker. However, the crosslinking did not interfere with activity, and at the same time, the activity was not influenced by optical switching. Thus, the lateral gate opening is not restricted by the long span and flexibility of the crosslinker used. Our previous study utilizing BMH which immobilized the same residues at the *trans* side to ~13Å interfered with translocation but this is likely due to the compound's rigidity as DTME that in length is only slightly longer, i.e., ~13.3Å, did not inhibit translocation. Thus, our results suggest that the lateral gate at the periplasmic side is more promiscuous to such perturbation than the mid or *cis* sections of the lateral gate.

5. Acknowledgments

This work was supported by Ministry of National Education of the Republic of Indonesia scholarship to I.T.

Chapter 4

Monitoring the Activity of Single Translocon

Intan Taufik, Alexej Kedrov, Marten Exterkate and Arnold J.M. Driessen

Journal of Molecular Biology (2013) 425 (22):4145-4153

CHAPTER FOUR

Monitoring the Activity of Single Translocon

Abstract – Recent studies introduced a novel view that the SecYEG translocon functions as a monomer and interacts with the dimeric SecA ATPase, which fuels the preprotein translocation reaction. Here, we used nanodisc-reconstituted SecYEG to characterize the functional properties of single copies of the translocon. Using a method based on intermolecular Förster's resonance energy transfer, we show for the first time that isolated nanodisc-reconstituted SecYEG monomers support preprotein translocation. When several copies of SecYEG were co-reconstituted within a nanodisc, no change in translocation kinetics was observed, suggesting that SecYEG oligomers do not facilitate enhanced translocation. In contrast, nanodisc-reconstituted monomers of the PrlA4 variant of SecYEG showed increased translocation rates. Experiments based on intramolecular Förster's resonance energy transfer within the nanodisc-isolated monomeric SecYEG demonstrated a nucleotide-dependent opening of the channel upon interaction with SecA. In conclusion, the nanodisc-reconstituted SecYEG monomers are functional for preprotein translocation and provide a new prospect for single-molecule analysis of dynamic aspects of protein translocation.

1. Introduction

The molecular mechanism of bacterial protein secretion has been intensively studied since the identification of the *sec* genes three decades ago[27,330]. Multidisciplinary efforts have led to a rigorous characterization of the essential components of the pathway, such as the membrane-embedded protein-conducting channel, or translocon, SecYEG, and the ATPase SecA[131]. Biochemical and biophysical data, together with the recently available molecular structures of individual components and their complexes, imply a functional model of protein translocation in bacteria[130]. In the current view, a single heterotrimer SecYEG forms a narrow pore within the membrane and interacts at its cytoplasmic membrane face with the motor protein SecA. The SecA ATPase directs the unfolded, translocation-competent preprotein into the SecYEG pore and employs the energy of ATP hydrolysis to facilitate preprotein transport. Other components involved in the pathway include a small ATP-independent chaperone SecB that prevents the preprotein from premature folding in the cytoplasm due to competing hydrophobic interactions[107,164], and the integral membrane complex SecD/SecF that is described as a proton-driven "lever" facilitating preprotein transpor[241]. The N-terminal signal sequence of the preprotein targets it to the SecYEG translocon and primes the translocon for transport[147]. During translocation, the signal sequence of the preprotein is removed from the translocating preprotein by the leader peptidase and released to the lipid bilayer.

Although the overall organization of the Sec pathway is generally accepted, several specific issues remain the focus of intense discussion, such as the functional oligomeric state of the SecYEG translocon upon SecA binding and preprotein translocation[331]. A variety of approaches, such as native PAGE, cryo-electron microscopy and crosslinking, have suggested that the translocon undergoes oligomerization, however the vast majority of experiments were performed in a non-physiological detergent environment[332,333]. The significance of SecYEG oligomers was challenged by the first crystal structure of SecYEβ homologue of archaea revealing a transmembrane channel formed within a single translocon protomer[10]. Since the channel was captured in its closed idle state, it was further suggested that the second protomer may be essential for opening the pore for translocation[84]. More recently, two independent functional studies demonstrated that a single SecYEG monomer is required for binding and translocation of the preprotein. Experiments based on *in vitro* fluorescence spectroscopy and *in vivo* chemical crosslinking[110,334] investigated the membrane-embedded translocon during its functional cycle including its association with the SecA ATPase and preprotein. The active translocon appeared largely monomeric and neither SecA binding, nor preprotein transport, led to the formation of oligomeric SecYEG complexes. However, an analysis of the translocation dynamics has not been performed so far, and thus transient SecYEG oligomerization at an intermediate stage of the translocation reaction could not be excluded.

In an alternative approach, analysis of the SecYEG oligomeric state within the lipid membranes was conducted on translocons reconstituted into nanodiscs, small lipid patches of defined size (~10 nm)[335,336]. The dimensions of these nanodiscs allow isolating either single or several copies of the translocon within single nanodiscs, such that their functional properties may be measured in a direct way. It was suggested that only the dimeric form of SecYEG embedded into pure DOPG lipids supports the ATPase activity of SecA[335], but in that study, translocation was not addressed experimentally. Although anionic lipids, such as DOPG, are required for translocon activity and DOPG-formed membranes alone have a strong propensity to stimulate the SecA ATPase activity[170], SecYEG translocation activity requires the presence of both charged and non-bilayer lipids, such as DOPE, within the membrane[337]. Remarkably, when SecYEG was reconstituted into nanodiscs with the physiologically-relevant *E. coli* lipids, no SecA translocation ATPase activity was observed[335] which suggested that technical issues interfered with this analysis.

Here, we aimed to investigate the functional properties of nanodisc-reconstituted SecYEG within a native-like lipid bilayer using a direct translocation assay. Our results demonstrate that monomers of SecYEG conduct preprotein translocation. The rate of translocation is not stimulated further when several SecYEG molecules are reconstituted into the nanodisc, demonstrating that the monomeric state of SecYEG is necessary and sufficient for protein translocation.

2. Detergent-solubilized SecYEG is monomeric

Nanodisc-reconstituted translocon represents an attractive lipid-based system that allows isolation of a single copy of SecYEG and testing it directly for its functional properties. To control the number of SecYEG translocons reconstituted into these nanodiscs, it is important to ensure that the detergent-solubilized SecYEG is in a monodispersed state. Previous reports suggested that the oligomeric state of SecYEG in detergent is dynamic and that the subtle equilibrium between monomers and dimers can be fine-tuned by different physicochemical factors, such as the detergent concentration[332,333]. To characterize the oligomeric state of purified SecYEG prior to reconstitution into nanodiscs, we employed fluorescence correlation spectroscopy/ fluorescence cross-correlation spectroscopy (FCCS) using SecYEG molecules independently labeled with two different fluorophores[338,339]. This high-sensitivity technique analyzes fluorescence fluctuation of spectrally separated fluorophores and their temporal correlation when illuminating those within two aligned laser confocal volumes (Fig. 1A). A positive correlation between fluorescence levels may reflect co-diffusion of fluorescently labeled species, for example, as a result of binding or oligomerization, while independent diffusion results in zero cross-correlation. For the fluorescence experiments we used a SecYEG mutant containing a unique cysteine L148C within a periplasmic loop that connects helices 3 and 4 ($SecY_{C148}EG$)[110].

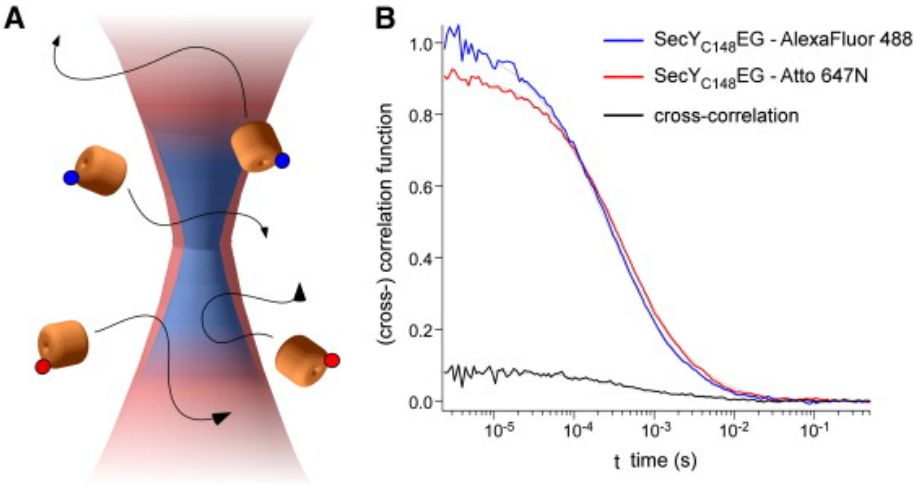

Figure 1. SecYEG is monomeric in detergent. (A) The oligomeric state of DDM-solubilized and fluorescently-labeled SecY$_{C148}$EG was analyzed by means of fluorescence cross-correlation spectroscopy (FCCS). AlexaFluor 488- and Atto 647N-labeled translocons diffuse through the aligned laser excitation volumes, and corresponding fluorescence fluctuations are cross-correlated if SecYEG form dual-labeled oligomers[339]. **(B)** FCS/FCCS analysis on SecY$_{C148}$EG diffusion in detergent. Temporal auto-correlation in fluorescence in individual blue (505-570 nm) and red (640-700 nm) channels reported on the translocon diffusion speed, and the cross-correlation between these channels indicated the fluorophore coupling, thus described SecYEG oligomerization. FCS analysis provided a diffusion coefficient for SecYEG of 28.3±1.6 cm^2/s (mean ± S.D., n = 10) as determined in the blue channel, in good agreement with previous measurements[90]. The cross-correlation level was within 10% of both auto-correlation traces that matched closely the unspecific labeling of SecYEG. The fluorophores AlexaFluor 488-C$_5$-maleimide and Atto 647N-maleimide were purchased from Life Technologies/Molecular Probes and Atto-Tech, respectively. FC(C)S data was recorded using LSM 710 inverted confocal microscope equipped with a Confocor 3 unit (Carl Zeiss GmbH, Germany). Data were fitted within 20 µs to 500 ms range assuming normal three-dimensional diffusion of molecules (shown in thin black lines) using ZET 2010 software (Carl Zeiss GmbH, Germany). SecYEG was present at 100 nM total concentration in 0.1% DDM, 100 mM KCl, 10% glycerol, and 50 mM KPi pH 7.4.

E. coli membranes containing over-expressed SecY$_{C148}$EG translocons were incubated in the presence of two maleimide-containing fluorophores, AlexaFluor 488 and Atto 647N, simultaneously; thus, the individual protomers of SecYEG could be stochastically labeled with the fluorophores[339]. Fluorophore-conjugated SecY$_{C148}$EG was purified, and analysis of the labeling revealed an ≈55% labeling efficiency for both fluorophores, suggesting complete labeling of the single cysteine positions but also limited unspecific labeling[110]. Next, FCCS was used to determine the amount of oligomeric complexes that bear both fluorophores. Due to stochastical labeling and fluorophore distribution, the value could be also used

to estimate the amount of equally labeled oligomers. When conducted in a solution containing 0.1% n-dodecyl β-D-maltoside (DDM) FCCS experiments showed that the cross-correlation signal was within 10% of both auto-correlation traces (Fig. 1B). As the value matched closely the total level of the unspecific labeling, the signal was largely related to single SecYEG protomers bearing both fluorophores. Thus, we concluded that the detergent-solubilized SecYEG translocon was present almost exclusively as monomers.

3. Nanodisc-isolated SecYEG monomers support translocation

To investigate the role of the SecYEG oligomeric state in the translocation cycle, we reconstituted SecYEG into nanodiscs constricted by the MSP1E3D1 scaffold protein (MSP)[340]. To achieve the monomeric state of SecYEG within these nanodiscs (SecYEG^{mono}-Nd), we reconstituted the translocon in presence of an excess amount of MSP (10-fold) and lipids (500-fold) following established protocols[90,340]. We used lipid bilayers composed of a mixture of DOPE, DOPG and DOPC that efficiently support efficient SecYEG translocation activity[110]. The formed nanodiscs were fractionated by size-exclusion chromatography (SEC) and their assembly was verified by SDS-PAGE and negative stain electron microscopy (Fig. 2A and B). The monomeric state of SecY_{C148}EG labeled with two fluorophores and reconstituted into nanodiscs was confirmed by FCCS, as the cross-correlation signal remained below 10% in the peak SEC fractions (Fig. 2C). When the amount of SecYEG in the reconstitution reaction was increased, multiple copies of the translocon could be reconstituted into single nanodiscs that resulted in high cross-correlation signal (Fig. 2D; see below).

To characterize the interaction of the nanodisc-isolated translocon with the SecA motor protein we analyzed its stimulatory effect on the SecA ATPase hydrolysis activity. SecYEG^{mono}-Nd stimulated the SecA translocation ATPase in a conventional ATPase assay in presence of the preprotein proOmpA[69], while the ATP hydrolysis remained at background levels when assayed in presence of nanodiscs loaded with pure lipids (Fig. 3A). Thus, a single membrane-embedded copy of SecYEG was sufficient to interact with the cytosolic motor protein SecA and stimulate its ATPase activity in a preprotein-dependent manner[65,110].

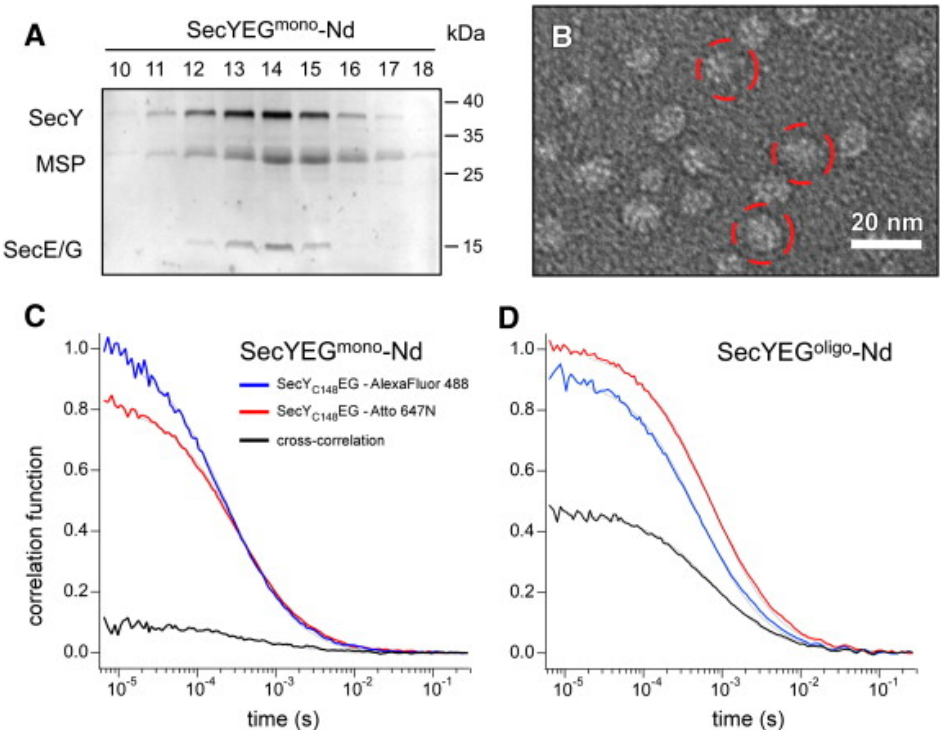

Figure 2. Preparation of SecYEG-containing nanodiscs. (A) Detergent-solubilized $SecY_{C148}EG$ was reconstituted into the lipid bilayer consisting of DOPG, DOPE, and DOPC at 1:1:1 molar ratio in the presence of the major scaffold protein MSP1E3D1 (MSP) resulting in nanodiscs formation. Reconstituted molecular complexes were subjected to SEC[90], with a maximum elution near fraction #14. Coomassie-stained SDS-PAGE shows content proteins (indicated on the left). Positions for molecular weight markers (PageRuler Prestained Protein Ladder, Thermo Scientific) are shown on the right. **(B)** Individual nanodiscs (encircled in red) as visualized by uranil acetate negative-stain electron microscopy. **(C and D)** FCCS analysis of the SecYEG oligomeric state within nanodiscs. Using an excess of MSP and lipids relative to SecYEG during the reconstitution (molar ratio SecYEG:MSP:lipids of 1:10:500) allowed trapping single copies of the translocon within nanodiscs, as confirmed by low cross-correlation level, probably arising from dual-labeled SecYEG protomers (see Fig. 1B). If SecYEG and MSP were used at stoichiometric amounts upon the reconstitution (molar ratio SecYEG:MSP:lipids of 10:10:500), nanodiscs largely contained multiple copies of SecYEG that resulted in a high cross-correlation level[339] (D). The fraction of "oligomers" was estimated around 80%. The same color coding for FCS/FCCS data was used for panels C and D, that is described in the panel C. SecYEG-Nd were present in 100 mM KCl, 5% glycerol, and 50 mM Tris-HCl pH 7.5. FCS/FCCS data were fitted within 20 μs to 500 ms range assuming normal three-dimensional diffusion of molecules (shown in thin black lines). Deviations from the diffusion model at time range 5-10 ms probably arise from large particles, such as occasionally formed proteoliposomes.

Figure 3. SecYEG is functional as a monomer. (A) Single and multiple copies of SecYEG support ATPase activity of SecA. Functional interactions of SecA with nanodisc-reconstituted SecYEG were assayed in presence of the preprotein proOmpA[322]. Either form of the translocon, but not empty nanodiscs, supported the ATPase activity of SecA in the translocation reaction. **(B)** Translocation activity of SecYEG-Nd probed in real-time FRET-based assay[110]. FRET-pair fluorophores Cy3 (Pierce) and Atto 647N were conjugated to preprotein fusion proOmpA$_{C282}$-DhfR and SecY$_{C148}$, respectively, at indicated positions. DhfR domain was pre-folded in presence of ligands MTX and NADPH and so could not be translocated via the SecYEG pore[341]. Formation of the stable translocation intermediate was followed as a change in FRET signal. **(C)** SecYEG monomers and dimers are active in translocation. Either form of the translocon could associate with the preprotein and translocate the unfolded proOmpA domain upon adding ATP giving rise to FRET-based acceptor fluorescence. The translocation rates estimated from single-exponential fitting (solid black lines) were within 20% for SecYEG monomers and oligomers. No translocation was observed in presence of AMP-PNP. For the reaction 100 nM of nanodisc-embedded SecY$_{C148}$EG-Atto 647N was incubated at 37°C

with 200 nM pre-folded proOmpA$_{C282}$-DhfR-Cy3 and 1.8 µM SecA as described before[110]. Reactions were initiated by adding 5 mM ATP or AMP-PNP. **(D)** Translocation rate depends on the structural features of SecYEG. The translocation-enhanced mutant SecYEG PrlA4 reconstituted into nanodiscs as monomers demonstrated faster kinetics and higher total translocation efficiency than wild-type SecYEG that agreed with previous data[342]. Cysteine at the solvent-exposed position 148 was introduced into wild-type and PrlA SecYEG over-expression plasmids pET2302 and pET2306, respectively[342], yielding plasmids pET2302c and pET2306c. Expression, purification and fluorescent labeling were performed according to the established protocol[110]. FRET assay was performed using SLM2 spectrofluorometer (Aminco Bowmann), as previously described[110].

The translocation activity of SecYEG was assessed in real-time using a recently developed fluorescence-based assay[110]. The assay employs Förster's resonance energy transfer (FRET) between fluorophores conjugated to the substrate preprotein and the translocon that occurs upon the formation of a translocation intermediate (Fig. 3B)[110]. Briefly, membrane-reconstituted SecYEG is incubated at 37°C in presence of the SecA ATPase, the chaperone SecB and the preprotein proOmpA fused to a folded domain of dihydrofolate reductase (DhfR). Upon addition of ATP, the proOmpA-DhfR substrate is partially translocated until the globular DhfR domain blocks further transport and traps it within the SecYEG pore, thus forming a stable translocation intermediate[341]. Upon formation of the translocation intermediate, the fluorescence donor (i.e., Cy3) within the translocated proOmpA domain comes into close proximity to the acceptor fluorophore (i.e., Atto 647N or Cy5) conjugated at the periplasmic side of SecY, and thus FRET between the fluorophores occurs (Fig. 3B). As the donor fluorophore is conjugated at the C-terminal end of proOmpA at position 282, the measured FRET signal implies that a large part of the preprotein has been translocated. Formation of SecYEG:preprotein translocation intermediate complexes is monitored in time as an increased emission of the acceptor fluorophore and the validity of this assay was previously established with membrane-embedded SecYEG[110]. Here, the FRET-based assay was conducted with SecY_{C148}EG^{mono}-Nd in the presence of an excess of SecA and proOmpA-DhfR to analyze whether the SecYEG monomer is able to translocate preproteins. Upon addition of ATP we observed an increase in fluorescence of the translocon-conjugated acceptor dye Atto 647N (Fig. 3C). The effect was ATP-dependent, as the non-hydrolysable ATP analogue AMP-PNP did not cause an increase in the dye emission. Taken together, since the nanodiscs support the SecA translocation ATPase activity and preprotein translocation, these results strongly imply that a single SecYEG copy is sufficient to form a functional translocon. Importantly, as SecYEG monomers are isolated within individual nanodiscs, this assay excludes the possibility that transient oligomerization of SecYEG is required for the activity.

To further validate that the observed translocation represents an authentic activity of the membrane-reconstituted translocon, we employed a mutant of SecYEG that displays the *prlA* phenotype. The point mutation N408I within the transmembrane domain 10 of the SecY subunit resulted in a relaxation of the central constriction pore and favors a tight association with the SecA motor protein[342]. Due to these properties, the SecYEG *prlA4* mutant displays enhanced preprotein translocation rates and is capable of translocating preproteins with a defective signal sequence, or even lacking one[343]. The additional mutation F286Y at the periplasmic side of helix 7 serves to stabilize the translocon structure[342]. To analyze the effect of the *prlA4*-mutations on the translocation kinetics in nanodiscs, we introduced a solvent-exposed cysteine residue at position 148 into the wild-type SecYEG ($SecY_{WT}EG$) and its PrlA4 derivate ($SecY_{PrlA4}EG$). Both translocon variants were purified, labeled with Atto 647N-maleimide fluorophore, and reconstituted into nanodiscs as monomers. Translocation was assayed as described above using the FRET-based assay. Indeed, the $SecY_{PrlA4}EG$-Nd translocon showed an enhanced activity in comparison to the wild-type variant, as stable translocation intermediates were formed much faster upon the addition of ATP (Fig. 3D). Also, the maximum FRET signal approached a significantly higher level for the PrlA4 translocon suggesting more efficient formation of the translocation intermediate. Previously, we have shown that the PrlA4 mutant also exhibits a lower level of preprotein rejection at the initiation stage, allowing it to achieve a higher translocation yield as compared to the wild-type[304]. Therefore, we conclude that the elevated FRET level observed in $SecY_{PrlA4}EG$-Nd is due to the more efficient formation of translocation intermediates, while the fast kinetics arise from a tighter interaction with the SecA ATPase.

4. Multiple SecYEG copies do not affect the translocation rate

Previous reports suggested that oligomeric species of SecYEG are required for the translocation reaction by either ensuring docking of the SecA ATPase[344] or facilitating the internal dynamics of the translocon, such as displacement of the central plug domain[84]. Our experiments on $SecYEG^{mono}$-Nd demonstrate that a single translocon is sufficient for translocation, but a beneficial effect of the oligomerization on the translocation kinetics cannot be ruled out. To investigate the role of the SecYEG oligomeric state in translocation we prepared nanodiscs containing multiple copies of SecYEG ($SecYEG^{oligo}$-Nd). For this purpose we increased the amount of SecYEG 10-fold upon the nanodisc reconstitution, reaching the SecYEG:nanodisc ratio of 2:1. The formed nanodiscs contained single and multiple copies of SecYEG[335], and their respective fractions were determined by the Poisson distribution[339]. The presence of multiple SecYEG complexes within nanodiscs was confirmed by FCCS (Fig. 2D) showing high levels of fluorescence cross-correlation when the dual-labeled SecYEG complexes were reconstituted at high density into the nanodiscs. From the cross-correlation

value it appeared that about 50% of nanodiscs contained differently labeled $SecY_{C148}EG$, and the same amount of nanodiscs likely contained equally labeled translocons, which could not be detected by FCCS. Thus, the total number of SecYEG oligomers was estimated at 80-90%. Since both orientations of SecYEG within the lipid bilayer were possible, only co-oriented protomers within a disc might be able to form a dimer. Assuming stochastic orientation of protomers upon reconstitution, dimers could be formed in 50% of nanodiscs containing two copies of SecYEG, and the fraction increased for higher number of copies. Thus, more than 50% of formed nanodiscs contained dimers of SecYEG.

The functional properties of $SecYEG^{oligo}$-Nd were analyzed as described above and compared to $SecYEG^{mono}$-Nd, keeping equal concentrations of SecYEG in both samples. Multiple co-reconstituted copies of SecYEG within the $SecYEG^{oligo}$-Nd sample stimulated the SecA translocation ATPase activity at the same level as the monomeric SecYEG (Fig. 3A). Thus, multiple translocons did not favor the functional interactions with the SecA ATPase. When the translocation activity of $SecYEG^{oligo}$-Nd was analyzed in the FRET assay, the real-time recording of translocation matched closely the data obtained for the $SecYEG^{mono}$-Nd (Fig. 3C). The apparent translocation rates estimated from a single-exponential fit matched within 20%, implying that multiple copies of SecYEG did not manifest faster intermediate formation, demonstrating that there is no catalytic advance in translocation upon SecYEG oligomerization.

5. Structural dynamics of isolated SecYEG

Next, we aimed to examine the conformational change of single SecYEG complexes upon translocation intermediate formation in particular focusing on the opening of the "lateral gate" formed by transmembrane domains 2 and 8 of SecY[88]. Using a library of single-cysteine $SecYEG^{110}$ we observed that cysteine residue at position 313 was accessible for the Atto 647N-maleimide dye, but could barely be labeled with Cy3-maleimide, while both dyes efficiently conjugated to cysteine at position 148 (Fig. S1A). Thus, a double-cysteine mutant of SecYEG was designed, which harbors cysteines in positions 148 and 313 at periplasmic loops 3-4 and 7-8, respectively, i.e. at opposite sides of the lateral gate. The liposome-reconstituted SecYEG variant supported translocation and was able to form a translocation intermediate with fluorescein-labeled $proOmpA_{C282}$-DhfR (Fig. S1B). The translocon was dual-labeled by incubating it step-wise with the Cy3 and Atto 647N maleimide derivates. The procedure allowed specific conjugation of fluorophores at the pre-defined positions, i.e. Cy3 at cysteine 148 and Atto 647N at cysteine 313 (Fig. 4A and Fig. S1A). We achieved similar labeling efficiencies of approximately 80% for each fluorophore with unspecific labeling at levels well within 10% as assessed with the cysteine-less SecYEG variant. Limited proteolysis by the outer membrane protease OmpT was employed to verify the specific labeling of SecYEG[88]. Cleaving $SecY_{C148,C313}EG$-Cy3-Atto 647N within the loop between helices 6-7 by the OmpT protease

resulted in two defined fragments. The Cy3 dye was almost exclusively found at the N-terminal fragment of SecY, while the majority of Atto 647N was conjugated to the C-terminal fragment (Fig. S1C).

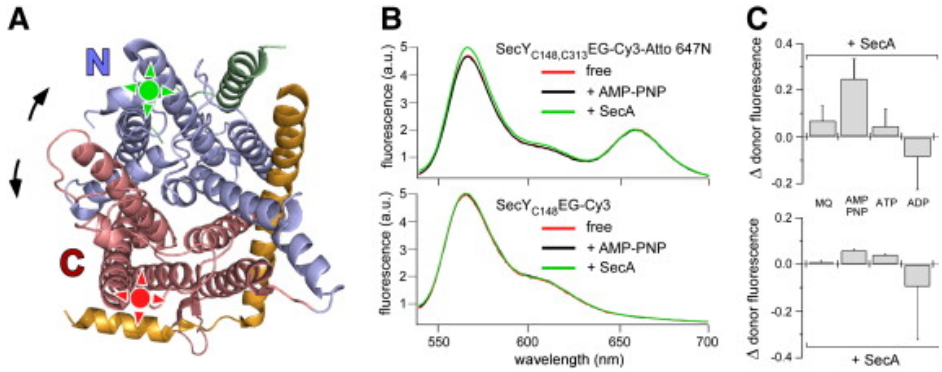

Figure 4. Conformational dynamics of SecYEG. (A) Site-specific labeling of SecY N-terminal and C-terminal fragments with Cy3 (green star) and Atto 647N (red star) fluorophores, respectively, allowed the monitoring of dynamics of lateral gate opening (indicated with the arrows) of the nanodisc-isolated translocon. **(B)** Binding of SecA to dual-labeled SecY$_{C148,C313}$EG caused pre-opened state of the translocon that was characterized by enhanced donor fluorescence due to separation of N- and C-terminal fragments of SecYEG and opening the gate (panel above). No change in fluorescence of SecY$_{C148}$EG-conjugated Cy3 was observed in absence of the acceptor dye (panel below). Fluorescence emission spectra were recorded using SLM2 spectrofluorometer. Reaction was carried out at 25°C using 100 nM nanodisc-embedded SecYEG, 500 nM SecA, 200 nM pre-folded proOmpA-DhfR and 2 mM AMP-PNP. The donor fluorophore Cy3 was excited at 520 nm. **(C)** SecA binding alters SecYEG conformation. Changes in the FRET donor fluorescence reflected dynamics of the translocon. The conformational change of SecY$_{C148,C313}$EG was only triggered by SecA complexed with AMP-PNP that stably mimics the ATP-bound state of the ATPase (panel above). Other nucleotides barely affected the donor fluorescence. No nucleotide-specific changes in donor fluorescence were observed for single-labeled SecY$_{C148}$EG-Cy3 (panel below). For sensitivity considerations, change in FRET was measured as a change in the donor (Cy3) fluorescence. Reaction was carried out at 25°C using 100 nM nanodisc-embedded SecYEG, 500 nM SecA, 200 nM pre-folded proOmpA-DhfR and 2 mM of respective nucleotide. The conformational changes occurred independently of the presence of a preprotein (proOmpA-DhfR; Fig. S2). Fluorescence spectra were recorded before adding nucleotide and after 5 min incubation of the reaction. Spectra were recorded 3 times, and independent triplicate measurements were performed to estimate standard deviations. Prolonged incubation of nanodiscs in the presence of ADP caused decrease in the overall SecYEG fluorescence after 20 min. Partial protein aggregation at these conditions might be a potential reason that would also explain variations between individual recordings and associated high standard deviations (Fig. 4C).

Next, the dual-labeled $SecY_{C148,C313}EG$-Cy3-Atto 647N was reconstituted into nanodiscs constricted by MSP1E3D1 to obtain the monomeric state of the translocon. When the dual-labeled $SecY_{C148,C313}EG$ was excited at 520 nm, emission from both Cy3 and Atto 647N fluorophores was observed demonstrating FRET between these dyes, as no direct excitation of the acceptor fluorophore Atto 647N alone was detected at 520 nm (Fig. S1d). As the fluorescent FRET-pair dyes are situated within the same $SecY_{C148,C313}EG$ molecule at opposite sides of the lateral gate, conformational changes within the translocon, such as lateral gate opening can be monitored via intramolecular FRET. The nanodisc-reconstituted system allows the background from protein:protein interactions and associated intermolecular FRET to be excluded, even at low lipid:protein ratios. We analyzed different conformational states of nanodisc-reconstituted $SecY_{C148,C313}EG$-Cy3-Atto 647N by monitoring changes in the fluorescence emission spectrum that contained characteristic peaks for the FRET donor and acceptor. In the presence of proOmpA-DhfR and SecA the translocon should be primed for preprotein transport that is assumed to pre-open the lateral gate[175,201]. When using AMP-PNP to stabilize the complex, we reproducibly observed a significant increase in donor fluorescence indicating separation of two dyes, as expected for the opening of the lateral gate (Fig. 4B, C). Control experiments with $SecY_{C148}EG$-Cy3 complexes labeled with the donor fluorophore alone revealed no change in donor fluorescence under the conditions that resulted in the altered FRET. The change in FRET for the dual-labeled SecYEG was nucleotide-specific and SecA-specific (Fig. 4C) but preprotein-independent (Fig. S2). As the structure of AMP-PNP is almost identical with that of ATP, the formed complex may mimic a naturally occurring state when ATP-bound SecA primes the translocon. As AMP-PNP cannot be hydrolyzed by SecA, this conformational state is stable. ADP-bound SecA did not change the emission spectra, suggesting that the ATPase in its post-hydrolysis state cannot prime the translocon.

Novel robust approaches for membrane protein reconstitution into lipid bilayers of nanodiscs[340] or possibly amphiphilic systems[345] allow biophysical and biochemical studies on membrane protein dynamics in the native state, as well as protein quaternary structure[346,347]. Here, we used the nanodisc-reconstituted SecYEG translocon to investigate its functional properties and the potential effect of translocon oligomerization on protein translocation. Preprotein translocation by monomeric SecYEG could be measured directly for the first time by employing a FRET-based method to detect the formation of a translocation intermediate. Our data support recent findings that the monomeric SecYEG is functional for translocation but importantly now excludes the possibility of transient oligomerization during the functional cycle. The presence of multiple SecYEG complexes within a nanodisc had little effect on the translocation kinetics, whereas translocation could be greatly enhanced when employing the monomeric SecYEG PrlA4 mutant[304]. Thus, we conclude that multiple copies of SecYEG do

not provide a catalytic advantage relative to the monomer. Therefore, these data do not support the hypothesis that SecYEG functions as a dimer with one protomer exclusively functioning as a SecA binding site and the other protomer functioning as a protein conducting channel[344]. The most recent study suggested that SecYEG dimers are recruited upon translocation of SecB-dependent preproteins[348]. However, the general significance of those findings remains to be determined as SecB is not an essential component of the translocase and is even absent in most bacterial species. Obviously, the specificity of particular oligomeric states of SecYEG for different substrates can be investigated in future using nanodisc-based experiments. We also demonstrated that the nanodisc-reconstituted monomeric SecYEG undergoes a conformational change upon binding of SecA trapped in an AMP-PNP-bound state. The decrease in FRET efficiency between fluorophores introduced in the N- and C-terminal domains of SecY is consistent with an increased distance between these two domains as expected upon the opening of the lateral gate and central pore[175,201]. The active monomeric SecYEG reconstituted into nanodiscs constitutes a novel system for studying further aspects of protein translocation, such as kinetics and translocon dynamic assembly[109], and the impact of periplasmic factors, as well as providing a system amendable for studies on the single-molecule level.

6. Acknowledgements

We would like to thank Prof. Stephan Sligar for a gift of MSP expression plasmid, Natalya Dudkina for negative stain electron microscopy experiments, and Daniel N. Wilson for critical reading of the manuscript. This work was financially supported by the Netherlands Foundation for Scientific Research, Chemical Sciences and Earth and Life Sciences. I.T. is a recipient of a scholarship from the Ministry of National Education of the Republic of Indonesia.

7. Supplementary Data

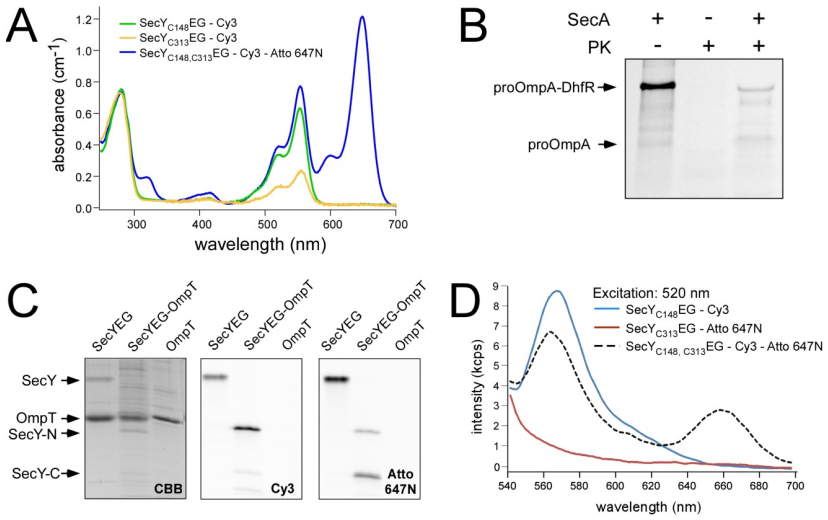

Figure S1. **(A)** Position-specific labeling of SecYEG with FRET-pair fluorophores. Cy3-maleimide fluorophore could be conjugated at high efficiency to the cysteine residue at position 148 within SecY. Low Cy3 labeling was observed for position 313. The double-cysteine mutant $SecY_{C148,C313}EG$ was pre-bound to Ni^{+}-NTA agarose beads and incubated for 2 h with excess of Cy3-maleimide to achieve labeling of the residue C148. After the non-reacted fluorophore was removed, the protein was incubated with an excess of Atto 647N-maleimide that could occupy available cysteine residues. Unreacted dye was removed upon extensive washing of the column-bound SecYEG, and the protein complex was eluted in presence of 300 mM imidazole. Light absorbance was recorded using Cary 100 UV-Vis spectrophotometer. Labeling efficiency was calculated using following extinction coefficients: SecYEG ε_{280} = 70.000 cm^{-1} M^{-1}, Cy3 ε_{560} = 150.000 cm^{-1} M^{-1}, and Atto 647N ε_{650} = 150.000 cm^{-1} M^{-1}. **(B)** Double-cysteine mutant $SecY_{C148,C313}EG$-Cy3-Atto 647N could efficiently form the translocation intermediate of proOmpA-DhfR. Fluorescein-labeled substrate protein $proOmpA_{C282}$-DhfR was completely degraded in absence of SecA, but became protected as full-length (proOmpA-DhfR) and cleaved (proOmpA) forms upon the translocation reaction. In-gel fluorescence was recorded using LAS 4000 fluorescence imager (Fuji) with appropriate excitation and emission filter settings. **(C)** Specific localization of fluorophores within $SecY_{C148,C313}EG$. Site-specific proteolysis of SecYEG by OmpT protease resulted in two distinct N- and C-terminal fragments of SecY. Fluorescence imaging demonstrated the specific localization of conjugated fluorophores Cy3 at the N-terminal fragment SecY-N (position 148), and Atto 647N at the C-terminal fragment SecY-C (position 313). **(D)** Intramolecular FRET between Cy3 and Atto 647N. Fluorescence excitation of the donor fluorophore Cy3 within the double-labeled $SecY_{C148,C313}EG$-Cy3-Atto 647N protein resulted in two emission peaks

at 570 nm (Cy3) and 665 nm (Atto 647N). No direct excitation of Atto 647N was observed at 520 nm for single-labeled $SecY_{C313}EG$-Atto 647N protein. Thus, dual-labeled SecYEG allowed for intra-molecular FRET. Fluorescence emission spectra were recorded using QuantaMaster 40 spectrofluorometer (Photon Technology International).

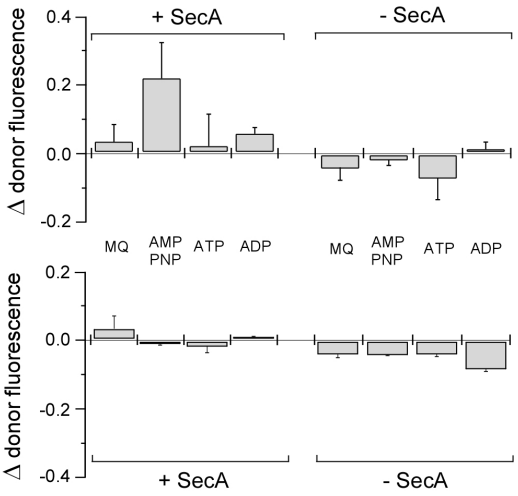

Figure S2. SecA binding alone triggers the lateral gate opening in SecYEG. FRET between fluorophores Cy3 and Atto 647N conjugated to nanodisc-embedded $SecY_{C148,C313}EG$ was analyzed upon binding of SecA in the absence of the preprotein proOmpA-DhfR as described in the caption of Figure 4C. When the SecYEG:SecA complex was stabilized by AMP-PNP, an increase in donor fluorescence was observed. No significant changes in fluorescence were detected when using other nucleotides or AMP-PNP alone (upper panel). No change in Cy3 fluorescence was observed in absence of the acceptor fluorophore (lower panel). It was concluded that SecA binding in presence of AMP-PNP stabilized the pre-open state of the translocon even in absence of the preprotein.

Chapter 5

Dynamics of the Interaction between the Two Helix Finger of SecA ATPase and SecYEG

Amalina Ghaisani Komarudin, Intan Taufik and Arnold J.M. Driessen

CHAPTER FIVE

Dynamics of the Interaction between the Two Helix Finger of SecA ATPase and SecYEG

Abstract – The Sec translocon is the major route for protein translocation across or into the cytoplasmic membrane of bacteria. In its minimal form, it consists of protein conducting channel SecYEG and the motor protein SecA. Based on structural studies of the *Thermotoga maritima* SecA-SecYEG complex, SecA enters the SecYEG channel via the so-called two-helix finger (2HF), which consists of two short helices present in the α-helical wing domain. The role of this interaction with SecYEG is not fully understood and two hypotheses prevail, i.e., the 2HF acts as a lever to push proteins across the translocation pore, or the 2HF functions in the opening of the SecYEG channel. Here we have analyzed the dynamics of interaction between the 2HF of SecA with SecYEG using Forster Resonance Energy Transfer (FRET). The data demonstrate a strong FRET signal upon the initial interaction between the 2HF of SecA and acceptor positions at the transmembrane domains 2-4 of SecY, that result in the pre-open state but this interaction is not further changed under conditions of translocation.

1. Introduction

Cellular processes depend on many systems of which proteinaceous complexes constitute a major role. More than one-third of the cellular proteins in bacteria, are localized at the cytoplasmic membrane or outside the cell. After their synthesis at ribosomes in the cytoplasm, the majority of these proteins are directed to the Sec translocase, and either inserted into the cytoplasmic membrane or translocated to the trans side of the cytoplasmic membrane [130]. The Sec translocase in its minimal form consists of a translocation pore SecYEG and an ATP-driven molecular motor, the SecA protein [41,147]. SecA is found in cells either as soluble cytosolic form or peripherally associated with cytoplasmic membrane [169] where it can bind to acidic phospholipids [170] and to SecYEG [69,70]. The exact mechanism of translocation is still not fully understood. Phospholipid bound SecA can diffuse along the membrane surface, and in this state, it is triggered for the high affinity binding to SecYEG. SecA accepts unfolded preproteins from the molecular chaperone SecB [277,278]. Subsequently, ATP binding initiates the insertion of signal sequence of the preprotein into the SecYEG pore [282], and this is coupled to the opening of vectorial aqueous channel [281]. ATP binding also effects the release of SecB that can rebind a newly synthesized preprotein in the cytosol [72]. ATP hydrolysis causes a dissociation of SecA from the preprotein whereupon SecA can undergo cycles of ATP binding and hydrolysis that are associated with preprotein binding and release and stepwise translocation [78,124]. In the absence of SecA association, larger segments of the preprotein can translocate by sliding [124,341]

The structure of SecA has been solved either as a soluble protein as well as in a SecYEG-bound form. This has led to major insights in the potential binding mechanism and conformational changes in association with the translocation process. Preprotein binding occurs at preprotein crosslinking domain (PPXD) or preprotein binding domain (PBD) that forms a clamp-like structure to capture the polypeptide [178–180]. Conversion of energy from ATP binding and hydrolysis is carried out by DEAD (Asp-Glu-Ala-Asp) motor-domain [184180,186]. Other domains are the C-terminal linker (CTL) and α-helical scaffold domain (HSD) of the C-domain [181], whereas the 'two-helix finger' (2HF) of HSD has been proposed to direct the polypeptide at the entrance of SecYEG pore [87]. From the structure of *Thermotoga maritima* SecA-SecYEG complex, two possible mechanisms for protein translocation involving the two-helix finger can be derived, namely a power stroke mechanism in which the 2HF functions as a lever to push proteins into the translocation pore [78,124,125], or a Brownian-ratchet mechanism in which the 2HF facilitates opening of the translocation pore to allow polypeptide segments to slide into the translocation pore [94,126].

In power stroke mechanism, movement of the 2HF of SecA would results a change in molecular distance between the 2HF and specific regions of SecY. In the Brownian ratchet mechanism, the 2HF likely remains similarly positioned

relative to its site of interaction with SecY, but the position may change relative to other sites on SecY. Here, we conducted a systematic study to monitor the dynamics of the movement of the 2HF of SecA ATPase by measuring FRET signals of a fluorophore conjugated to this region of SecA relative to positions on SecY. A donor and an acceptor fluorophore were conjugated to a set of cysteine mutants of SecA and SecY, respectively. Conformational changes were recorded using FRET to explore the 2HF-SecY interaction at different stages of the translocation process.

2. Experimental Procedures

Chemicals and reagents

N,N'-Dimethyl-N-(Iodoacetyl)-N'-(7-Nitrobenz-2-Oxa-1,3-Diazol-4-yl) ethylene-diamine (IANBD) amide and Texas Red C_2-maleimide were purchased from Invitrogen. Cy3-maleimide and Cy5-maleimide were purchased from GE Healthcare Life Sciences. Fluorescein-maleimide was purchased from Molecular Probes. Cation exchange chromatography and buffer exchange were performed on HiTrap SP and HiTrap Desalting columns with Sephadex G-25 resin from GE Healthcare, respectively.

Bacterial strains and plasmids

E. coli strains and plasmids are listed in Table 1. DNA manipulations were performed using *E. coli* DH5α. Single cysteine mutants of SecY were constructed from cysteine-less template, and resulting fragments were used to substitute the corresponding nucleotide region of SecY in pEK20. Introduction of cysteine residue were accomplished according to Stratagene QuickChange® site-directed mutagenesis kit. All substitutions were confirmed by sequence analysis. DNA restriction enzymes were from Fermentas, while other chemicals were from Sigma.

Table 4. Strains and plasmids used in this study

Strains/plasmids	Relevant characteristics	Source
E. coli SF100	*F⁻, ΔlacX74, galE, galK, thi, rpsL, strA 4, ΔphoA*(pvuII), *ΔompT*	[295]
E. coli DH5α	*supE44, ΔlacU169 (Δ80lacZ_M15) hsdR17, recA, endA1, gyrA96, thi-1. relA1*	[349]
E. coli BL21(DE3)	F-*ompT* hsdSB(rB-, mB-) *gal dcm* (λDE3)	[350]
pAGK002	Wild type SecA	This study
pET503	proOmpA C290S	[293]
pET80	proOmpAC290S-DHFR	[351]
pEK20	Cysteine-less SecYEG	[213]
pEK20-100C	SecY(P100C)EG	This study
pEK20-109C	SecY(G109C)EG	This study
pEK20-179C	SecY(T179C)EG	This study

pT7SecA-Co	Cysteine-less SecA	This study
pT7SecA-792C	SecA R792C	This study
pT7SecA-794C	SecA Y794C	This study
pT7SecA-795C	SecA A795C	This study
pT7SecA-797C	SecA K797C	This study
pT7SecA-801C	SecA Q801C	This study

Overexpression, purification and labeling of SecA and SecY mutants

Inner membrane vesicles (IMVs) containing overexpressed SecYEG were isolated as described [293]. SecB, proOmpA C290S and proOmpA-DHFR were purified as described [293]. ProOmpA C290S was labeled with fluorescein maleimide [322].

Labeling of single cysteine SecYEG were accomplished by first incubating 1.5 mg of IMVs containing designated overexpressed SecYEG with 1 mM Tris 2-carboxyethylphosphine (TCEP) for 30 minutes followed by incubation in buffer containing either 500 µM of Cy5-maleimide or Texas Red C_2-maleimide at 4°C on a rolling bank for 2 hours. The labeled IMVs were stripped using urea buffer (8 M urea, 20 mM HEPES-KOH pH 7) and the pellet were resuspended with 20% glycerol, 50 mM Tris-HCl pH 8, and were analyzed by 12% SDS PAGE. The fluorescence was visualized using Fujifilm LAS-4000 image analyzer.

SecA was purified as described elsewhere [109]. *E. coli* BL21 (DE3) harboring wild type SecA or its mutants was grown at 37°C and induced by addition of 0.5 mM Isopropyl β-D-1-thiogalactopyranoside at A_{600} of 0.6 and further grown for 2 hours. Cells were harvested at 6000 x g for 15 min at 4°C, resuspended in 20 mM HEPES- KOH, pH 6.5, and stored at -80°C. The cell free extract was subjected to HiTrap SP HP column equilibrated with buffer A (20 mM HEPES-KOH, pH 6.5, 10% glycerol, 0.1 M NaCl). Column was washed with buffer A supplemented with 0.1 M NaCl and proteins were eluted with 0.5 M NaCl gradient in buffer A.

Labeling of SecA was accomplished by incubating the protein with a 10-fold molar excess of either Cy3-maleimide or IANBD at 4°C on a rolling bank for 2 hours. The protein were then subjected to desalting column using buffer D (50 mM Tris-HCl pH 7.5, 10% glycerol, 50 mM KCl) in order to remove free dyes. Protein concentration were estimated spectrophotometrically, corrected for fluorophore absorption at 280 nm. The extinction coefficients used were: ε_{280} = 75,750 cm^{-1} M^{-1} for SecA, ε_{550} = 150.000 cm^{-1} M^{-1} for Cy3-maleimide and ε_{480} = 21.000 cm^{-1} M^{-1} for IANBD.

In vitro translocation of proOmpA

In vitro translocation of proOmpA was assayed by employing fluorescein-labeled proOmpA [322]. Translocation reactions were started by adding ATP to the translocation buffer containing SecA, SecB and SecYEG IMVs and incubated at 37°C. Translocation reactions were terminated after 10 minutes on ice by proteinase K treatment. The translocation activity was analyzed by means of SDS

PAGE as previously described [268]. Fluorescence imaging was carried out with a Fujifilm LAS-4000 image analyzer and quantified using ImageJ software.

FRET measurements

Interaction of SecA and SecY was measured by FRET assay. Fluorescence emission spectra was recorded using QuantaMaster 40 Spectrofluorimeter (Photon Technology International). Reactions were carried out at 37°C in 50 mM HEPES/KOH, pH 7.4, 50 mM KCl, 2 mM $MgCl_2$, 2 mM Dithiothreitol and 0.1 mg/mL bovine serum albumin. Observation is started with adding approximately 75 nM of SecA, followed by 1 μg of IMVs containing designated overexpressed SecYEG, 2 mM nucleotide and 25 nM proOmpA-DHFR, where folding DHFR domain was performed as described [110]. Donor fluorophore was excited at 470 nm; all spectra were corrected for background. FRET was calculated on the basis of ratio between acceptor to donor intensity as described [352].

3. Results

Introduction of unique cysteines into SecA and SecY

The crystal structure of SecA and protein translocation channel SecYEG from *Thermotoga maritima* shows several regions of interaction [175]. Critical interfaces occur between the polypeptide crosslinking domain (PPXD) of SecA and the large cytoplasmic TM 6-7 loop of SecY [175]. The structure also shows that the 2HF of the HSD of SecA inserts into the translocation pore and contacts the loop that connects TM 6-7 of SecY. To study the dynamics of the interaction of the 2HF of SecA with SecY in the translocation process, a set of SecA single cysteine mutants was created. Unique cysteine residues were introduced on the tip region of the 2HF (Fig. 1A) via site-directed mutagenesis using the cysteine-less SecA template vector resulting SecA R792C, SecA Y794C, SecA A795C, SecA K797C, SecA Q801C. These proteins were expressed in *E. coli* BL21 (DE3) and purified (Fig. 1B).

In order to not interfere with the SecA-SecY interactions, FRET pairs were created between SecA and the first halve of SecY, TM 1-5 away from the contact point between the 2HF of SecA and SecY (Fig. 1). Ligand induced channel opening may thus be recorded by a reduced FRET signal between SecA and SecY. Single cysteine mutations were generated into the cysteine-less SecY, i.e., on the *cis* interface of TM2b, TM3 and TM4 residues resulting SecY P100C, SecY G109C and SecY T179C, respectively. Each of the aforementioned mutants of SecY was cloned into an expression vector and overproduced in *E. coli* SF100. Inner membrane vesicles containing the overexpressed SecYEG mutants were isolated (Fig. 1C).

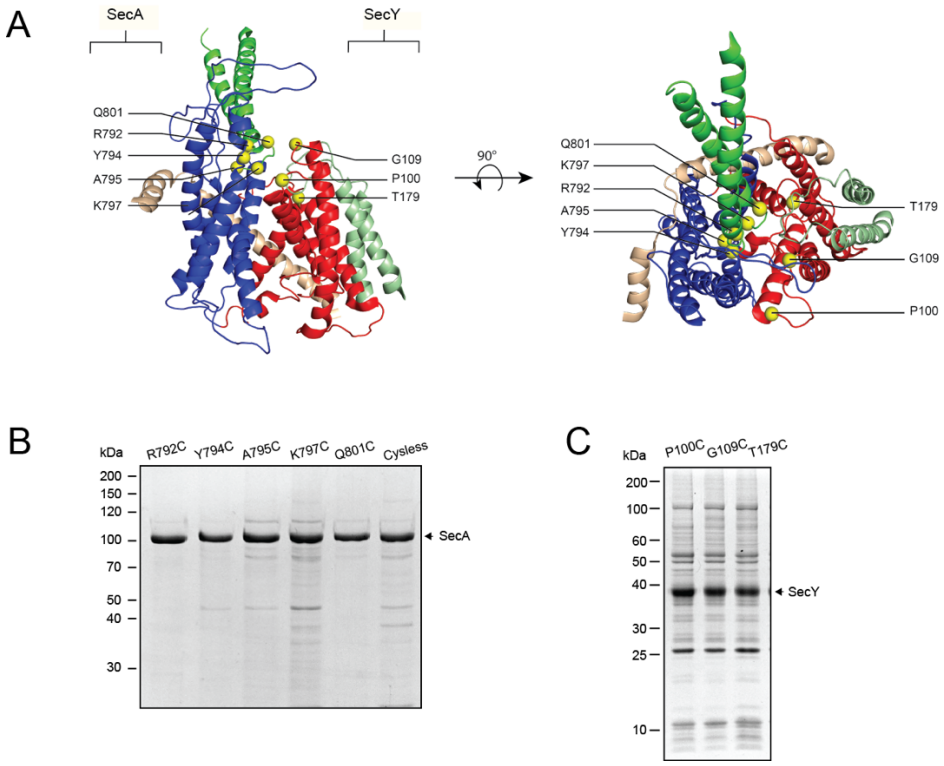

Fig. 1. Cysteine mutation introduction to SecA and SecY. (A) Positions of cysteine mutations in SecY and SecA as mapped on *Thermotoga maritima* SecYEG and SecA co-structure (PDB: 3DIN) from two angles. Image on the left is view of translocon from 'lateral gate', whereas image on the right is view from *cis* side of the membrane. Image showing two halves of SecY colored in red (TM 1-5) and blue (TM 6-10); SecE in light brown and SecG in pale green; SecA is only represented by its two-helix finger colored in green for clarity. A short segment of TM8 and cytosolic loop of SecY is omitted from the illustration to provide better view of the cysteine positions. Yellow balls represent the position of single cysteine mutants. **(B)** Coomassie stained SDS-PAGE of purified SecA cysteine mutants. **(C)** IMVs containing overexpressed of SecY P100C, SecY G109C and T179C which correspond to TM2, TM3 and TM4, respectively.

Labeling of SecA and SecY with fluorescence dyes

The unique cysteine residues allowed the conjugation of the donor and acceptor fluorophore specifically via maleimide chemistry to SecA and SecY, respectively. Purified mutants of SecA and inner membrane vesicles harboring overproduced levels of SecY mutants were labeled with various dyes. We selected the Cy3-Cy5-maleimide and IANBD-Texas Red C_2-maleimide pair since these two pair have been used successfully in the previous FRET studies [110,353]. The Cy dyes are relatively bulky, with IANBD being relatively smaller than Cy dyes and Texas C_2

maleimide (Fig. 2A and 3A). To ensure specificity of the SecA and SecY cysteine labeling, we treated Cys-less SecA, SecA Q801C, IMVs containing Cys-less SecY and SecY T179C with each of the fluorescent probes (Fig. 2B and 3B).

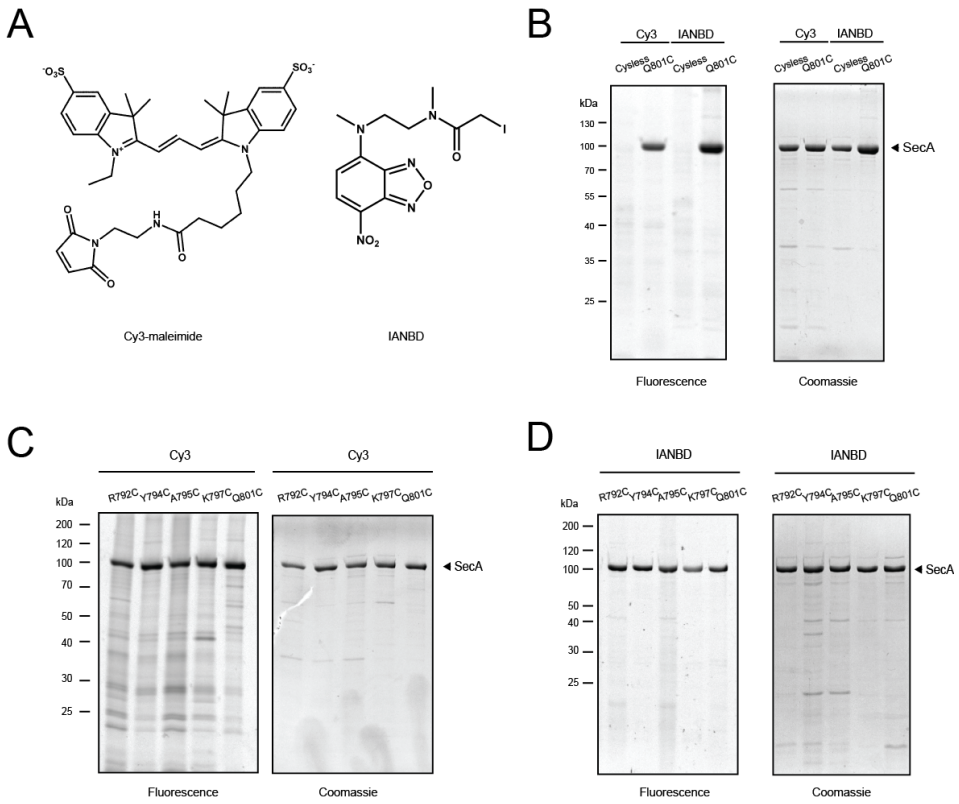

Fig. 2. Fluorescent labeling of SecA cysteine mutants (A) Structures of donor fluorophores, Cy3-maleimide and IANBD. **(B)** Specificity of Cy3-maleimide and IANBD labeling. Cys-less SecA and Q801C SecA mutant were labeled with either Cy3-maleimide or IANBD. **(C)** SecA was labeled with Cy3-maleimide. **(D)** SecA was labeled with IANBD. Similar labeling efficiency were achieved for all mutants. All the sample were run on an SDS-PAGE gel, followed by visualization with Fujifilm LAS-400 Image Analyzer and Coomassie Brilliant Blue R250 staining.

The donor and acceptor fluorophores could successfully label the SecA Q801C mutant and SecY T179C, respectively, but were unable to label the Cys-less SecA and Cys-less SecY (Fig. 2B and 3B). Next, the other SecA mutants were then labeled with Cy3-maleimide (Fig. 2C) and IANBD (Fig. 2D). Labeling efficiency with IANBD was about 80% for SecA K797C; and 90% for the other SecA mutants, with either Cy3 maleimide or IANBD.

The three cysteine mutants of SecY were labeled with either Cy5-maleimide or Texas Red C_2-maleimide. Labeling was done by incubating the IMVs containing

the SecY mutants with either dyes followed by urea treatment to inactivate and remove the endogenous SecA and to remove loosely associated dye. The IMVs

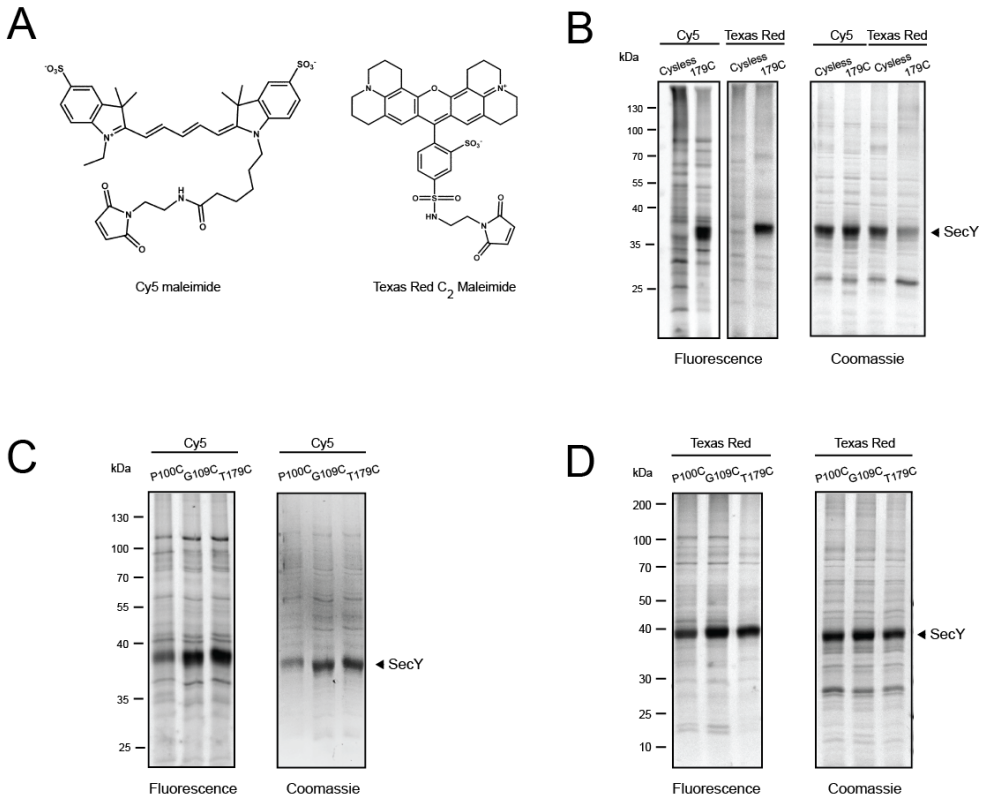

Fig. 3. Fluorescent Labeling of SecY Cysteine mutants. (A) Structures of acceptor fluorophores, Cy5-maleimide and Texas Red C_2-maleimide. **(B)** Specificity of Cy5-maleimide and Texas Red labeling. IMVs containing the overexpressed Cys-less or T179C SecY mutant were labeled with either Cy5-maleimide or Texas Red C_2-maleimide. **(C)** Cy5-maleimide and Texas Red C_2-maleimide labeling of different single cysteine SecY mutants. The reduced Cy5-maleimide fluorescence for SecY P100C is explained by lower protein loaded on the gel as seen as from the Coomassie staining. **(D)** Texas Red C_2-maleimide labeling of different single cysteine SecY mutants.

were collected by centrifugation and extensively washed to remove the remaining free dyes. SecY cysteine mutants have a similar degree of labeling efficiency with either Cy5-maleimide and Texas Red C_2-maleimide as assessed by the fluorescence over coomassie staining ratio assessed in gel (Fig. 3C and 3D). These data show that the SecA and SecY mutants can be effectively labeled with a range of fluorophores for FRET analysis.

Translocation activity of labeled SecA and SecY variants

Since the cysteine mutations and the fluorophore attachment addresses the functional 2HF domain of SecA, each mutant was tested for its ability in supporting translocation by means of *in vitro* translocation assay. The activities of unlabeled and labeled SecA mutants were assessed using wild-type SecY. The cysteine-less SecA mutant showed similar translocation activity as wild-type SecA. SecA R792C, SecA A795C, SecA K797C and SecA Q801C are all active, but their activity is lower as compared to wild type SecA. Substitution of the tyrosine residue in position 794 for a cysteine severely perturbed the protein function (Fig. 4A, black bar). Our data shows that introduction of a cysteine at the C-terminal end of the 2HF is more tolerable than at the N-terminal end. When the SecA mutants were labeled with Cy3-maleimide, all SecA mutants lost 80% of its activity (Fig. 4A, gray bar). However, the variants labeled with IANBD retained high levels of activity (Fig. 4A, white bar). Remarkably, labeling of SecA Y794C with IANBD even restored some of the activity of this mutant that is essentially inactive after mutation. The SecA mutants K797C and Q801C show substantial translocation activity after IANBD labeling and were further used for the FRET analysis.

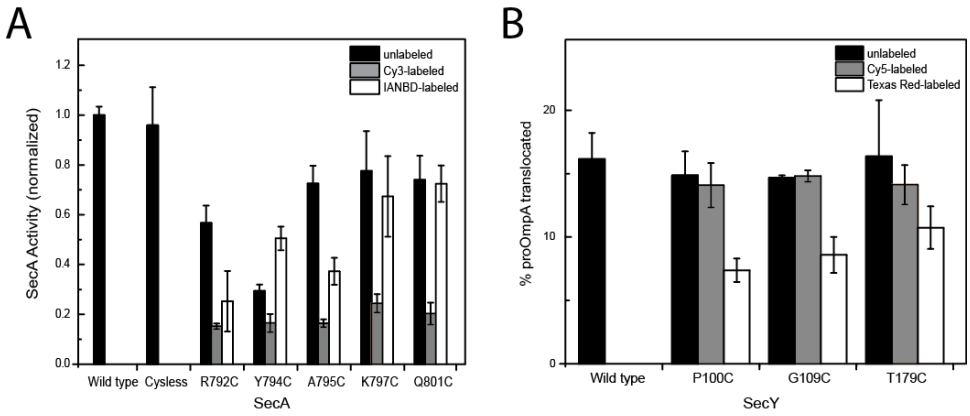

Fig. 4. Translocation activity of SecA and SecY cysteine mutants. (A) Normalized translocation activity of the wild-type, cysteine-less and cysteine mutants of SecA that were unlabeled (black bars), labeled with Cy3 (grey bars) or IANBD (white bars). **(B)** Translocation activity of wild-type and cysteine mutants of SecY that were unlabeled (black bars), labeled with Cy5 (grey bars) or Texas Red (white bars).

The effect of cysteine mutations and subsequent fluorophore labelling in SecY was also tested for translocation activity with wild type SecA. All SecY mutants were active as wild-type SecY in translocation (Fig. 4B, black bar), additionally its activity was not affected after labeling with Cy5-maleimide dye (Fig. 4B, gray bar). The conjugation of Texas Red C_2-maleimide to SecY still allows translocation, although the activity is slightly reduced as compared to the unlabeled SecY (Fig. 4B, white bar).

FRET analysis of the SecA-SecY interaction

To examine the interaction between SecA and SecY, and associated dynamical changes, FRET was recorded between the IANBD donor fluorophore introduced into the 2HF of SecA and the Texas Red acceptor fluorophore present at the *cis* interface of SecYEG. Fluorescence emission spectra were recorded showing a clear FRET signal between SecA K797-IANBD or Q801C-IANBD and the various Texas Red-labeled SecY proteins. Excitation at 470 nm of IANBD-conjugated SecA in solution generated a spectrum with maximum emission at 537 nm. As shown for the SecY G109C-Texas Red and IANBD labeled SecA proteins (Fig. 5A), addition of Texas Red C_2-maleimide-conjugated SecY lowered the fluorescence intensity at 537 nm concomitantly with an emission peak at 611 nm. All measurements were corrected for background emission of Texas Red-labeled SecY excited at 470 nm. Binding of unlabeled SecA to the Texas Red-labeled SecY did not result in any change in the Texas red fluorescence (data not shown).

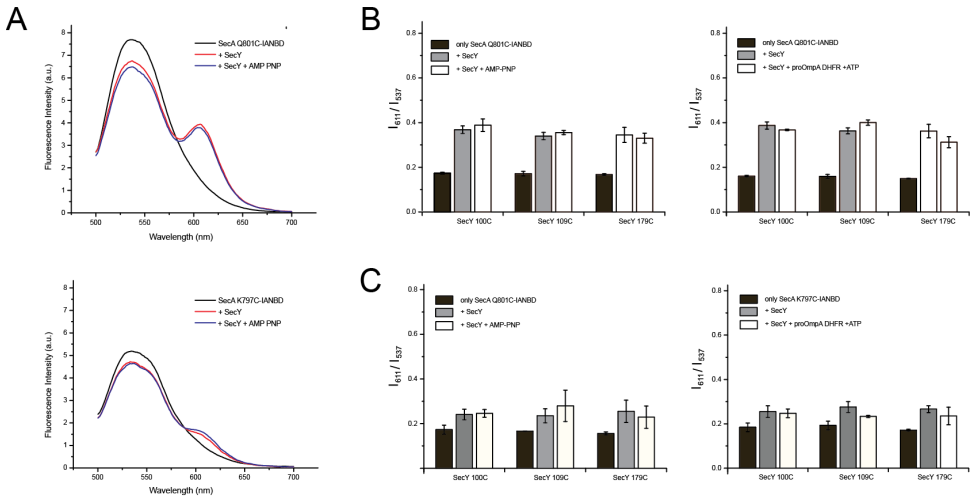

Fig.5 Dynamics of two-helix finger in binding and in initial substrate processing. (A) Emission spectra recording for IANBD (donor)-conjugated SecA mutants and Texas Red C2-maleimide SecY mutants. The upper and lower spectra correspond to SecA Q801C-IANBD and SecA K797C-IANBD, respectively, with SecY G109C-Texas Red. IANBD-labeled SecA is excited at 470 nm and the emission spectra was generated with a single peak maximum emission at 537 (black line). Addition of SecY-Texas Red decreases the emission of donor fluorophore, and results in enhanced emission at 611 nm indicating energy transfer (FRET) to that of acceptor fluorophore (red line). Addition of nucleotide (AMP PNP) (blue line) did not significantly change the FRET. These spectra were corrected by background emission of buffer and SecY-Texas Red alone excited at 470 nm. **(B)** FRET was measured as ratio of fluorescence intensity at 611 nm (acceptor) to that of 537 nm (donor). This bar plot corresponds to SecA Q801C-IANBD supplemented with various SecY-Texas Red mutants and other translocation components. **(C)** FRET measurement of SecA K797C-IANBD supplemented with various SecY-Texas Red mutants and other translocation components.

IANBD is known to change its fluorescence depending on the polarity of the environment where it resides [354]. Our measurement indicate a difference in the fluorescence intensity of IANBD-labeled K797C versus Q801C SecA mutant (Fig. 5A, black line). This difference also resulted in a lower FRET signal for IANBD labeled-SecA K797C and the respective SecY-Texas Red mutants. The FRET signal from all pairs were measured as ratio of the fluorescence intensity at 611 nm to the fluorescence intensity at 537 nm ($I_{611/537}$) (Fig. 5B). The initial value of the SecA Q801C-IANBD alone is 0.18 whereas the addition of IMVs containing SecY-Texas Red increases the ratio to around 0.4 indicating a binding event between SecA and SecY. The SecA K797-IANBD and SecY-Texas Red pair yielded a ratio of about 0.28.

To assure that the FRET signal resulted from the SecA-SecY interaction, a competition experiment was performed with the IANBD labeled SecA Q801C mutant. Addition of a 5-fold excess of unlabeled SecA to the SecA-SecY mixture eliminated the fluorescence at 611 nm with a corresponding increase in the fluorescence at 537 nm (Fig. 6). Likewise, the FRET signal was reduced when SecY-containing IMVs were added to the mixture of IANBD-labeled SecA Q801C and 5-fold unlabeled SecA Q801C. This suggests that SecA-SecY interaction is dynamic, and that the recorded FRET signals emerged from a specific interaction between SecA and SecY.

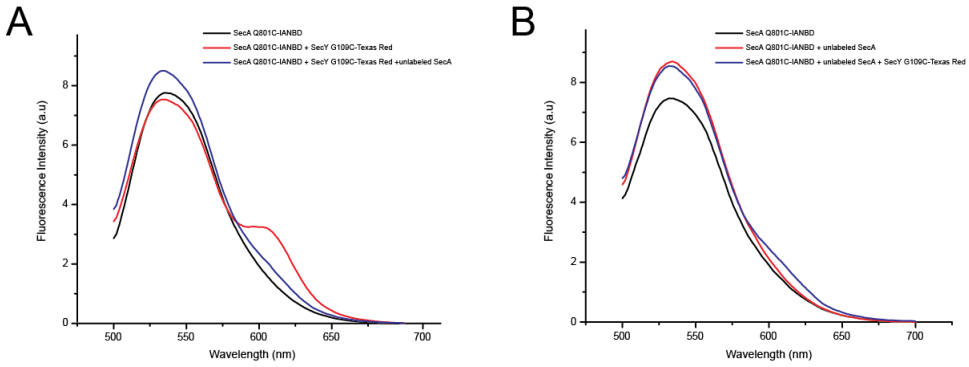

Fig. 6. Unlabeled SecA quenches the FRET signal between Q801C-IANBD and SecY G109C-Texas Red. The FRET signal was reduced after the addition of 5-fold molar excess of unlabeled SecA Q801C to mixture of SecY G109C-Texas-Red and SecA Q801C-IANBD **(A)** or SecA Q801C-IANBD **(B)** Excitation was at 470 nm.

Next, the effect of additional translocation components on the FRET signal was examined. Herein, AMP-PNP and ATP were added to the SecA-SecYEG complexes (Fig. 5), but this did not alter FRET signals as compared to the signal in the absence of nucleotides. Also, ATP and substrate proOmpA or proOmpA-DHFR were used to simulate translocation and an arrested translocation event, respectively. The presence of methotrexate-induced folding of the C-terminal

DHFR domain, causing the accumulation of translocation intermediate consisting of large DHFR domain on the *cis* side of the translocon [341]. Again, these conditions did not lead to an altered FRET signal (Fig. 5B and 5C). These data demonstrate a strong FRET signal between the 2HF region of SecA and fluorophores positioned at TM 2-4 at the *cis* side of SecY, but indicate that no further changes in the distance between the 2HF region of SecA and the TM 2-4 of SecY once the interaction has been established.

4. Discussion

SecA is the motor domain of the Sec-translocase. It recognizes and accepts preprotein by means of the signal peptide-binding domain that involves residues of the preprotein crosslinking domain (PPXD) and helical scaffold domain (HSD) [180]. Together with the helical wing domain (HWD), these regions form a peptide-binding groove [173]. Once the preprotein is bound, the PPXD swings away from the HWD toward nucleotide binding domain 2 (NBD2) in order to release signal sequence and forms a clamp, creating continuous polypeptide guiding channel that is further stabilized by interaction with SecYEG [175,279]. Upon the release, the signal sequence inserts into the lateral gate of SecY, causing the displacement of the plug domain and the widening of a central channel [355]. By comparing molecular structures of SecA and the SecA-SecYEG co-complex, various conformational changes of SecA have been proposed. Further in conjunction with disulfide-bridge crosslinking experiments, it was suggested that the tip of the 2HF of SecA directly interact with the translocating polypeptide and it was proposed that this structure moves up-and-down during the ATPase cycle to pushes the polypeptide to go through SecYEG channel [87,175].

To test the above hypothesis, we have used FRET experiments to directly address the movement of the 2HF relative to fixed position on SecY. Through the use of appropriate fluorescent dyes movements within an atomic range can be measured, although relative motion of the probes and extent of energy transfer could limit the accuracy [356]. Nevertheless, FRET can be used as a molecular ruler to detect such conformational changes that can be predicted on the basis of the structural information. Movement of C-domain has already been observed by FRET where modulation of temperature and nucleotide binding change the proximity of the PPXD and the C-domain [357]. We have engineered eight single cysteine mutants consisting of five mutants in the 2HF of SecA and three mutants on cis interface of SecY, using the structural and sequence homology of the E. coli proteins to that of T. maritima SecA and SecYEG (PDB: 3DIN). As electrostatic interaction for binding of SecY with the PPXD and HSD domains of SecA mostly occurred through loop of TM 6-7 and 8-9 [175], the cysteine substitutions and fluorescent labeling at cis ends of TM 2b, 3 and 4 of SecY will not inhibit binding or interfere with translocation activity as indeed verified with translocation assays using the Cy5-maleimide and Texas Red C2-malemide labeled SecY mutants (Fig.3).

On the other hand, the 2HF appears as a catalytically active domain as some of the cysteine mutations resulted in a decreased activity of SecA, in particular the Y794C mutation (Fig. 2A). Also, the incorporation of the bulky fluorophore Cy3-maleimide disrupted the SecA function, but conjugation with the less bulky fluorophore IANBD yielded a set of labeled SecA cysteine mutants with high activity. Remarkably, labeling of the Y794C mutant with IANBD even restored some of the activity of this catalytically inactive mutant. This finding is in a good agreement with a previous study that showed Tyr 794 could be replaced by bulky amino acids [87].

Using combinations of donor labeled SecA proteins and inner membrane vesicles containing the acceptor labeled SecY protein, FRET experiments were carried out. In the assay, strong FRET signals were observed when SecA was added to the IMVs containing overexpressed SecY (Fig. 5A) indicating the binding event can be recorded by FRET. SecA Q801C-IANBD showed a higher FRET ratio with the various labeled positions on SecY than SecA K797C-IANBD.

Moreover, this FRET signal is specific for the SecA binding reaction as it could be quenched by unlabeled SecA that competes with labeled SecA for binding to SecYEG. Remarkably, any combination of nucleotide and substrate tested, including the formation of an arrested proOmpA-DHFR intermediate, did not result in an altered FRET signal, which suggests that potential conformational changes involving the positioning of the 2HF already occur at the stage of SecA binding to SecYEG.

These observations are not in accordance with the hypothesis that the 2HF acts as an ATP-dependent lever, but does not exclude a lever action in the initial stages of SecA-SecYEG binding. The lack of an ATP effect on the position of the 2HF relative to SecY positions at the cis interface of TM2b, TM3 and TM4, is more in line with a study where the tip of SecA 2HF was cysteine crosslinked to the loop of TM 6-7 of SecY, and that was found to remain fully functional [193]. As we observed lack of change of FRET signal, it indicated no change in distance between SecA 2HF and the cis interface of TM1-5 of SecY. Hence, the protein conformation remained similar. Therefore, we propose the need for further exploration of delicate functioning of the 2HF in facilitating the channel opening.

5. Acknowledgements

I.T. is a recipient of a scholarship from the Ministry of National Education of the Republic of Indonesia.

References

-

References

-

1. Fraser CM, Gocayne JD, White O, et al. The Minimal Gene Complement of Mycoplasma genitalium. *Science*. 1995;270(5235):397-403. doi:10.1126/ science.270.5235.397.
2. Wallin E, von Heijne G. Genome-wide analysis of integral membrane proteins from eubacterial, archaean, and eukaryotic organisms. *Protein Sci*. 1998;7(4): 1029-38. doi:10.1002/pro.5560070420.
3. Perry AJ. Protein Translocation across Membranes. *Encycl Life Sci*. 2010;241 (4871). doi:10.1002/9780470015902.a0000632.pub2.
4. Blobel G. Intracellular protein topogenesis. *Proc Natl Acad Sci U S A*. 1980;77(3): 1496-500. doi:10.1073/pnas.77.3.1496.
5. Pohlschröder M, Prinz W a, Hartmann E, Beckwith J. Protein translocation in the three domains of life: variations on a theme. *Cell*. 1997;91(5):563-566. doi:10.1016/S0092-8674(00)80443-2.
6. Pohlschröder M, Hartmann E, Hand NJ, Dilks K, Haddad A. Diversity and Evolution of Protein Translocation. *Annu Rev Microbiol*. 2005;59(1):91-111. doi:10.1146/annurev.micro.59.030804.121353.
7. Hartmann E, Sommer T, Prehn S, Görlich D, Jentsch S, Rapoport TA. Evolutionary conservation of components of the protein translocation complex. *Nature*. 1994;367(6464):654-657. doi:10.1038/367654a0.
8. Hanada M, Nishiyama KI, Mizushima S, Tokuda H. Reconstitution of an efficient protein translocation machinery comprising SecA and the three membrane proteins, SecY, SecE, and SecG (p12). *J Biol Chem*. 1994;269(38):23625-23631.
9. Kinch LN, Saier MH, Grishin N V. Sec61beta - A component of the archaeal protein secretory system. *Trends Biochem Sci*. 2002;27(4):170-171. doi:10.1016/S0968-0004(01)02055-2.
10. van den Berg B, Clemons WJ, Collinson I, et al. X-ray structure of a protein-conducting channel. *Nature*. 2003;427(6969):36-44. doi:10.1038/nature02218.
11. Simon SM, Blobel G. A protein-conducting channel in the endoplasmic reticulum. *Cell*. 1991;65(3):371-380. doi:10.1016/0092-8674(91)90455-8.
12. Schatz G, Dobberstein B. Common Principles of Protein Translocatibn Across Membranes. *Science*. 1995;271(5255):1519-26. doi:10.1126/ science.271. 5255.1519.
13. Wickner W, Schekman R. Protein Translocation across Biological Membranes. *Science*. 2005;310(5753):1452-1456. doi:10.1126/science.1113752.

14. Wickner W, Driessen AJM, Hartl FU. The Enzymology Of Protein Translocation Across The Escherichia Coli Plasma Membrane. *Annu Rev Biochem*. 1991;60(1):101-124. doi:10.1146/annurev.biochem.60.1.101.

15. Danese PN, Silhavy TJ. Targeting and Assembly of Periplasmic and Outer-Membrane Proteins in Escherichia coli. *Annu Rev Genet*. 1998;32(1):59-94. doi:10.1146/annurev.genet.32.1.59.

16. Brundage L, Hendrick JP, Schiebel E, Driessen a. JM, Wickner W. The purified E. coli integral membrane protein SecY/E is sufficient for reconstitution of SecA-dependent precursor protein translocation. *Cell*. 1990;62(4):649-657. doi:10.1016/0092-8674(90)90111-Q.

17. Asbeck F, Beyreuther K, Köhler H, Von Wettstein G, Barunitzer G. Virusproteine, IV. Die Konstitution des Hüllproteins des Phagen fd. *Hoppe-Seyler´s Zeitschrift für Physiol Chemie*. 1969;350(2):1047-1066. doi:10.1515/bchm2.1969.350.2.1047.

18. Silhavy TJ, Casadaban MJ, Shuman HA, Beckwith JR. Conversion of beta-galactosidase to a membrane-bound state by gene fusion. *Proc Natl Acad Sci U S A*. 1976;73(10):3423-3427.

19. Randall LL, Hardy SJ. Synthesis of exported proteins by membrane-bound polysomes from Escherichia coli. *Eur J Biochem*. 1977;75(1):43-53. doi:10.1111/ j.1432-1033.1977.tb11502.x.

20. Smith WP, Tai P, Thompson RC, Davis BD. Extracellular labeling of nascent polypeptides traversing the membrane of Escherichia coli Biochemistry : *Proc Natl Acad Sci U S A*. 1977;74(7):2830-2834.

21. Chang CN, Blobel G, Model P. Detection of prokaryotic signal peptidase in an Escherichia coli membrane fraction: endoproteolytic cleavage of nascent f1 pre-coat protein. *Proc Natl Acad Sci*. 1978;75(1):361-365. doi:10.1073/pnas.75.1.361.

22. Ito K, Mandel G, Wickner W. Soluble precursor of an integral membrane protein: synthesis of procoat protein in Escherichia coli infected with bacteriophage M13. *Proc Natl Acad Sci U S A*. 1979;76(3):1199-1203.

23. Bedouelle H, Bassford PJ, Fowler A V, Zabin I, Beckwith J, Hofnung M. Mutations which alter the function of the signal sequence of the maltose binding protein of Escherichia coli. *Nature*. 1980;285(5760):78-81. doi:10.1038/285078a0.

24. Oliver DB, Beckwith J. E. coli mutant pleiotropically defective in the export of secreted proteins. *Cell*. 1981;25(3):765-772. doi:10.1016/0092-8674(81)90184-7.

25. Emr SD, Hanley-Way S, Silhavy TJ. Suppressor mutations that restore export of a protein with a defective signal sequence. *Cell*. 1981;23(1):79-88. doi:10.1016/ 0092-8674(81)90272-5.

26. Kumamoto CA, Beckwith J. Mutations in a new gene, secB, cause defective protein localization in Escherichia coli. *J Bacteriol*. 1983;154(1):253-260.

27. Ito K, Wittekind M, Nomura M, et al. A temperature-sensitive mutant of E. coli exhibiting slow processing of exported proteins. *Cell*. 1983;32(3):789-797. doi:10.1016/0092-8674(83)90065-X.

28. Wolfe PB, Wickners W, Goodman M. Sequence of the leader peptidase gene of Escherichia coli and the orientation of leader peptidase in the bacterial envelope. *J Biol Chem*. 1983;158(19):12073-12080.

29. Yamagata H, Daishima K, Mizushima S. Cloning and expression of a gene coding for the prolipoprotein signal peptidase of Escherichia coli. *FEBS Lett*. 1983;158(2):301-304. doi:10.1016/0014-5793(83)80600-0.

30. Innis MA, Tokunaga M, Williams ME, et al. Nucleotide sequence of the Escherichia coli prolipoprotein signal peptidase (lsp) gene. *Proc Natl Acad Sci U S A*. 1984;81(12):3708-12.

31. Yu F, Yamada H, Daishima K, Mizushima S. Nucleotide sequence of the lspA gene, the structural gene for lipoprotein signal peptidase of Escherichia coli. *FEBS Lett*. 1984;173(1):264-268. doi:10.1016/0014-5793(84)81060-1.

32. Schatz PJ, Riggs PD, Jacq A, Fath MJ, Beckwith J. The secE gene encodes an integral membrane protein required for protein export in Escherichia coli. *Genes Dev*. 1989;3(7):1035-1044. doi:10.1101/gad.3.7.1035.

33. Bost S, Belin D. prl Mutations in the Escherichia coli secG gene. *J Biol Chem*. 1997;272(7):4087-4093. doi:10.1074/jbc.272.7.4087.

34. Date T, Zwizinski C, Ludmerer S, Wickner W. Mechanisms of membrane assembly: effects of energy poisons on the conversion of soluble M13 coliphage procoat to membrane-bound coat protein. *Proc Natl Acad Sci, USA*. 1980;77(2):827-831.

35. Date T, Goodman JM, Wickner WT. Procoat, the precursor of M13 coat protein, requires an electrochemical potential for membrane insertion. *Proc Natl Acad Sci USA*. 1980;77(8):4669-4673.

36. Chen L, Tai PC. ATP is essential for protein translocation into Escherichia coli membrane vesicles. *Proc Natl Acad Sci U S A*. 1985;82(13):4384-4388. doi:10.1073/pnas.82.13.4384.

37. Geller BL, Movva NR, Wickner W. Both ATP and the electrochemical potential are required for optimal assembly of pro-OmpA into Escherichia coli inner membrane vesicles. *Proc Natl Acad Sci U S A*. 1986;83(12):4219-22.

38. Ito K. Purification of the precursor form of maltose-binding protein, a periplasmic protein of Escherichia coli. *J Biol Chem*. 1982;257(17):9895-9897.

39. Zwizinski C, Wickner W. The purification of M13 procoat, a membrane protein precursor. *Embo J*. 1982;1(5):573-578.

40. Wolfe PB, Silver P, Wickner W. The isolation of homogeneous leader peptidase from a strain of Escherichia coli which overproduces the enzyme. *J Biol Chem*. 1982;257(13):7898-7902.

41. Cabelli RJ, Chen L, Tai PC, Oliver DB. SecA protein is required for secretory protein translocation into E. coli membrane vesicles. *Cell*. 1988;55(4):683-692. doi:10.1016/0092-8674(88)90227-9.

42. Weiss JB, Ray PH, Bassford PJ. Purified secB protein of Escherichia coli retards folding and promotes membrane translocation of the maltose-binding protein in

vitro. *Proc Natl Acad Sci U S A*. 1988;85(23):8978-8982. doi:10.1073/pnas.85.23.8978.

43. Matsuyama S ichi, Fujita Y, Sagara K, Mizushima S. Overproduction, purification and characterization of SecD and SecF, integral membrane components of the protein translocation machinery of Escherichia coli. *Biochim Biophys Acta (BBA)/Protein Struct Mol*. 1992;1122(1):77-84. doi:10.1016/0167-4838(92)90130-6.

44. Nakamura K, Nakamura A, Takamatsu H, Yoshikawa H, Yamane K. Cloning and characterization of a Bacillus subtilis gene homologous to E. coli secY. *J Biochem*. 1990;107(4):603-607.

45. Koivula T, Palva I, Hemilä H. Nucleotide sequence of the secY gene from Lactococcus lactis and identification of conserved regions by comparison of four SecY proteins. *FEBS Lett*. 1991;288(1-2):114-118. doi:10.1016/0014-5793(91)81015-Z.

46. Nakai M, Goto A, Nohara T, Sugita D, Endo T. Identification of the SecA protein homolog in pea chloroplasts and its possible involvement in thylakoidal protein transport. *J Biol Chem*. 1994;269(50):31338-31341.

47. Kim JK, Kim JH, Kim SJ, et al. Cloning and sequencing of the secY gene homolog from Mycobacterium bovis BCG. *Biochem Mol Biol Int*. 1997;43(2):391-8.

48. Douglas SE. A secY homologue is found in the plastid genome of Cryptomonas Φ. *FEBS Lett*. 1992;298(1):93-96. doi:10.1016/0014-5793(92)80029-G.

49. Nakai M, Sugita D, Omata T, Endo T. Sec-Y protein is localized in both the cytoplasmic and thylakoid membranes in the cyanobacterium Synechococcus PCC7942. *Biochem Biophys Res Commun*. 1993;193(1):228-234. doi:10.1006/bbrc.1993.1613.

50. Gu L, Remacha M, Wenman WM, Kaul R. Cloning and characterization of a secY homolog from Chlamydia trachomatis. *MGG Mol Gen Genet*. 1994;243(4):482-487. doi:10.1007/BF00280480.

51. Kobayashi M, Fugono N, Asai Y, et al. Cloning and sequencing of the secY homolog from Coryneform bacteria. *Gene*. 1994;139(1):99-103.

52. Kath T, Schäfer G. A secY homologous gene in the crenarchaeon Sulfolobus acidocaldarius. *BBA - Gene Struct Expr*. 1995;1264(2):155-158. doi:10.1016/ 0167-4781(95)00165-D.

53. Laidler V, Chaddock AM, Knott TG, Walker D, Robinson C. A SecY homolog in Arabidopsis thaliana: Sequence of a full-length cDNA clone and import of the precursor protein into chloroplasts. *J Biol Chem*. 1995;270(30):17664-17667. doi:10.1074/jbc.270.30.17664.

54. Ostiguy S, Gilbert M, Shareck F, Kluepfel D, Morosoli R. Cloning and sequencing of the sec Y homolog from Streptomyces lividans 1326. *Gene*. 1996;176(1-2):265-267. doi:10.1016/0378-1119(96)00229-6.

55. Suh TW, Boylan SA, Oh SH, Price CW. Genetic and transcriptional organization of the Bacillus subtilis spc-α region. *Gene*. 1996;169(1):17-23. doi:10.1016/0378-1119(95)00757-1.

56. Nakamura K, Takamatsu H, Akiyama Y, Ito K, Yamane K. Complementation of the protein transport defect of an Escherichia coli secY mutant (secY24) by Bacillus subtilis secY homologue. *FEBS Lett*. 1990;273(1-2):75-8.

57. Duong F, Wickner W. Distinct catalytic roles of the SecYE, SecG and SecDFyajC subunits of preprotein translocase holoenzyme. *EMBO J*. 1997;16(10):2756-68. doi:10.1093/emboj/16.10.2756.

58. Braunstein M, Brown AM, Kurtz S, Jacobs W.R. J. Two nonredundant SecA homologues function in mycobacteria. *J Bacteriol*. 2001;183(24):6979-6990. doi:10.1128/JB.183.24.6979-6990.2001.

59. Bensing BA, Sullam PM. An accessory sec locus of Streptococcus gordonii is required for export of the surface protein GspB and for normal levels of binding to human platelets. *Mol Microbiol*. 2002;44(4):1081-1094. doi:10.1046/j.1365-2958.2002.02949.x.

60. Murakami A, Nakatogawa H, Ito K. Translation arrest of SecM is essential for the basal and regulated expression of SecA. *Proc Natl Acad Sci U S A*. 2004;101(33):12330-5. doi:10.1073/pnas.0404907101.

61. Ohno Iwashita Y, Wickner W. Reconstriction of rapid and asymmetric assembly of M13 procoat protein into liposomes which have bacterial leader peptidase. *J Biol Chem*. 1983;258(3):1895-1900.

62. Müller M, Blobel G. In vitro translocation of bacterial proteins across the plasma membrane of Escherichia coli. *Proc Natl Acad Sci U S A*. 1984;81(23):7421-5.

63. Driessen AJ, Wickner W. Solubilization and functional reconstitution of the protein-translocation enzymes of Escherichia coli. *Proc Natl Acad Sci U S A*. 1990;87(8):3107-11.

64. Görlich D, Rapoport TA. Protein translocation into proteoliposomes reconstituted from purified components of the endoplasmic reticulum membrane. *Cell*. 1993;75(4):615-630. doi:10.1016/0092-8674(93)90483-7.

65. Alami M, Dalal K, Lelj-Garolla B, Sligar SG, Duong F. Nanodiscs unravel the interaction between the SecYEG channel and its cytosolic partner SecA. *EMBO J*. 2007;26(8):1995-2004. doi:10.1038/sj.emboj.7601661.

66. Kumamoto CA, Chen L, Fandl J, Tai PC. Purification of the Escherichia coli secB gene product and demonstration of its activity in an in vitro protein translocation system. *J Biol Chem*. 1989;264(4):2242-2249.

67. Lecker S, Lill R, Ziegelhoffer T, et al. Three pure chaperone proteins of Escherichia coli--SecB, trigger factor and GroEL--form soluble complexes with precursor proteins in vitro. *EMBO J*. 1989;8(9):2703-2709.

68. Liu G, Topping TB, Randall LL. Physiological role during export for the retardation of folding by the leader peptide of maltose-binding protein. *Proc Natl Acad Sci U S A*. 1989;86(23):9213-9217. doi:10.1073/pnas.86.23.9213.

69. Lill R, Cunningham K, Brundage LA, Ito K, Oliver D, Wickner W. SecA protein hydrolyzes ATP and is an essential component of the protein translocation ATPase of Escherichia coli. *EMBO J*. 1989;8(3):961-966.

70. Hartl FU, Lecker S, Schiebel E, Hendrick JP, Wickner W. The binding cascade of SecB to SecA to SecY E mediates preprotein targeting to the E. coli plasma membrane. *Cell*. 1990;63(2):269-279. doi:10.1016/0092-8674(90)90160-G.

71. Douville K, Price A, Eichler J, Economou A, Wickner W. SecYEG and SecA Are the Stoichiometric Components of Preprotein Translocase. *J Biol Chem*. 1995; 270(34):20106-20111. doi:10.1074/jbc.270.34.20106.

72. Fekkes P, van der Does C, Driessen AJM. The molecular chaperone SecB is released from the carboxy-terminus of SecA during initiation of precursor protein translocation. *EMBO J*. 1997;16(20):6105-6113. doi:10.1093/ emboj/ 16.20.6105.

73. Valent QA, Scotti PA, High S, et al. The Escherichia coli SRP and SecB targeting pathways converge at the translocon. *EMBO J*. 1998;17(9):2504-2512. doi:10.1093/emboj/17.9.2504.

74. Koch HG, Hengelage T, Neumann-Haefelin C, et al. In vitro studies with purified components reveal signal recognition particle (SRP) and SecA/SecB as constituents of two independent protein-targeting pathways of Escherichia coli. *Mol Biol Cell*. 1999;10(7):2163-2173.

75. Beck K, Wu L, Brunner J, Muller M. Discrimination between SRP- and SecA/SecB-dependent substrates involves selective recognition of nascent chains by SRP and trigger factor. *EMBO J*. 2000;19(1):134-143. doi:10.1093/emboj/19.1.134.

76. Bieker-Brady K, Silhavy TJ. Suppressor analysis suggests a multistep, cyclic mechanism for protein secretion in Escherichia coli. *EMBO J*. 1992;11(9):3165-3174.

77. Economou A, Wickner W. SecA promotes preprotein translocation by undergoing ATP-driven cycles of membrane insertion and deinsertion. *Cell*. 1994;78(5):835-843. doi:10.1016/S0092-8674(94)90582-7.

78. Van Der Wolk JPW, De Wit JG, Driessen AJM. The catalytic cycle of the Escherichia coli SecA ATPase comprises two distinct preprotein translocation events. *EMBO J*. 1997;16(24):7297-7304. doi:10.1093/emboj/16.24.7297.

79. Or E, Navon A, Rapoport TA. Dissociation of the dimeric SecA ATPase during protein translocation across the bacterial membrane. *EMBO J*. 2002;21(17):4470-4479. doi:10.1093/emboj/cdf471.

80. de Keyzer J, van der Does C, Kloosterman TG, Driessen AJM. Direct demonstration of ATP-dependent release of SecA from a translocating preprotein by surface plasmon resonance. *J Biol Chem*. 2003;278(32):29581-29586. doi:10.1074/ jbc.M303490200.

81. Crowley KS, Liao S, Worrell VE, Reinhart GD, Johnson AE. Secretory proteins move through the endoplasmic reticulum membrane via an aqueous, gated pore. *Cell*. 1994;78(3):461-471. doi:10.1016/0092-8674(94)90424-3.

82. Martoglio B, Hofmann MW, Brunner J, Dobberstein B. The protein-conducting channel in the membrane of the endoplasmic reticulum is open laterally toward the lipid bilayer. *Cell*. 1995;81(2):207-214. doi:10.1016/0092-8674(95)90330-5.

83. Cannon KS, Or E, Clemons WM, Shibata Y, Rapoport TA. Disulfide bridge formation between SecY and a translocating polypeptide localizes the translocation pore to the center of SecY. *J Cell Biol*. 2005;169(2):219-225. doi:10.1083/jcb.200412019.

84. Tam PCK, Maillard AP, Chan KKY, Duong F. Investigating the SecY plug movement at the SecYEG translocation channel. *EMBO J*. 2005;24(19):3380-3388. doi:10.1038/sj.emboj.7600804.

85. Li W, Schulman S, Boyd D, Erlandson K, Beckwith J, Rapoport TA. The plug domain of the SecY protein stabilizes the closed state of the translocation channel and maintains a membrane seal. *Mol Cell*. 2007;26(4):511-21. doi:10.1016/j.molcel.2007.05.002.

86. Saparov SM, Erlandson K, Cannon K, et al. Determining the Conductance of the SecY Protein Translocation Channel for Small Molecules. *Mol Cell*. 2007;26(4):501-509. doi:10.1016/j.molcel.2007.03.022.

87. Erlandson KJ, Miller SBM, Nam Y, Osborne AR, Zimmer J, Rapoport TA. A role for the two-helix finger of the SecA ATPase in protein translocation. *Nature*. 2008;455(7215):984-987. doi:10.1038/nature07439.

88. du Plessis DJF, Berrelkamp G, Nouwen N, Driessen AJM. The lateral gate of SecYEG opens during protein translocation. *J Biol Chem*. 2009;284(23):15805-15814. doi:10.1074/jbc.M901855200.

89. Bonardi F, Halza E, Walko M, et al. Probing the SecYEG translocation pore size with preproteins conjugated with sizable rigid spherical molecules. *Proc Natl Acad Sci U S A*. 2011;108(19):7775-80. doi:10.1073/pnas.1101705108.

90. Wu ZC, de Keyzer J, Kedrov A, Driessen AJM. Competitive binding of the SecA ATPase and ribosomes to the SecYEG translocon. *J Biol Chem*. 2012;287(11):7885-7895. doi:10.1074/jbc.M111.297911.

91. Knyazev DG, Lents A, Krause E, et al. The bacterial translocon secYEG opens upon ribosome binding. *J Biol Chem*. 2013;288(25):17941-17946. doi:10.1074/jbc.M113.477893.

92. Ge Y, Draycheva A, Bornemann T, Rodnina M V, Wintermeyer W. Lateral opening of the bacterial translocon on ribosome binding and signal peptide insertion. *Nat Commun*. 2014;5:5263. doi:10.1038/ncomms6263.

93. Taufik I, Kedrov A, Exterkate M, Driessen AJM. Monitoring the activity of single translocons. *J Mol Biol*. 2013;425(22):4145-4153. doi:10.1016/ j.jmb.2013.08.012.

94. Allen WJ, Corey RA, Oatley P, et al. Two-way communication between SecY and SecA suggests a Brownian ratchet mechanism for protein translocation. *Elife*. 2016;5(Md). doi:10.7554/eLife.15598.

95. Hanein D, Matlack KE, Jungnickel B, et al. Oligomeric rings of the Sec61p complex induced by ligands required for protein translocation. *Cell*. 1996;87(4):721-32. doi:10.1016/S0092-8674(00)81391-4.

96. Beckmann R, Bubeck D, Grassucci R, et al. Alignment of conduits for the nascent polypeptide chain in the ribosome-Sec61 complex. *Science*. 1997;278(5346): 2123-6. doi:10.1126/science.278.5346.2123.

97. Meyer TH, Ménétret JF, Breitling R, Miller KR, Akey CW, Rapoport TA. The bacterial SecY/E translocation complex forms channel-like structures similar to those of the eukaryotic Sec61p complex. *J Mol Biol*. 1999;285(4):1789-800. doi:10.1006/jmbi.1998.2413.

98. Manting EH, van Der Does C, Remigy H, Engel A, Driessen AJ. SecYEG assembles into a tetramer to form the active protein translocation channel. *EMBO J*. 2000;19(5):852-861. doi:10.1093/emboj/19.5.852.

99. Xu Z, Knafels JD, Yoshino K. Crystal structure of the bacterial protein export chaperone secB. *Nat Struct Biol*. 2000;7(12):1172-1177. doi:10.1038/82040.

100. Dekker C, De Kruijff B, Gros P. Crystal structure of SecB from Escherichia coli. *J Struct Biol*. 2003;144(3):313-319. doi:10.1016/j.jsb.2003.09.012.

101. Hunt JF, Weinkauf S, Henry L, et al. Nucleotide control of interdomain interactions in the conformational reaction cycle of SecA. *Science*. 2002;297(5589):2018-2026. doi:10.1126/science.1074424.

102. Vassylyev DG, Mori H, Vassylyeva MN, et al. Crystal Structure of the Translocation ATPase SecA from Thermus thermophilus Reveals a Parallel, Head-to-Head Dimer. *J Mol Biol*. 2006;364(3):248-258. doi:10.1016/j.jmb.2006.09.061.

103. Zimmer J, Li W, Rapoport TA. A novel dimer interface and conformational changes revealed by an X-ray structure of B. subtilis SecA. *J Mol Biol*. 2006;364(3):259-65. doi:10.1016/j.jmb.2006.08.044.

104. Frauenfeld J, Gumbart J, Sluis EO van der, et al. Cryo-EM structure of the ribosome-SecYE complex in the membrane environment. *Nat Struct Mol Biol*. 2011;18(5):614-621. doi:10.1038/nsmb.2026.

105. Ménétret J-F, Schaletzky J, Clemons WM, et al. Ribosome Binding of a Single Copy of the SecY Complex : Implications for Protein Translocation. *Mol Cell*. 2007;28(6):1083-1092. doi:10.1016/j.molcel.2007.10.034.

106. Becker T, Bhushan S, Jarasch A, et al. Structure of monomeric yeast and mammalian Sec61 complexes interacting with the translating ribosome. *Science*. 2009;326(5958):1369-1373. doi:10.1126/science.1178535.

107. Bechtluft P, van Leeuwen RGH, Tyreman M, et al. Direct observation of chaperone-induced changes in a protein folding pathway. *Science*. 2007;318(5855):1458-61. doi:10.1126/science.1144972.

108. Wirth A, Jung M, Bies C, et al. The Sec61p complex is a dynamic precursor activated channel. *Mol Cell*. 2003;12(1):261-268. doi:10.1016/S1097-2765(03)00283-1.

109. Kusters I, Van Den Bogaart G, Kedrov A, et al. Quaternary structure of SecA in solution and bound to SecYEG probed at the single molecule level. *Structure*. 2011;19(3):430-439. doi:10.1016/j.str.2010.12.016.

110. Kedrov A, Kusters I, Krasnikov V V, Driessen AJM. A single copy of SecYEG is sufficient for preprotein translocation. *EMBO J*. 2011;30(21):4387-4397. doi:10.1038/emboj.2011.314.

111. Gari RRS, Frey NC, Mao C, Randall LL, King GM. Dynamic structure of the translocon SecYEG in membrane: Direct single molecule observations. *J Biol Chem*. 2013;288(23):16848-16854. doi:10.1074/jbc.M113.471870.

112. Samuelson JC, Chen M, Jiang F, et al. YidC mediates membrane protein insertion in bacteria. *Nature*. 2000;406(6796):637-641. doi:10.1038/35020586.

113. Scotti PPA, Urbanus MLML, Brunner J, et al. YidC, the Escherichia coli homologue of mitochondrial Oxa1p, is a component of the Sec translocase. *EMBO J*. 2000;19(4):542-549. doi:10.1093/emboj/19.4.542.

114. Urbanus ML, Scotti P a, Froderberg L, et al. Sec-dependent membrane protein insertion: sequential interaction of nascent FtsQ with SecY and YidC. *EMBO Rep*. 2001;2(6):524-529. doi:10.1093/embo-reports/kve108.

115. van der Laan M, Houben EN, Nouwen N, et al. Reconstitution of Sec-dependent membrane protein insertion: nascent FtsQ interacts with YidC in a SecYEG-dependent manner. *EMBO Rep*. 2001;2(6):519-23. doi:10.1093/embo-reports/kve106.

116. Nouwen N, Driessen AJM. SecDFyajC forms a heterotetrameric complex with YidC. *Mol Microbiol*. 2002;44(5):1397-1405. doi:10.1046/j.1365-2958.2002.02972.x.

117. Sachelaru I, Petriman NA, Kudva R, et al. YidC occupies the lateral gate of the SecYEG translocon and is sequentially displaced by a nascent membrane protein. *J Biol Chem*. 2013;288(23):16295-16307. doi:10.1074/jbc.M112.446583.

118. Kumazaki K, Kishimoto T, Furukawa A, et al. Crystal structure of Escherichia coli YidC, a membrane protein chaperone and insertase. *Sci Rep*. 2014;4:7299. doi:10.1038/srep07299.

119. Haider S, Hall BA, Sansom MSP. Simulations of a protein translocation pore: SecY. *Biochemistry*. 2006;45(43):13018-13024. doi:10.1021/bi061013d.

120. Tian P, Andricioaei I. Size, motion, and function of the SecY translocon revealed by molecular dynamics simulations with virtual probes. *Biophys J*. 2006;90(8):2718-2730. doi:10.1529/biophysj.105.073304.

121. Zhang B, Miller TF. Hydrophobically stabilized open state for the lateral gate of the Sec translocon. *Proc Natl Acad Sci*. 2010;107(12):5399-5404. doi:10.1073/pnas.0914752107.

122. Ismail N, Hedman R, Schiller N, von Heijne G. A biphasic pulling force acts on transmembrane helices during translocon-mediated membrane integration. *Nat Struct Mol Biol*. 2012;19(10):1018-1022. doi:10.1038/nsmb.2376.

123. Halegoua S, Inouye M. Translocation and assembly of outer membrane proteins of Escherichia coli Selective accumulation of precursors and novel assembly intermediates caused by phenethyl alcohol. *J Mol Biol*. 1979;130(1):39-61. doi:10.1016/0022-2836(79)90551-5.

124. Schiebel E, Driessen AJM, Hartl FU, Wickner W. ΔμH+ and ATP function at different steps of the catalytic cycle of preprotein translocase. *Cell*. 1991;64(5):927-939. doi:10.1016/0092-8674(91)90317-R.

125. Uchida K, Mori H, Mizushima S. Stepwise movement of preproteins in the process of translocation across the cytoplasmic membrane of Escherichia coli. *J Biol Chem*. 1995;270(52):30862-30868. doi:10.1074/jbc.270.52.30862.

126. Simon SM, Peskin CS, Oster GF. What drives the translocation of proteins? *Proc Natl Acad Sci U S A*. 1992;89(9):3770-3774. doi:10.1073/pnas.89.9.3770.

127. Benach J, Chou Y Te, Fak JJ, et al. Phospholipid-induced monomerization and signal-peptide-induced oligomerization of SecA. *J Biol Chem*. 2003;278(6):3628-3638. doi:10.1074/jbc.M205992200.

128. Sharma V, Arockiasamy A, Ronning DR, et al. Crystal structure of Mycobacterium tuberculosis SecA, a preprotein translocating ATPase. *Proc Natl Acad Sci U S A*. 2003;100(5):2243-8. doi:10.1073/pnas.0538077100.

129. Tomkiewicz D, Nouwen N, Driessen AJM. Pushing, pulling and trapping - Modes of motor protein supported protein translocation. *FEBS Lett*. 2007;581(15):2820-2828. doi:10.1016/j.febslet.2007.04.015.

130. Driessen AJM, Nouwen N. Protein translocation across the bacterial cytoplasmic membrane. *Annu Rev Biochem*. 2008;77(1):643-667. doi:10.1146/annurev.biochem.77.061606.160747.

131. Kusters I, Driessen AJM. SecA, a remarkable nanomachine. *Cell Mol Life Sci*. 2011;68(12):2053-2066. doi:10.1007/s00018-011-0681-y.

132. Bauer BW, Shemesh T, Chen Y, Rapoport TA. A "push and slide" mechanism allows sequence-insensitive translocation of secretory proteins by the SecA ATPase. *Cell*. 2014;157(6):1416-1429. doi:10.1016/j.cell.2014.03.063.

133. von Heijne G. The signal peptide. *J Membr Biol*. 1990;115(3):195-201. doi:10.1007/BF01868635.

134. Blobel G, Dobberstein B. Transfer of proteins across membranes. I. Presence of proteolytically processed and unprocessed nascent immunoglobulin light chains on membrane bound ribosomes of murine myeloma. *J Cell Biol*. 1975;67(3):835-851. doi:10.1083/jcb.67.3.835.

135. Bassford P, Beckwith J. Escherichia coli mutants accumulating the precursor of a secreted protein in the cytoplasm. *Nature*. 1979;277(5697):538-541. doi:10.1038/277538a0.

136. Moreno F, Fowler A V, Hall M, Silhavy TJ, Zabin I, Schwartz M. A signal sequence is not sufficient to lead beta-galactosidase out of the cytoplasm. *Nature*. 1980;286(5771):356-359. doi:10.1038/286356a0.

137. Dalbey RE, Lively MO, Bron S, van Dijl JM. The chemistry and enzymology of the type I signal peptidases. *Protein Sci*. 1997;6(6):1129-1138. doi:10.1002/pro.5560060601.

138. Paetzel M, Karla A, Strynadka NCJ, Dalbey RE. Signal peptidases. *Chem Rev*. 2002;102(12):4549-80.

139. Nakamoto H, Bardwell JCA. Catalysis of disulfide bond formation and isomerization in the Escherichia coli periplasm. *Biochim Biophys Acta*. 2004;1694(1-3):111-9. doi:10.1016/j.bbamcr.2004.02.012.

140. Mogensen JE, Otzen DE. Interactions between folding factors and bacterial outer membrane proteins. *Mol Microbiol*. 2005;57(2):326-46. doi:10.1111/j.1365-2958.2005.04674.x.

141. Gruber CW, Cemazar M, Heras B, Martin JL, Craik DJ. Protein disulfide isomerase: the structure of oxidative folding. *Trends Biochem Sci*. 2006;31(8):455-64. doi:10.1016/j.tibs.2006.06.001.

142. Paetzel M, Dalbey RE, Strynadka NC. Crystal structure of a bacterial signal peptidase in complex with a beta-lactam inhibitor. *Nature*. 1998;396(6707):186-190. doi:10.1038/24196.

143. Paetzel M. Structure and mechanism of Escherichia coli type I signal peptidase. *Biochim Biophys Acta - Mol Cell Res*. 2014;1843(8):1497-1508. doi:10.1016/j.bbamcr.2013.12.003.

144. Wolfe PB, Wickner W. Bacterial leader peptidase, a membrane protein without a leader peptide, uses the same export pathway as pre-secretory proteins. *Cell*. 1984;36(4):1067-1072. doi:10.1016/0092-8674(84)90056-4.

145. Randall LL, Hardy SJS. Correlation of competence for export with lack of tertiary structure of the mature species: A study in vivo of maltose-binding protein in E. coli. *Cell*. 1986;46(6):921-928. doi:10.1016/0092-8674(86)90074-7.

146. Randall LL, Hardy SJS. High selectivity with low specificity: how SecB has solved the paradox of chaperone binding. *Trends Biochem Sci*. 1995;20(2):65-69. doi:10.1016/S0968-0004(00)88959-8.

147. Fekkes P, Driessen a J. Protein targeting to the bacterial cytoplasmic membrane. *Microbiol Mol Biol Rev*. 1999;63(1):161-173.

148. Müller JP, Bron S, Venema G, Maarten van Dijl J. Chaperone-like activities of the CsaA protein of Bacillus subtilis. *Microbiology*. 2000;146(1):77-88. doi:10.1099/00221287-146-1-77.

149. Tani K, Tokuda H, Mizushima S. Translocation of proOmpA possessing an intramolecular disulfide bridge into membrane vesicles of Escherichia coli: Effect of membrane energization. *J Biol Chem*. 1990;265(28):17341-17347.

150. Driessen AJ. Precursor protein translocation by the Escherichia coli translocase is directed by the protonmotive force. *EMBO J*. 1992;11(3):847-53.

151. Luirink J, High S, Wood H, Giner A, Tollervey D, Dobberstein B. Signal-Sequence Recognition by an Escherichia coli Ribonucleoprotein Complex. *Nature*. 1992;359(6397):741-743. doi:Doi 10.1038/359741a0.

152. Valent Q a, Kendall D a, High S, Kusters R, Oudega B, Luirink J. Early events in preprotein recognition in E. coli: interaction of SRP and trigger factor with nascent polypeptides. *EMBO J*. 1995;14(22):5494-5505.

153. Keenan RJ, Freymann DM, Stroud RM, Walter P. The Signal Recognition Particle. *Annu Rev Biochem*. 2001;70(1):755-775. doi:10.1146/annurev.biochem.70.1.755.

154. Egea PF, Stroud RM, Walter P. Targeting proteins to membranes: Structure of the signal recognition particle. *Curr Opin Struct Biol*. 2005;15(2):213-220. doi:10.1016/j.sbi.2005.03.007.

155. Bernstein HD, Poritz MA, Strub K, Hoben PJ, Brenner S, Walter P. Model for signal sequence recognition from amino-acid sequence of 54K subunit of signal recognition particle. *Nature*. 1989;340(6233):482-6. doi:10.1038/340482a0.

156. Prinz A, Behrens C, Rapoport TA, Hartmann E, Kalies KU. Evolutionarily conserved binding of ribosomes to the translocation channel via the large ribosomal RNA. *EMBO J*. 2000;19(8):1900-1906. doi:10.1093/emboj/19.8.1900.

157. Neumann-Haefelin C, Schäfer U, Müller M, Koch HG. SRP-dependent co-translational targeting and SecA-dependent translocation analyzed as individual steps in the export of a bacterial protein. *EMBO J*. 2000;19(23):6419-6426. doi:10.1093/emboj/19.23.6419.

158. White SH, von Heijne G. How translocons select transmembrane helices. *Annu Rev Biophys*. 2008;37:23-42. doi:10.1146/annurev.biophys.37.032807.125904.

159. Cymer F, von Heijne G, White SH. Mechanisms of Integral Membrane Protein Insertion and Folding. *J Mol Biol*. 2015;427(5):999-1022. doi:10.1016/ j.jmb.2014.09.014.

160. Dalbey RE, Kuhn A. YidC family members are involved in the membrane insertion, lateral integration, folding, and assembly of membrane proteins. *J Cell Biol*. 2004;166(6):769-74. doi:10.1083/jcb.200405161.

161. Laan M van der, Nouwen NP, Driessen AJ. YidC – an evolutionary conserved device for the assembly of energy-transducing membrane protein complexes. *Curr Opin Microbiol*. 2005;8(2):182-187. doi:10.1016/j.mib.2005.02.004.

162. Prabudiansyah I, Driessen AJM. The Canonical and Accessory Sec System of Gram-positive Bacteria. In: Springer Berlin Heidelberg; 2016:1-23. doi:10.1007/ 82_2016_9.

163. Zhou J, Xu Z. Structural determinants of SecB recognition by SecA in bacterial protein translocation. *Nat Struct Biol*. 2003;10(11):942-947. doi:10.1038/ nsb980.

164. Driessen AJM. SecB, a molecular chaperone with two faces. *Trends Microbiol*. 2001;9(5):193-196. doi:10.1016/S0966-842X(01)01980-1.

165. Poritz MA, Bernstein HD, Strub K, Zopf D, Wilhelm H, Walter P. An E. coli ribonucleoprotein containing 4.5S RNA resembles mammalian signal recognition particle. *Science*. 1990;250(4984):1111-1117. doi:10.1126/science.1701272.

166. Estrozi LF, Boehringer D, Shan S-O, Ban N, Schaffitzel C. Cryo-EM structure of the E. coli translating ribosome in complex with SRP and its receptor. *Nat Struct Mol Biol*. 2011;18(1):88-90. doi:10.1038/nsmb.1952.

167. Ataide SF, Schmitz N, Shen K, et al. The crystal structure of the signal recognition particle in complex with its receptor. *Science*. 2011;331(6019):881-886. doi:10.1126/science.1196473.

168. Jomaa A, Boehringer D, Leibundgut M, Ban N. Structures of the E. coli translating ribosome with SRP and its receptor and with the translocon. *Nat Commun*. 2016;7:10471. doi:10.1038/ncomms10471.

169. Oliver DB, Beckwith J. Regulation of a membrane component required for protein secretion in Escherichia coli. *Cell*. 1982;30(1):311-319. doi:10.1016/0092-8674(82)90037-X.

170. Lill R, Dowhan W, Wickner W. The ATPase activity of secA is regulated by acidic phospholipids, secY, and the leader and mature domains of precursor proteins. *Cell*. 1990;60(2):271-280. doi:10.1016/0092-8674(90)90742-W.

171. Koch S, de Wit JG, Vos I, et al. Lipids activate SecA for high affinity binding to the SecYEG complex. *J Biol Chem*. 2016:jbc.M116.743831. doi:10.1074/jbc.M116.743831.

172. Ding H, Hunt JF, Mukerji I, Oliver D. Bacillus subtilis SecA ATPase exists as an antiparallel dimer in solution. *Biochemistry*. 2003;42(29):8729-8738. doi:10.1021/bi0342057.

173. Osborne AR, Clemons WM, Rapoport TA. A large conformational change of the translocation ATPase SecA. *Proc Natl Acad Sci U S A*. 2004;101(30):10937-42. doi:10.1073/pnas.0401742101.

174. Papanikolau Y, Papadovasilaki M, Ravelli RBG, et al. Structure of dimeric SecA, the Escherichia coli preprotein translocase motor. *J Mol Biol*. 2007;366(5):1545-57. doi:10.1016/j.jmb.2006.12.049.

175. Zimmer J, Nam Y, Rapoport TA. Structure of a complex of the ATPase SecA and the protein-translocation channel. *Nature*. 2008;455(7215):936-43. doi:10.1038/nature07335.

176. Zimmer J, Rapoport TA. Conformational flexibility and peptide interaction of the translocation ATPase SecA. *J Mol Biol*. 2009;394(4):606-12. doi:10.1016/j.jmb.2009.10.024.

177. Li L, Park E, Ling J, Ingram J, Ploegh H, Rapoport TA. Crystal structure of a substrate-engaged SecY protein-translocation channel. *Nature*. 2016;531(7594): 395-399. doi:10.1038/nature17163.

178. Papanikou E, Karamanou S, Baud C, et al. Identification of the preprotein binding domain of SecA. *J Biol Chem*. 2005;280(52):43209-17. doi:10.1074/ jbc.M509990200.

179. Musial-Siwek M, Rusch SL, Kendall DA. Probing the affinity of SecA for signal peptide in different environments. *Biochemistry*. 2005;44(42):13987-96. doi:10.1021/bi050882k.

180. Gelis I, Bonvin AMJJ, Keramisanou D, et al. Structural basis for signal-sequence recognition by the 204-kDA translocase motor SecA as determined by NMR. *Cell*. 2007;131(4):756-69. doi:10.1016/j.cell.2007.09.039.

181. Cooper DB, Smith VF, Crane JM, Roth HC, Lilly AA, Randall LL. SecA, the motor of the secretion machine, binds diverse partners on one interactive surface. *J Mol Biol*. 2008;382(1):74-87. doi:10.1016/j.jmb.2008.06.049.

182. Fekkes P, De Wit JG, Van Der Wolk JPW, Kimsey HH, Kumamoto CA, Driessen AJM. Preprotein transfer to the Escherichia coli translocase requires the co-operative binding of SecB and the signal sequence to SecA. *Mol Microbiol*. 1998;29(5):1179-1190. doi:10.1046/j.1365-2958.1998.00997.x.

183. Breukink E, Nouwen N, van Raalte A, Mizushima S, Tommassen J, de Kruijff B. The C terminus of SecA is involved in both lipid binding and SecB binding. *J Biol Chem*. 1995;270(14):7902-7. doi:10.1074/jbc.270.14.7902.

184. Koonin E V., Gorbalenya AE. Autogenous translation regulation by Escherichia coli ATPase SecA may be mediated by an intrinsic RNA helicase activity of this protein. *FEBS Lett*. 1992;298(1):6-8. doi:10.1016/0014-5793(92)80009-6.

185. Robson A, Booth AEG, Gold VAM, Clarke AR, Collinson I. A Large Conformational Change Couples the ATP Binding Site of SecA to the SecY Protein Channel. *J Mol Biol*. 2007;374(4):965-976. doi:10.1016/j.jmb.2007.09.086.

186. Sianidis G, Karamanou S, Vrontou E, et al. Cross-talk between catalytic and regulatory elements in a DEAD motor domain is essential for SecA function. *EMBO J*. 2001;20(5):961-970. doi:10.1093/emboj/20.5.961.

187. Karamanou S, Vrontou E, Sianidis G, et al. A molecular switch in SecA protein couples ATP hydrolysis to protein translocation. *Mol Microbiol*. 1999;34(5):1133-1145. doi:10.1046/j.1365-2958.1999.01686.x.

188. Mori H, Ito K. The long α-helix of SecA is important for the ATPase coupling of translocation. *J Biol Chem*. 2006;281(47):36249-36256. doi:10.1074/ jbc.M606906200.

189. Van Der Does C, Manting EH, Kaufmann A, Lutz M, Driessen AJM. Interaction between SecA and SecYEG in micellar solution and formation of the membrane-inserted state. *Biochemistry*. 1998;37(1):201-210. doi:10.1021/bi972105t.

190. Eichler J, Wickner W. Both an N-terminal 65-kDa domain and a C-terminal 30-kDa domain of SecA cycle into the membrane at SecYEG during translocation. *Proc Natl Acad Sci U S A*. 1997;94(11):5574-81. doi:10.1073/pnas.94.11.5574.

191. Chen Y, Bauer BW, Rapoport TA, Gumbart JC. Conformational changes of the clamp of the protein translocation ATPase SecA. *J Mol Biol*. 2015;427(14):2348-2359. doi:10.1016/j.jmb.2015.05.003.

192. Bauer BW, Rapoport TA. Mapping polypeptide interactions of the SecA ATPase during translocation. *Proc Natl Acad Sci U S A*. 2009;106(49):20800-20805. doi:10.1073/pnas.0910550106.

193. Whitehouse S, Gold VAM, Robson A, Allen WJ, Sessions RB, Collinson I. Mobility of the SecA 2-helix-finger is not essential for polypeptide translocation via the SecYEG complex. *J Cell Biol*. 2012;199(6):919-929. doi:10.1083/jcb.201205191.

194. Zhang Q, Lahiri S, Banerjee T, Sun Z, Oliver D, Mukerji I. Alignment of the protein substrate hairpin along the SecA two-helix finger primes protein transport in Escherichia coli. *Proc Natl Acad Sci U S A*. 2017;114(35):9343-9348. doi:10.1073/pnas.1702201114.

195. Catipovic MA, Bauer BW, Loparo JJ, Rapoport TA. Protein translocation by the SecA ATPase occurs by a power-stroke mechanism. *EMBO J*. 2019. doi:10.15252/embj.2018101140.

196. Breyton C, Haase W, Rapoport TA, Kühlbrandt W, Collinson I. Three-dimensional structure of the bacterial protein-translocation complex SecYEG. *Nature*. 2002;418(6898):662-5. doi:10.1038/nature00827.

197. Mitra K, Schaffitzel C, Shaikh T, et al. Structure of the E. coli protein-conducting channel bound to a translating ribosome. *Nature*. 2005;438(7066):318-324. doi:10.1038/nature05086.

198. Hizlan D, Robson A, Whitehouse S, et al. Structure of the SecY Complex Unlocked by a Preprotein Mimic. *Cell Rep*. 2012;1(1):21-28. doi:10.1016/ j.celrep.2011.11.003.

199. Voorhees RM, Hegde RS. Structure of the Sec61 channel opened by a signal sequence. *Science*. 2016;351(6268):88-91. doi:10.1126/science.aad4992.

200. Tsukazaki T, Mori H, Fukai S, et al. Conformational transition of Sec machinery inferred from bacterial SecYE structures. *Nature*. 2008;455(7215):988-91. doi:10.1038/nature07421.

201. Egea PF, Stroud RM. Lateral opening of a translocon upon entry of protein suggests the mechanism of insertion into membranes. *Proc Natl Acad Sci U S A*. 2010;107(40):17182-17187. doi:10.1073/pnas.1012556107.

202. Tanaka Y, Sugano Y, Takemoto M, et al. Crystal Structures of SecYEG in Lipidic Cubic Phase Elucidate a Precise Resting and a Peptide-Bound State. *Cell Rep*. 2015;13(8):1561-1568. doi:10.1016/j.celrep.2015.10.025.

203. Murphy CK, Beckwith J. Residues essential for the function of SecE, a membrane component of the Escherichia coli secretion apparatus, are located in a conserved cytoplasmic region. *Proc Natl Acad Sci U S A*. 1994;91(7):2557-61.

204. Kihara A, Akiyama Y, Ito K. FtsH is required for proteolytic elimination of uncomplexed forms of SecY, an essential protein translocase subunit. *Proc Natl Acad Sci U S A*. 1995;92(10):4532-4536. doi:10.1073/pnas.92.10.4532.

205. Schatz PJ, Bieker KL, Ottemann KM, Silhavy TJ, Beckwith J. One of three transmembrane stretches is sufficient for the functioning of the SecE protein, a membrane component of the E. coli secretion machinery. *EMBO J*. 1991;10(7):1749-57.

206. Tokuda H, Akimaru J, Matsuyama S, Nishiyama K, Mizushima S. Purification of SecE and reconstitution of SecE-dependent protein translocation activity. *FEBS Lett*. 1991;279(2):233-6. doi:10.1016/0014-5793(91)80156-W.

207. Nishiyama K, Mizushima S, Tokuda H. The carboxyl-terminal region of SecE interacts with SecY and is functional in the reconstitution of protein translocation activity in Escherichia coli. *J Biol Chem*. 1992;267(10):7170-6.

208. Pohlschröder M, Murphy C, Beckwith J. In vivo analyses of interactions between SecE and SecY, core components of the Escherichia coli protein translocation machinery. *J Biol Chem*. 1996;271(33):19908-14. doi:10.1074/jbc.271.33.19908.

209. Lycklama a Nijeholt JA, de Keyzer J, Prabudiansyah I, Driessen AJM. Characterization of the supporting role of SecE in protein translocation. *FEBS Lett*. 2013;587(18):3083-8. doi:10.1016/j.febslet.2013.07.046.

210. Nishiyama K, Mizushima S, Tokuda H. A novel membrane protein involved in protein translocation across the cytoplasmic membrane of Escherichia coli. *EMBO J*. 1993;12(9):3409-15.

211. Nishiyama K, Hanada M, Tokuda H. Disruption of the gene encoding p12 (SecG) reveals the direct involvement and important function of SecG in the protein translocation of Escherichia coli at low temperature. *EMBO J*. 1994;13(14):3272-7.

212. Hanada M, Nishiyama K, Tokuda H. SecG plays a critical role in protein translocation in the absence of the proton motive force as well as at low temperature. *FEBS Lett*. 1996;381(1-2):25-8.

213. Van der Sluis EO, Nouwen N, Driessen AJM. SecY-SecY and SecY-SecG contacts revealed by site-specific crosslinking. *FEBS Lett*. 2002;527(1-3):159-165. doi:10.1016/S0014-5793(02)03202-7.

214. Satoh Y, Matsumoto G, Mori H, Ito K. Nearest neighbor analysis of the SecYEG complex. 1. Identification of a SecY-SecG interface. *Biochemistry*. 2003;42(24):7434-41. doi:10.1021/bi034331a.

215. Mori H, Shimokawa N, Satoh Y, Ito K. Mutational analysis of transmembrane regions 3 and 4 of SecY, a central component of protein translocase. *J Bacteriol*. 2004;186(12):3960-9. doi:10.1128/JB.186.12.3960-3969.2004.

216. Kato Y, Nishiyama K, Tokuda H. Depletion of SecDF-YajC causes a decrease in the level of SecG: implication for their functional interaction. *FEBS Lett*. 2003;550(1-3):114-8. doi:10.1016/S0014-5793(03)00847-0.

217. Mori H, Sugiyama H, Yamanaka M, Sato K, Tagaya M, Mizushima S. Amino-Terminal Region of SecA Is Involved in the Function of SecG for Protein Translocation into Escherichia coli Membrane Vesicles. *J Biochem*. 1998;124(1):122-129. doi:10.1093/oxfordjournals.jbchem.a022070.

218. Suzuki H, Nishiyama K, Tokuda H. Coupled structure changes of SecA and SecG revealed by the synthetic lethality of the secAcsR11 and ΔsecG::kan double mutant. *Mol Microbiol*. 1998;29(1):331-41. doi:10.1046/j.1365-2958.1998.00937.x.

219. Das S, Oliver DB. Mapping of the SecA-SecY and SecA-SecG interfaces by site-directed in vivo photocross-linking. *J Biol Chem*. 2011;286(14):12371-12380. doi:10.1074/jbc.M110.182931.

220. Nishiyama K, Suzuki T, Tokuda H. Inversion of the membrane topology of SecG coupled with SecA-dependent preprotein translocation. *Cell*. 1996;85(1):71-81. doi:10.1016/S0092-8674(00)81083-1.

221. Matsumoto G, Mori H, Ito K. Roles of SecG in ATP- and SecA-dependent protein translocation. *Proc Natl Acad Sci U S A*. 1998;95(23):13567-13572. doi:10.1073/pnas.95.23.13567.

222. Nagamori S, Nishiyama K, Tokuda H. Membrane topology inversion of SecG detected by labeling with a membrane-impermeable sulfhydryl reagent that causes a close association of SecG with SecA. *J Biochem*. 2002;132(4):629-34.

223. Sugai R, Takemae K, Tokuda H, Nishiyama K. Topology inversion of SecG is essential for cytosolic SecA-dependent stimulation of protein translocation. *J Biol Chem*. 2007;282(40):29540-8. doi:10.1074/jbc.M704716200.

224. van der Sluis EO, van der Vries E, Berrelkamp G, Nouwen N, Driessen AJM. Topologically fixed SecG is fully functional. *J Bacteriol*. 2006;188(3):1188-90. doi:10.1128/JB.188.3.1188-1190.2006.

225. Homma T, Yoshihisa T, Ito K. Subunit interactions in the Escherichia coli protein translocase: SecE and SecG associate independently with SecY. *FEBS Lett*. 1997;408(1):11-15. doi:10.1016/S0014-5793(97)00376-1.

226. Flower AM, Hines LL, Pfennig PL. SecG is an auxiliary component of the protein export apparatus of Escherichia coli. *Mol Gen Genet*. 2000;263(1):131-136. doi:10.1016/j.molcel.2007.03.022.

227. Gumbart J, Schulten K. The Roles of Pore Ring and Plug in the SecY Protein-conducting Channel. *J Gen Physiol*. 2008;132(6):709-719. doi:10.1085/jgp.200810062.

228. Park E, Rapoport TA. Preserving the membrane barrier for small molecules during bacterial protein translocation. *Nature*. 2011;473(7346):239-42. doi:10.1038/nature10014.

229. Lycklama A Nijeholt JA, Bulacu M, Marrink SJ, Driessen AJM. Immobilization of the plug domain inside the SecY channel allows unrestricted protein translocation. *J Biol Chem*. 2010;285(31):23747-23754. doi:10.1074/ jbc.M110.124636.

230. Ménétret J-F, Neuhof A, Morgan DG, et al. The Structure of Ribosome-Channel Complexes Engaged in Protein Translocation. *Mol Cell*. 2000;6(5):1219-1232. doi:10.1016/S1097-2765(00)00118-0.

231. van der Sluis EO, Nouwen N, Koch J, et al. Identification of Two Interaction Sites in SecY that Are Important for the Functional Interaction with SecA. *J Mol Biol*. 2006;361(5):839-849. doi:10.1016/j.jmb.2006.07.017.

232. Mori H, Ito K. Different modes of SecY-SecA interactions revealed by site-directed in vivo photo-cross-linking. *Proc Natl Acad Sci U S A*. 2006;103(44):16159-64. doi:10.1073/pnas.0606390103.

233. Plath K, Mothes W, Wilkinson BM, Stirling CJ, Rapoport TA. Signal sequence recognition in posttranslational protein transport across the yeast ER membrane. *Cell*. 1998;94(6):795-807. doi:10.1016/S0092-8674(00)81738-9.

234. Fessl T, Watkins D, Oatley P, et al. Dynamic action of the Sec machinery during initiation, protein translocation and termination revealed by single molecule fluorescence. 2018. doi:10.1101/248310.

235. Junne T, Schwede T, Goder V, Spiess M. The plug domain of yeast Sec61p is important for efficient protein translocation, but is not essential for cell viability. *Mol Biol Cell*. 2006;17(9):4063-4068. doi:10.1091/mbc.E06-03-0200.

236. Maillard AP, Lalani S, Silva F, Belin D, Duong F. Deregulation of the SecYEG translocation channel upon removal of the plug domain. *J Biol Chem*. 2007;282(2):1281-1287. doi:10.1074/jbc.M610060200.

237. Harris CR, Silhavy TJ. Mapping an interface of SecY (PrlA) and SecE (PrlG) by using synthetic phenotypes and in vivo cross-linking. *J Bacteriol*. 1999;181 (11):3438-44.

238. Lycklama A Nijeholt JA, Wu ZC, Driessen AJM. Conformational dynamics of the plug domain of the SecYEG protein-conducting channel. *J Biol Chem*. 2011;286(51):43881-43890. doi:10.1074/jbc.M111.297507.

239. Sagara K, Matsuyama SI, Mizushima S. SecF stabilizes SecD and SecY, components of the protein translocation machinery of the Escherichia coli cytoplasmic membrane. *J Bacteriol*. 1994;176(13):4111-4116.

240. Gardel C, Johnson K, Jacq A, Beckwith J. The secD locus of E. coli codes for two membrane proteins required for protein export. *EMBO J*. 1990;9(10):4205-4206.

241. Tsukazaki T, Mori H, Echizen Y, et al. Structure and function of a membrane component SecDF that enhances protein export. *Nature*. 2011;474(7350):235-238. doi:10.1038/nature09980.

242. Pogliano J a, Beckwith J. SecD and SecF facilitate protein export in Escherichia coli. *EMBO J*. 1994;13(3):554-561.

243. Luirink J, Samuelsson T, De Gier JW. YidC/Oxa1p/Alb3: Evolutionarily conserved mediators of membrane protein assembly. *FEBS Lett*. 2001;501(1):1-5. doi:10.1016/S0014-5793(01)02616-3.

244. Samuelson JC, Jiang F, Yi L, et al. Function of YidC for the Insertion of M13 Procoat Protein in Escherichia coli. *J Biol Chem*. 2001;276(37):34847-34852. doi:10.1074/jbc.M105793200.

245. Chen M, Samuelson JC, Jiang F, Muller M, Kuhn A, Dalbey RE. Direct interaction of YidC with the Sec-independent Pf3 coat protein during its membrane protein insertion. *J Biol Chem*. 2002;277(10):7670-7675. doi:10.1074/jbc.M110644200.

246. Van Der Laan M, Bechduft P, Kol S, Nouwen N, Driessen AJM. F1F0 ATP synthase subunit c is a substrate of the novel YidC pathway for membrane protein biogenesis. *J Cell Biol*. 2004;165(2):213-222. doi:10.1083/jcb.200402100.

247. Price CE, Kocer A, Kol S, Van Der Berg JP, Driessen AJM. In vitro synthesis and oligomerization of the mechanosensitive channel of large conductance, MscL, into a functional ion channel. *FEBS Lett*. 2011;585(1):249-254. doi:10.1016/ j.febslet.2010.11.057.

248. Klostermann E, Droste Gen Helling I, Carde J-P, Schünemann D. The thylakoid membrane protein ALB3 associates with the cpSecY-translocase in Arabidopsis thaliana. *Biochem J*. 2002;368(Pt 3):777-781. doi:10.1042/BJ20021291.

249. van der Laan M, Urbanus ML, Ten Hagen-Jongman CM, et al. A conserved function of YidC in the biogenesis of respiratory chain complexes. *Proc Natl Acad Sci U S A*. 2003;100(10):5801-5806. doi:10.1073/pnas.0636761100.

250. Yi L, Celebi N, Chen M, Dalbey RE. Sec/SRP requirements and energetics of membrane insertion of subunits a, b, and c of the Escherichia coli F1F0 ATP synthase. *J Biol Chem*. 2004;279(38):39260-39267. doi:10.1074/ jbc.M405490200.

251. Van Bloois E, Haan GJ, De Gier JW, Oudega B, Luirink J. Distinct requirements for translocation of the N-tail and C-tail of the Escherichia coli inner membrane protein CyoA. *J Biol Chem*. 2006;281(15):10002-10009. doi:10.1074/ jbc.M511357200.

252. Du Plessis DJF, Nouwen N, Driessen AJM. Subunit a of cytochrome o oxidase requires both YidC and SecYEG for membrane insertion. *J Biol Chem*. 2006;281(18):12248-12252. doi:10.1074/jbc.M600048200.

253. Kol S, Majczak W, Heerlien R, van der Berg JP, Nouwen N, Driessen AJM. Subunit a of the F1F0 ATP Synthase Requires YidC and SecYEG for Membrane Insertion. *J Mol Biol*. 2009;390(5):893-901. doi:10.1016/j.jmb.2009.05.074.

254. Price CE, Driessen AJM. Conserved negative charges in the transmembrane segments of subunit K of the NADH:ubiquinone oxidoreductase determine its dependence on YidC for membrane insertion. *J Biol Chem*. 2010;285(6):3575-3581. doi:10.1074/jbc.M109.051128.

255. Wagner S, Pop O, Haan GJ, et al. Biogenesis of MalF and the MalFGK2 maltose transport complex in Escherichia coli requires YidC. *J Biol Chem*. 2008;283(26):17881-17890. doi:10.1074/jbc.M801481200.

256. Zhu L, Kaback HR, Dalbey RE. YidC protein, a molecular chaperone for LacY protein folding via the SecYEG protein machinery. *J Biol Chem*. 2013;288(39):28180-28194. doi:10.1074/jbc.M113.491613.

257. de Sousa Borges A, de Keyzer J, Driessen AJM, Scheffers D-J. The Escherichia coli membrane protein insertase YidC assists in the biogenesis of penicillin binding proteins. *J Bacteriol*. 2015;197(8):1444-50. doi:10.1128/JB.02556-14.

258. Saller MJ, Wu ZC, De Keyzer J, Driessen AJM. The YidC/Oxa1/Alb3 protein family: Common principles and distinct features. *Biol Chem*. 2012;393(11):1279-1290. doi:10.1515/hsz-2012-0199.

259. Hennon SW, Soman R, Zhu L, Dalbey RE. YidC/Alb3/Oxa1 family of insertases. *J Biol Chem*. 2015;290(24):14866-14874. doi:10.1074/jbc.R115.638171.

260. Angelini S, Deitermann S, Koch H-G. FtsY, the bacterial signal-recognition particle receptor, interacts functionally and physically with the SecYEG translocon. *EMBO Rep*. 2005;6(5):476-481. doi:10.1038/sj.embor.7400385.

261. Shimoike T, Taura T, Kihara A, et al. Product of a new gene, syd, functionally interacts with SecY when overproduced in Escherichia coli. *J Biol Chem*. 1995;270(10):5519-5526. doi:10.1074/jbc.270.10.5519.

262. Matsuo EI, Mori H, Shimoike T, Ito K. Syd, a secY-interacting protein, excludes SecA from the SecYE complex with an altered SecY24 subunit. *J Biol Chem*. 1998;273(30):18835-18840. doi:10.1074/jbc.273.30.18835.

263. Matsuo E, Ito K. Genetic analysis of an essential cytoplasmic domain of Escherichia coli SecY based on resistance to Syd, a SecY-interacting protein. *Mol Gen Genet*. 1998;258(3):240-249. doi:10.1007/s004380050728.

264. Dalal K, Nguyen N, Alami M, et al. Structure, binding, and activity of Syd, a SecY-interacting protein. *J Biol Chem*. 2009;284(12):7897-7902. doi:10.1074/jbc.M808305200.

265. Sachelaru I, Petriman NA, Kudva R, Koch HG. Dynamic interaction of the Sec translocon with the chaperone PpiD. *J Biol Chem*. 2014;289(31):21706-21715. doi:10.1074/jbc.M114.577916.

266. Geng Y. Membrane protein insertases of the YidC/Oxa1/Alb3 protein Family. University of Groningen. 2015.

267. Musial-Siwek M, Rusch SL, Kendall DA. Selective Photoaffinity Labeling Identifies the Signal Peptide Binding Domain on SecA. *J Mol Biol*. 2007;365(3):637-648. doi:10.1016/j.jmb.2006.10.027.

268. Cunningham K, Lill R, Crooke E, et al. SecA protein, a peripheral protein of the Escherichia coli plasma membrane, is essential for the functional binding and translocation of proOmpA. *EMBO J*. 1989;8(3):955-959.

269. Hendrick JP, Wickner W. SecA protein needs both acidic phospholipids and SecY/E protein for functional high-affinity binding to the Escherichia coli plasma membrane. *J Biol Chem*. 1991;266(36):24596-600.

270. Floyd JH, You Z, Hsieh YH, Ma Y, Yang H, Tai PC. The dispensability and requirement of SecA N-terminal aminoacyl residues for complementation, membrane binding, lipid-specific domains and channel activities. *Biochem Biophys Res Commun*. 2014;453(1):138-142. doi:10.1016/j.bbrc.2014.09.080.

271. Bauer BW, Shemesh T, Chen Y, Rapoport TA. A "Push and Slide" Mechanism Allows Sequence-Insensitive Translocation of Secretory Proteins by the SecA ATPase. *Cell*. 2014;157(6):1416-1429. doi:10.1016/j.cell.2014.03.063.

272. Hoyt DW, Gierasch LM. A peptide corresponding to an export-defective mutant OmpA signal sequence with asparagine in the hydrophobic core is unable to insert into model membranes. *J Biol Chem*. 1991;266(22):14406-14412.

273. Killian J a, de Jong a M, Bijvelt J, Verkleij a J, de Kruijff B. Induction of non-bilayer lipid structures by functional signal peptides. *Embo J*. 1990;9(3):815-819.

274. Van Raalte ALJ, Demel RA, Verberkmoes G, Breukink E, Keller RCA, De Kruijff B. Influence of the signal sequence and chaperone SecB on the interaction between precursor protein prePhoE and phospholipids. *Eur J Biochem*. 1996;235(1-2):207-214.

275. Batenburg AM, Demel RA, Verkleij AJ, de Kruijff B. Penetration of the Signal Sequence of Escherichia coli PhoE Protein into Phospholipid Model Membranes Leads to Lipid-Specific Changes in Signal Peptide Structure and Alterations of Lipid Organization. *Biochemistry*. 1988;27(15):5678-5685. doi:10.1021/ bi00415a043.

276. de Vrije T, de Swart RL, Dowhan W, Tommassen J, de Kruijff B. Phosphatidylglycerol is involved in protein translocation across Escherichia coli inner membranes. *Nature*. 1988;334(6178):173-175. doi:10.1038/334173a0.

277. de Keyzer J, van der Sluis EO, Spelbrink REJ, et al. Covalently Dimerized SecA Is Functional in Protein Translocation. *J Biol Chem*. 2005;280(42):35255-35260. doi:10.1074/jbc.M506157200.

278. Rajapandi T, Dolan KM, Oliver DB. The first gene in the Escherichia coli secA operon, gene X, encodes a nonessential secretory protein. *J Bacteriol*. 1991;173(22):7092-7097.

279. Karamanou S, Gouridis G, Papanikou E, et al. Preprotein-controlled catalysis in the helicase motor of SecA. *EMBO J*. 2007;26(12):2904-2914. doi:10.1038/ sj.emboj.7601721.

280. Suo Y, Hardy SJS, Randall LL. Orientation of SecA and SecB in complex, derived from disulfide cross-linking. *J Bacteriol*. 2011;193(1):190-196. doi:10.1128/ JB.00975-10.

281. Natale P, Swaving J, Van Der Does C, De Keyzer J, Driessen AJM. Binding of SecA to the SecYEG Complex Accelerates the Rate of Nucleotide Exchange on SecA. *J Biol Chem*. 2004;279(14):13769-13777. doi:10.1074/jbc.M312892200.

282. Engelman DM, Steitz TA. The spontaneous insertion of proteins into and across membranes: The helical hairpin hypothesis. *Cell*. 1981;23(2):411-422. doi:10.1016/0092-8674(81)90136-7.

283. Joly JC, Wickner W. The SecA and SecY subunits of translocase are the nearest neighbors of a translocating preprotein, shielding it from phospholipids. *EMBO J*. 1993;12(1):255-63.

284. Economou A, Pogliano JA, Beckwith J, Oliver DB, Wickner W. SecA membrane cycling at SecYEG is driven by distinct ATP binding and hydrolysis events and is regulated by SecD and SecF. *Cell*. 1995;83(7):1171-1181. doi:10.1016/0092-8674(95)90143-4.

285. Dalbey RE, Chen M. Sec-translocase mediated membrane protein biogenesis. *Biochim Biophys Acta - Mol Cell Res*. 2004;1694(1-3 SPEC.ISS.):37-53. doi:10.1016/j.bbamcr.2004.03.009.

286. Gogala M, Becker T, Beatrix B, et al. Structures of the Sec61 complex engaged in nascent peptide translocation or membrane insertion. *Nature*. 2014;506(7486):107-10. doi:10.1038/nature12950.

287. Bonardi F, London G, Nouwen N, Feringa BL, Driessen AJM. Light-induced control of protein translocation by the SecYEG complex. *Angew Chemie - Int Ed*. 2010;49(40):7234-7238. doi:10.1002/anie.201002243.

288. Gumbart J, Chipot C, Schulten K. Free energy of nascent-chain folding in the translocon. *J Am Chem Soc*. 2011;133(19):7602-7607. doi:10.1021/ja2019299.

289. Gumbart J, Schulten K. Structural determinants of lateral gate opening in the protein translocon. *Biochemistry*. 2007;46(39):11147-11157. doi:10.1021/ bi700835d.

290. Mori T, Ishitani R, Tsukazaki T, Nureki O, Sugita Y. Molecular mechanisms underlying the early stage of protein translocation through the Sec translocon. *Biochemistry*. 2010;49(5):945-950. doi:10.1021/bi901594w.

291. Zhang B, Miller TF. Direct simulation of early-stage sec-facilitated protein translocation. *J Am Chem Soc*. 2012;134(33):13700-13707. doi:10.1021/ ja3034526.

292. Van der Does C, De Keyzer J, Van der Laan M, Driessen AJM. Reconstitution of Purified Bacterial Preprotein Translocase in Liposomes. *Methods Enzymol*. 2003;372(2000):86-98. doi:10.1016/S0076-6879(03)72005-9.

293. Kusters I, van den Bogaart G, de Wit J, Krasnikov V, Poolman B, Driessen A. Purification and functional reconstitution of the bacterial protein translocation pore, the SecYEG complex. In: *Methods in molecular biology (Clifton, N.J.)*.Vol 619.; 2010:131-143. doi:10.1007/978-1-60327-412-8_8.

294. Hanahan D. Studies on transformation of Escherichia coli with plasmids. *J Mol Biol*. 1983;166(4):557-580. doi:10.1016/S0022-2836(83)80284-8.

295. Baneyx F, Georgiou G. In vivo degradation of secreted fusion proteins by the Escherichia coli outer membrane protease OmpT. *J Bacteriol*. 1990;172(1):491-494.

296. Nouwen N, Van der Laan M, Driessen AJM. SecDFyajC is not required for the maintenance of the proton motive force. *FEBS Lett*. 2001;508(1):103-106. doi:10.1016/S0014-5793(01)03033-2.

297. Kramer RA, Dekker N, Egmond MR. Identification of active site serine and histidine residues in Escherichia coli outer membrane protease OmpT. *FEBS Lett*. 2000;468(2-3):220-224. doi:10.1016/S0014-5793(00)01231-X.

298. Klose M, Schimz KL, Van der Wolk J, Driessen AJM, Freudl R. Lysine 106 of the putative catalytic ATP-binding site of the Bacillus subtilis SecA protein is required for functional complementation of Escherichia coli secA mutants in vivo. *J Biol Chem*. 1993;268(6):4504-4510.

299. Wu Z, de Keyzer J, Kusters I, Driessen A. Analysis of the interaction between membrane proteins and soluble binding partners by surface plasmon resonance. In: *Methods in molecular biology (Clifton, N.J.)*.Vol 1033.; 2013:157-172. doi:10.1007/978-1-62703-487-6_11.

300. Li Y-J, Rothwarf DM, Scheraga HA. An unusual adduct of dithiothreitol with a pair of cysteine residues of a protein as a stable folding intermediate. *J Am Chem Soc*. 1998;120(11):2668-2669. doi:10.1021/ja973625e.

301. Li X, Han Y, Pan XM. Cysteine-25 of adenylate kinase reacts with dithiothreitol to form an adduct upon aging of the enzyme. *FEBS Lett*. 2001;507(2):169-173. doi:10.1016/S0014-5793(01)02954-4.

302. Begg GE, Speicher DW. Mass spectrometry detection and reduction of disulfide adducts between reducing agents and recombinant proteins with highly reactive cysteines. *J Biomol Tech*. 1999;10(1):17-20.

303. Manting EH, Kaufmann A, Van Der Does C, Driessen AJM. A single amino acid substitution in SecY stabilizes the interaction with SecA. *J Biol Chem*. 1999;274(34):23868-23874. doi:10.1074/jbc.274.34.23868.

304. Van Der Wolk JPW, Fekkes P, Boorsma A, Huie JL, Silhavy TJ, Driessen AJM. PrlA4 prevents the rejection of signal sequence defective preproteins by stabilizing the SecA-SecY interaction during the initiation of translocation. *EMBO J*. 1998;17(13):3631-3639. doi:10.1093/emboj/17.13.3631.

305. Kaufman H, Vratsanos SM, Erlanger BF. Photoregulation of an enzymic process by means of a light-sensitive ligand. *Science*. 1968;162(3861):1487-1489. doi:10.1126/science.162.3861.1487.

306. Bieth J, Vratsanos SM, Wassermann N, Erlanger BF. Photoregulation of Biological Activity By Photocromic Reagents, II. Inhibitors of Acetylcholinesterase. *Proc Natl Acad Sci*. 1969;64(3):1103-1106. doi:10.1073/pnas.64.3.1103.

307. Bieth J, Wassermann N, Vratsanos SM, Erlanger BF. Photoregulation of biological activity by photochromic reagents, IV. A model for diurnal variation of enzymic activity. *Proc Natl Acad Sci U S A*. 1970;66(3):850-4. doi:10.1073/pnas.66.3.850.

308. Bartels E, Wassermann NH, Erlanger BF. Photochromic activators of the acetylcholine receptor. *Proc Natl Acad Sci USA*. 1971;68(8):1820-1823. doi:10.1073/pnas.68.8.1820.

309. Changeux J, Podleski T. On the Excitability and Cooperativity of the Electroplax Membrane. *Proc Natl Acad Sci U S A*. 1968;59(3):944-950.

310. Deal WJ, Erlanger BF, Nachmansohn D. Photoregulation of biological activity by photochromic reagents, iii. photoregulation of bioelectricity by acetylcholine receptor inhibitors. *Proc Natl Acad Sci U S A*. 1969;64(4):1820-1823. doi:DOI 10.1073/pnas.64.4.1230.

311. Willner I, Rubin S, Riklin A. Photoregulation of papain activity through anchoring photochromic azo groups to the enzyme backbone. *J Am Chem Soc*. 1991;113(9):3321-3325. doi:10.1021/ja00009a016.

312. Xu Z, Shi L, Jiang D, Cheng J, Shao X, Li Z. Azobenzene Modified Imidacloprid Derivatives as Photoswitchable Insecticides: Steering Molecular Activity in a Controllable Manner. *Sci Rep*. 2015;5:13962. doi:10.1038/srep13962.

313. Velema WA, van der Berg JP, Hansen MJ, Szymanski W, Driessen AJM, Feringa BL. Optical control of antibacterial activity. *Nat Chem*. 2013;5(11):924-928. doi:10.1038/nchem.1750.

314. Velema WA, Hansen MJ, Lerch MM, Driessen AJM, Szymanski W, Feringa BL. Ciprofloxacin–Photoswitch Conjugates: A Facile Strategy for Photopharmacology. *Bioconjug Chem*. 2015;26(12):2592-2597. doi:10.1021/acs.bioconjchem. 5b00591.

315. Barber DM, Schönberger M, Burgstaller J, et al. Optical control of neuronal activity using a light-operated GIRK channel opener (LOGO). *Chem Sci*. 2016;7(3):2347-2352. doi:10.1039/C5SC04084A.

316. Volgraf M, Gorostiza P, Numano R, Kramer RH, Isacoff EY, Trauner D. Allosteric control of an ionotropic glutamate receptor with an optical switch. *Nat Chem Biol*. 2006;2(1):47-52. doi:10.1038/nchembio756.

317. Hess H, Bachand GD, Vogel V. Powering Nanodevices with Biomolecular Motors. *Chem A Eur J*. 2004;10(9):2110-2116. doi:10.1002/chem.200305712.

318. van Den Heuvel MGL, Dekker C. Motor proteins at work for nanotechnology. *Science*. 2007;317(5836):333-6. doi:10.1126/science.1139570.

319. Koçer A, Walko M, Meijberg W, Feringa BL. A Light-Actuated Nanovalve Derived from a Channel Protein. *Science*. 2005;309(5735):755-758. doi:10.1126/science.1114760.

320. Gorostiza P, Isacoff EY. Optical Switches for Remote and Noninvasive Control of Cell Signaling. *Science*. 2008;322(5900):395-399. doi:10.1126/science.1166022.

321. Kramer RA, Zandwijken D, Egmond MR, Dekker N. In vitro folding, purification and characterization of Escherichia coli outer membrane protease OmpT. *Eur J Biochem*. 2000;267(3):885-893. doi:10.1046/j.1432-1327.2000.01073.x.

322. de Keyzer J, van der Does C, Driessen AJM. Kinetic Analysis of the Translocation of Fluorescent Precursor Proteins into Escherichia coli Membrane Vesicles. *J Biol Chem*. 2002;277(48):46059-46065. doi:10.1074/jbc.M208449200.

323. Jackson M, Mantsch HH. Beware of proteins in DMSO. *Biochim Biophys Acta*. 1991;1078(2):231-5.

324. Mattos C, Ringe D. Proteins in organic solvents. *Curr Opin Struct Biol*. 2001;11(6):761-4.

325. Zheng Y, Ornstein RL. A Molecular Dynamics and Quantum Mechanics Analysis of the Effect of DMSO on Enzyme Structure and Dynamics: Subtilisin. *J Am Chem Soc*. 1996;118(10):4175-4180. doi:10.1021/ja9539195.

326. van der Spoel D, Berendsen HJ. Molecular dynamics simulations of Leu-enkephalin in water and DMSO. *Biophys J*. 1997;72(5):2032-41. doi:10.1016/ S0006-3495(97)78847-7.

327. Hughes ZE, Mark AE, Mancera RL. Molecular dynamics simulations of the interactions of DMSO with DPPC and DOPC phospholipid membranes. *J Phys Chem B*. 2012;116(39):11911-11923. doi:10.1021/jp3035538.

328. Vandeputte-Rutten L, Kramer RA, Kroon J, Dekker N, Egmond MR, Gros P. Crystal structure of the outer membrane protease OmpT from Escherichia coli suggests a novel catalytic site. *EMBO J*. 2001;20(18):5033-9. doi:10.1093/emboj/ 20.18.5033.

329. Kumar GS, Neckers DC. Photochemistry of azobenzene-containing polymers. *Chem Rev*. 1989;89(8):1915-1925. doi:10.1021/cr00098a012.

330. Shultz J, Silhavy TJ, Berman ML, Fiil N, Emr SD. A previously unidentified gene in the spc operon of Escherichia coli K12 specifies a component of the protein export machinery. *Cell*. 1982;31(1):227-235. doi:10.1016/0092-8674(82)90422-6.

331. Rusch SL, Kendall DA. Oligomeric states of the SecA and SecYEG core components of the bacterial Sec translocon. *Biochim Biophys Acta - Biomembr*. 2007;1768(1):5-12. doi:10.1016/j.bbamem.2006.08.013.

332. Bessonneau P, Besson V, Collinson I, Duong F. The SecYEG preprotein translocation channel is a conformationally dynamic and dimeric structure. *EMBO J*. 2002;21(5):995-1003. doi:10.1093/emboj/21.5.995.

333. Scheuring J, Braun N, Nothdurft L, et al. The oligomeric distribution of SecYEG is altered by SecA and translocation ligands. *J Mol Biol*. 2005;354(2):258-271. doi:10.1016/j.jmb.2005.09.058.

334. Park E, Rapoport TA. Bacterial protein translocation requires only one copy of the SecY complex in vivo. *J Cell Biol*. 2012;198(5):881-893. doi:10.1083/ jcb.201205140.

335. Dalal K, Chan CS, Sligar SG, Duong F. Two copies of the SecY channel and acidic lipids are necessary to activate the SecA translocation ATPase. *Proc Natl Acad Sci U S A*. 2012;109(11):1-6. doi:10.1073/pnas.1117783109.

336. Denisov IG, Grinkova Y V., Lazarides AA, Sligar SG. Directed Self-Assembly of Monodisperse Phospholipid Bilayer Nanodiscs with Controlled Size. *J Am Chem Soc*. 2004;126(11):3477-3487. doi:10.1021/ja0393574.

337. Van Der Does C, Swaving J, Van Klompenburg W, Driessen AJM. Non-bilayer lipids stimulate the activity of the reconstituted bacterial protein translocase. *J Biol Chem*. 2000;275(4):2472-2478. doi:10.1074/jbc.275.4.2472.

338. Schwille P, Meyer-Almes FJ, Rigler R. Dual-color fluorescence cross-correlation spectroscopy for multicomponent diffusional analysis in solution. *Biophys J*. 1997;72(4):1878-86. doi:10.1016/S0006-3495(97)78833-7.

339. Kedrov A, Sustarsic M, De Keyzer J, Caumanns JJ, Wu ZC, Driessen AJM. Elucidating the native architecture of the YidC: Ribosome complex. *J Mol Biol*. 2013;425(22):4112-4124. doi:10.1016/j.jmb.2013.07.042.

340. Ritchie TK, Grinkova Y V., Bayburt TH, et al. Chapter 11 Reconstitution of Membrane Proteins in Phospholipid Bilayer Nanodiscs. *Methods Enzymol*. 2009;464(C):211-231. doi:10.1016/S0076-6879(09)64011-8.

341. Arkowitz RA, Joly JC, Wickner W. Translocation can drive the unfolding of a preprotein domain. *EMBO J*. 1993;12(1):243-253.

342. De Keyzer J, Van der Does C, Swaving J, Driessen AJM. The F286Y mutation of PrlA4 tempers the signal sequence suppressor phenotype by reducing the SecA

binding affinity. *FEBS Lett*. 2002;510(1-2):17-21. doi:10.1016/S0014-5793 (01)03213-6.

343. Derman AI, Puziss JW, Bassford PJ, Beckwith J. A signal sequence is not required for protein export in prlA mutants of Escherichia coli. *EMBO J*. 1993;12(3):879-88.

344. Osborne AR, Rapoport TA. Protein Translocation Is Mediated by Oligomers of the SecY Complex with One SecY Copy Forming the Channel. *Cell*. 2007;129(1):97-110. doi:10.1016/j.cell.2007.02.036.

345. Popot JL, Althoff T, Bagnard D, et al. Amphipols from A to Z. *Annu Rev Biophys*. 2011;40(1):379-408. doi:10.1146/annurev-biophys-042910-155219.

346. Bayburt TH, Leitz AJ, Xie G, Oprian DD, Sligar SG. Transducin activation by nanoscale lipid bilayers containing one and two rhodopsins. *J Biol Chem*. 2007;282(20):14875-14881. doi:10.1074/jbc.M701433200.

347. Baas BJ, Denisov IG, Sligar SG. Homotropic cooperativity of monomeric cytochrome P450 3A4 in a nanoscale native bilayer environment. *Arch Biochem Biophys*. 2004;430(2):218-228. doi:10.1016/j.abb.2004.07.003.

348. Mao C, Cheadle CE, Hardy SJS, et al. Stoichiometry of SecYEG in the active translocase of Escherichia coli varies with precursor species. *Proc Natl Acad Sci U S A*. 2013;110(29):11815-20. doi:10.1073/pnas.1303289110.

349. Hanahan D. Studies on transformation of Escherichia coli with plasmids. *J Mol Biol*. 1983;166(4):557-80.

350. Zhang X, Studier FW. Mechanism of inhibition of bacteriophage T7 RNA polymerase by T7 lysozyme. *J Mol Biol*. 1997;269(1):10-27. doi:10.1006/jmbi.1997.1016.

351. Bol R, De Wit JG, Driessen AJM. The active protein-conducting channel of Escherichia coli contains an apolar patch. *J Biol Chem*. 2007;282(41):29785-29793. doi:10.1074/jbc.M702140200.

352. Goryashchenko AS, Khrenova MG, Savitsky AP. Detection of protease activity by fluorescent protein FRET sensors: from computer simulation to live cells. *Methods Appl Fluoresc*. 2018;6(2):022001. doi:10.1088/2050-6120/aa9e47.

353. Hsieh H V, Sherman DB, Andaluz SA, Amiss TJ, Pitner JB. Fluorescence resonance energy transfer glucose sensor from site-specific dual labeling of glucose/galactose binding protein using ligand protection. *J Diabetes Sci Technol*. 2012;6(6):1286-95. doi:10.1177/193229681200600607.

354. Malovrh P, Viero G, Serra MD, et al. A novel mechanism of pore formation: membrane penetration by the N-terminal amphipathic region of equinatoxin. *J Biol Chem*. 2003;278(25):22678-85. doi:10.1074/jbc.M300622200.

355. Tam PCK, Maillard AP, Chan KKY, Duong F. Investigating the SecY plug movement at the SecYEG translocation channel. *EMBO J*. 2005;24(19):3380-3388. doi:10.1038/sj.emboj.7600804.

356. Heyduk T. Measuring protein conformational changes by FRET/LRET. *Curr Opin Biotechnol*. 2002;13(4):292-296. doi:10.1016/S0958-1669(02)00332-4.

357. Ding H, Mukerji I, Oliver D. Nucleotide and Phospholipid-Dependent Control of PPXD and C-Domain Association for SecA ATPase. *Biochemistry*. 2003;42(46):13468-13475. doi:10.1021/bi035099b.

Summary and Perspective

-

Summary and Perspective

-

Introduction

Life relies on setting boundaries from uncontrolled activities in its surrounding. For instance, bacteria confine their bodily features by membranes that separate the interior from the external environment. Bacteria have developed various systems to communicate across this barrier membrane and conduct essential cellular processes such as growth and development. The main barrier that can be found throughout different forms of life is the inner or cytoplasmic membrane. This layer is composed of a bilayer of phospholipids and contains various cellular machineries that help to maintain a metabolic balance, preventing unintended loss of cellular components as well as the uptake of essential nutrients. The membrane is impermeable to small solutes, proteins and other cellular components, therefore, proteins needs to be actively transported to the exterior. To do so, selective translocation machineries in the membrane allow proteins to pass the membrane in a carefully orchestrated manner. This process of protein secretion has been extensively studied in the model bacteria Escherichia coli. The major and universally conserved route for protein transport into and across membrane is the Sec pathway. Proteins destined to be localized outside the cytoplasmic membrane are recognized via their signal sequence by the SecA motor protein, which in turn associates with the membrane-residing SecYEG channel and followed by a traverse of the unfolded protein through SecYEG channel.

Chapter 1 discuss the main components of the Sec translocase and provides current insights in the protein translocation mechanism. The canonical protein conducting channel comprises of three integral membrane proteins, in E. coli known as SecY, SecE and SecG. Based on high-resolution crystal structures of SecYEG and its archaeal homologue SecYE β complex (Fig. 1), the actual protein conducting channel is formed by SecY and adopts a pseudo symmetrically aligned hourglass clamshell-like structure. Each halve of the clamshell is comprised of 5 transmembrane segments, TMS1-5 and TMS6-10, that are connected by a hinge region. The two helices of SecE partially enwrap SecY, whereas Secβ which is homologous to the E. coli SecG is almost perpendicular to the membrane. SecY is the main component of the channel with a subcentral hydrophobic constriction ring where six hydrophobic amino acid residues maintain a seal preventing leakage of ions. At the trans side of the constriction ring, a small α-helix of a re-entrance loop forms a plug that occupies the channel and that further hinders the vectorial passage of ions and polypeptide substrates. At the cis side of the membrane, the two halves of the clamshell converge with an opening on one side,

which is termed the lateral gate. The lateral gate is formed by TM2b, TM3, TM7 and TM8, and upon channel opening, provides access to the lipid bilayer.

The various structures of the prokaryotic SecYEG/β complex and its eukaryote homolog Sec61, point at a highly dynamic channel with different conformational states (Fig. 1A-F) that may represent sub-states in the channel opening mechanism.

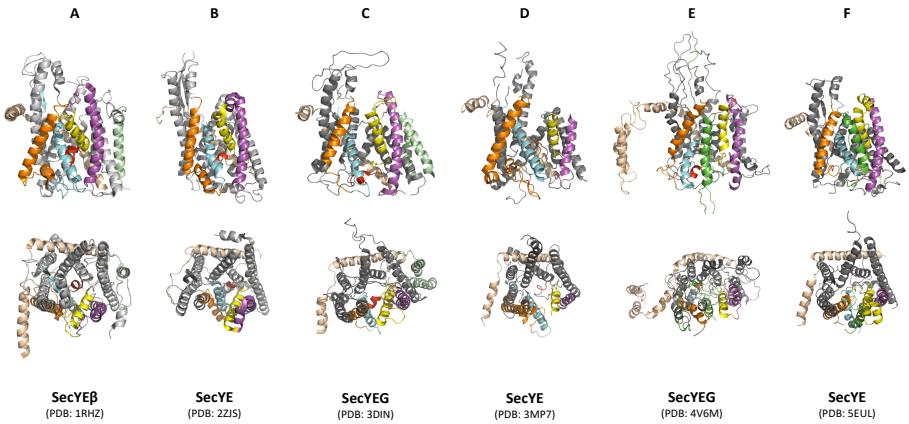

Figure 1. Cartoon representation of various SecYE(G/ β) complexes. SecY (grey), indicated with lateral gate helices TMS 2b (yellow), TMS 3 (magenta), TMS 7 (cyan) and TMS 8 (orange), and plug (red); SecE (beige); SecG (pale green), polypeptide (green). **(A)** SecYE β of Methanocaldococcus jannaschii; **(B)** SecYE of Thermus thermophilus; **(C)** SecYEG of Thermotoga maritima; **(D)** SecYE from Pyrococcus furiosus; **(E)** SecYEG of Escherichia coli; **(F)** SecYE of Geobacillus thermodenitrificans.

In the resting state (Fig. 1A), the structure is compact and the channel is closed. Upon binding of SecA, the lateral gate opens at cis-side (Fig. 1B) providing an entry site for the signal sequence to latch into the lateral gate. Such opening also present access towards the lipid bilayer. Figure 1C represent the structure of SecY bound to SecA in an ATP hydrolysis intermediate state, where there is a notable gap in the constriction ring region between TM2 and TM7 of about 5Å. Upon insertion of preprotein, the lateral gate opens further thereby also widening the hydrophobic restriction ring (Fig. 1D). Figure 1E displays a further separation of lateral gate which provide larger opening of the channel from the cis to the trans side of the membrane, and also a displacement of the plug domain to the trans-side. Figure 1F shows a structure where the signal sequence is intercalated into the lateral gate, resulting in an even larger widening of the hydrophobic ring and separation of the lateral gate.

Chapter 2 centers around the dynamics of lateral gate opening, particularly at its cis- and trans-side. Oxidation of a unique pair of introduced cysteine residues at the TM2-TM8 (cis-side) and TM3-TM7 (trans-side) fixed the lateral gate in a closed position, thus abolishing translocation. However, the 'closed' state of lateral gate still allowed for SecA binding. A range of crosslinkers were introduced that cover distances of 5 Å up to 13.3 Å at the cis- and trans-side of the channel to examine the structural dynamics of the lateral gate. Except for the largest spacer length introduced at the trans- side, crosslinking of the lateral gate opening at the aforementioned distances obstructed translocation. These findings suggest that the lateral gate needs to open to the full length from cis- to trans-side to fully support protein translocation.

In **Chapter 3**, we utilized a crosslinker at the trans-side of the lateral gate based on bismaleimidoazo-benzene that depending on specific wavelengths is able to switch between a length of 10 Å or 19 Å. With these switches introduced into this region of the lateral gate, translocation still occurred, indicating that the periplasmic side of the translocon is more promiscuous to perturbation than the mid or cis section of the lateral gate. Overall, these data suggest that the lateral gate opens as a wedge with the widest opening at the cis-side of the membrane.

In **Chapter 4**, we investigated the activity of a single translocon using nanodisc-reconstituted SecYEG, and provide evidence that the monomer of SecYEG is suffices for protein translocation. The translocon is a protein complex that is composed of flexible transmembrane segments. Docking of the cytoplasmic partner SecA most probably causes a conformational change which leads to partial or complete opening of the lateral gate and the central channel. To investigate the channel opening, we employed intramolecular Förster's resonance energy transfer (FRET) experiments by conjugating a donor and an acceptor fluorophore on each side of the lateral gate. Binding of SecA indeed already causes a partial opening of the lateral gate. Previous studies have shown that intermediate stages of translocation is a stepwise process where in two consecutive steps a defined stretch of polypeptide moves through the channel upon the binding by SecA and subsequent binding of ATP to SecA. It has been suggested that a segment called the two-helix-finger (2HF) of SecA plays a significant role in this event, but another study showed that crosslinking of the 2HF of SecA to an exposed loop of SecY has little effect on the translocation reaction.

In **Chapter 5** we further investigate the binding and dynamics of the 2HF of SecA during protein translocation. To monitor the intricate dynamics, we conjugated donor fluorophores on various amino acid position in the 2HF of SecA and acceptor fluorophores at various position at the cis-side of SecY on TM2b, TM3 and TM4,. We then employ a FRET assay to examine the dynamics. A significant FRET signal was observed upon the binding of SecA to SecY, but there were no further significant changes in the distance between the 2HF and the cis interface

of TM 2b, TM3 and TM4 of SecY upon the addition of nucleotides and/or substrate. These findings are more in line with the suggestion that SecA acts to open the channel rather than pushing the protein through the channel.

Perspective

As illustrated by the first figure in the first chapter in this thesis, various studies employing assorted techniques and technologies have elucidated the intricate interplay of bacterial protein transport events. The work in this thesis extents the current knowledge and has provided insight in how subunits of the translocon work cooperatively to guide polypeptides across the membrane. However, still many questions remain. The exact mechanism by which SecA drives proteins through the channel remains to be elucidate. Herein, application of single-molecule techniques will be very beneficial. This may lead to an integrated picture on how the components cooperate and reveal the dynamics of the interactions. Also, monitoring of the translocase and translocation events in living systems remains a major challenge. By the use of cryo-electronmicroscopy different stages of the translocation reaction may be structurally elucidated to obtain complete understanding of the translocation process at the molecular level.

Samenvatting en Perspectief

-

Samenvatting en Perspectief

-

Introductie

Leven is alleen mogelijk door grenzen te stellen aan ongecontroleerde activiteiten in de omgeving. Een voorbeeld hiervan zijn bacteriën, zij beperken hun fysieke kenmerken door membranen die het interieur van de externe omgeving scheiden. Bacteriën hebben verschillende systemen ontwikkeld om door deze membraanbarrière te communiceren en essentiële cellulaire processen, zoals groei en ontwikkeling, uit te voeren. De meest voorkomende barrière die in verschillende levensvormen wordt gevonden, is het binnenste of cytoplasmatische membraan en bestaat uit een dubbele laag van fosfolipiden. Het cytoplasmatische membraan bevat verschillende cellulaire machines die helpen bij; het handhaven van een metabolisch evenwicht, het voorkomen van onbedoeld verlies van cellulaire componenten en de opname van essentiële voedingsstoffen. Het membraan is ondoordringbaar voor kleine stoffen, eiwitten en andere cellulaire componenten, daardoor moeten eiwitten actief naar buiten worden getransporteerd. Selectieve translocatie complexen in het membraan verzorgen de passage van eiwitten op een zorgvuldig gecoördineerde manier. Dit proces van eiwit secretie is uitgebreid bestudeerd in de modelbacterie Escherichia coli. De belangrijkste en universeel geconserveerde weg voor eiwittransport in en over het cytoplasmatische membraan is via de Sec-route. Eiwitten voorbestemd voor een locatie buiten het cytoplasmatische membraan, worden via hun signaalsequentie herkend door het SecA-motoreiwit, dat zich daarna associeert met het membraan-verblijvende SecYEG-kanaal, waarna de verplaatsing van het ongevouwen eiwit door het SecYEG-kanaal plaats vindt.

Hoofdstuk 1 bespreekt de belangrijkste componenten van de Sec translocase en biedt actuele inzichten in het eiwittranslocatie mechanisme. Het canonieke eiwit geleidende kanaal bestaat uit drie integrale membraaneiwitten, in E. coli bekend als SecY, SecE en SecG. Gebaseerd op hoge-resolutie kristal structuren van SecYEG en zijn archaeal homologue SeYEβ (figuur 1), wordt het daadwerkelijke eiwit geleidende kanaal gevormd door SecY en neemt het de vorm aan van een pseudo symmetrisch uitgelijnde zandloper met een schelpachtige structuur. Elke helft van de schelp bestaat uit 5 transmembraansegmenten (TMS), TMS1-5 en TMS6-10, die verbonden zijn door een scharniersegment. De twee helices van SecE omwikkelen SecY gedeeltelijk, terwijl Secβ, dat homoloog is met de E. coli SecG, bijna loodrecht in het membraan zit. SecY is de voornaamste component van het kanaal met een subcentrale hydrofobe vernauwingsring bestaande uit zes hydrofobe aminozuurresiduen welke een afdichting vormen tegen de lekkage van ionen. Aan de trans-zijde van de vernauwingsring vormt een kleine α-helix van

een herintreding lus een plug die het kanaal bezet en die de vectoriale doorgang van ionen en polypeptidesubstraten verder belemmert.

Aan de cis-zijde van het membraan komen de twee helften van de schelp samen met een opening aan één zijde, die de laterale uitgang wordt genoemd. Deze uitgang wordt gevormd door TM2b, TM3, TM7 en TM8 en bij opening toegang tot de lipide dubbellaag biedt.

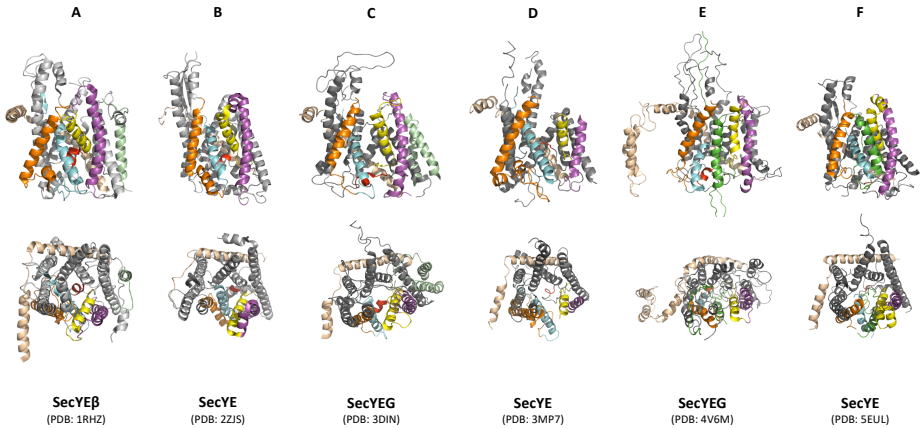

Figuur 1. Cartoonweergave van verschillende SecYE(G/β)-complexen. SecY (grijs), aangegeven met laterale poorthelices TMS 2b (geel), TMS 3 (magenta), TMS 7 (cyaan) en TMS 8 (oranje) en plug (rood); SecE (beige); SecG (lichtgroen), polypeptide (groen). **(A)** SecYEβ van Methanocaldococcus jannaschii; **(B)** SecYE van Thermus thermophilus; **(C)** SecYEG van Thermotoga maritima; **(D)** SecYE van Pyrococcus furiosus; **(E)** SecYEG van Escherichia coli; **(F)** SecYE van Geobacillus thermodenitrificans.

De verschillende structuren van het prokaryotische SecYEG/β -complex en zijn eukaryote homoloog Sec61, wijzen op een zeer dynamisch kanaal met verschillende conformationele toestanden (figuur 1A-F) die sub-toestanden in het kanaalopeningsmechanisme kunnen vertegenwoordigen. In de rusttoestand (figuur 1A) is de structuur compact en is het kanaal gesloten. Na de binding van SecA aan het translocon, opent de laterale uitgang aan de cis-zijde (figuur 1B) en vormt het een ingangspunt voor de signaalsequentie om zich in de laterale uitgang te positioneren. Deze opening biedt ook een doorgang naar de lipidebilaag. Figuur 1C toont een structuur van SecY gebonden aan SecA in een ATP-hydrolyse intermediaire toestand, waar er een opmerkelijke vergroting is in de vernauwingsring tussen TM2 en TM7 van ongeveer 5Å . Bij de insertie van de polypeptide keten gaat de laterale uitgang verder open waardoor ook de hydrofobe vernauwingsring wordt vergroot (figuur 1D). Figuur 1E toont een verdere opening van de laterale uitgang, waardoor er een grotere doorgang onstaat vanaf de cis naar de trans-zijde van het membraan, bovendien vindt er een verplaatsing van het plugdomein naar de trans-zijde plaats. Figuur 1F toont

een structuur waarbij de signaalsequentie zich volledig in de laterale uitgang bevindt, resulterend in een nog verdere vergroting van de hydrofobe vernauwingsring en scheiding van de laterale uitgang.

In **Hoofdstuk 2** staat de dynamiek van de laterale uitgang opening centraal, met name de veranderingen aan de cis- en trans-zijde. Oxidatie van een uniek paar cysteïneresiduen geïntroduceerde in de TM2-TM8 (cis-zijde) en TM3-TM7 (trans-zijde) resulteerde in een gesloten positie van de laterale uitgang, waardoor translocatie onmogelijk werd. De 'gesloten' staat van laterale uitgang stond echter nog steeds SecA-binding. Een reeks crosslinkers werd geïntroduceerd die afstanden van 5 tot 13,3 Å aan de cis- en trans-zijde van het kanaal aflegden om de structurele dynamiek van de laterale uitgang te onderzoeken. Met uitzondering van de langste crosslinker die aan de trans-zijde was geïntroduceerd, belemmerde de bovengenoemde afstanden translocatie. Deze bevindingen suggereren dat de laterale poort zich over de volledige lengte van cis- tot trans-side moet openen om eiwittranslocatie volledig te ondersteunen.

In **Hoofdstuk 3** gebruiken we een crosslinker aan de trans-zijde van de laterale uitgang op basis van bismaleimidoazo-benzeen, welke door middel van specifieke golflengtes kan wisselen tussen een lengte van 10 Å en 19 Å. Met deze crosslinkers in dit gebied van de laterale uitgang, vond translocatie nog steeds plaats, hetgeen aangeeft dat de periplasmatische zijde van het translocon meer vatbaar is voor verstoring dan het midden- of cis-gedeelte van de laterale poort. Over het algemeen suggereren deze resultaten dat de laterale uitgang opent als een wig met de breedste opening aan de cis-zijde van het membraan.

In **Hoofdstuk 4** hebben we de activiteit van een enkel translocon onderzocht met behulp van in nanodiscs gereconstitueerde SecYEG en bewijzen dat het monomeer van SecYEG voldoende is voor eiwittranslocatie. Het translocon is een eiwitcomplex dat bestaat uit flexibele transmembraansegmenten. Binding van de cytoplasmatische partner SecA veroorzaakt hoogstwaarschijnlijk een conformationele verandering die leidt tot gedeeltelijke of volledige opening van de laterale uitgang en het centrale kanaal. Om de kanaalopening te onderzoeken, gebruikten we intramoleculaire Förster's resonance energy transfer (FRET) experimenten door een donor en een acceptor fluorofoor aan elke zijde van de laterale uitgang te conjugeren. Binding van SecA veroorzaakt inderdaad al een gedeeltelijke opening van de zijuitgang. Eerdere studies hebben aangetoond dat tussenliggende toestanden van translocatie een stapsgewijs proces is waarbij in twee opeenvolgende stappen een gedefinieerd stuk polypeptide door het kanaal beweegt bij de binding door SecA en de daaropvolgende binding van ATP aan SecA. Er is gesuggereerd dat een segment genaamd de 2 helix vinger (2HF) van SecA een belangrijke rol speelt in dit proces, echter toont een ander onderzoek aan dat crosslinking van de 2HF van SecA met een blootgestelde lus van SecY weinig effect heeft op de translocatiereactie.

In **Hoofdstuk 5** onderzoeken we de binding en dynamiek van 2 helix vinger van SecA tijdens eiwittranslocatie verder. Om de ingewikkelde dynamiek te volgen, hebben we donorfluoroforen geconjugeerd op verschillende aminozuurposities in de 2HF van SecA en acceptorfluoroforen op verschillende posities aan de cis-zijde van SecY op TM2b, TM3 en TM4. We gebruiken vervolgens een FRET methode om de dynamiek te onderzoeken. Een significant FRET signaal werd waargenomen bij de binding van SecA aan SecY, maar er waren geen verdere significante veranderingen in de afstand tussen de 2HF en de cis-interface van TM 2b, TM3 en TM4 van SecY bij toevoeging van nucleotiden en/of substraat. Deze bevindingen komen meer overeen met de suggestie dat SecA het kanaal opent in plaats van het eiwit door het kanaal te duwen.

Perspectief

Zoals geïllustreerd door het eerste figuur in het eerste hoofdstuk van dit proefschrift, hebben verschillende studies met behulp van diverse technieken en technologieën het ingewikkelde samenspel van bacteriële eiwittransportgebeurtenissen opgehelderd. Het werk gepresenteerd in dit proefschrift verruimt de huidige kennis en heeft inzicht gegeven in hoe subeenheden van het translocon samenwerken om polypeptiden door het membraan te geleiden. Er blijven echter nog veel vragen over. Het exacte mechanisme waarmee SecA eiwitten door het kanaal drijft, moet nog worden opgehelderd. Toepassing van technieken welke meten op het niveau van een enkel-molecuul zullen hier zeer voordelig zijn. Dit kan leiden tot een meer volledig beeld van hoe de componenten samenwerken maar ook de dynamiek van de interacties onthullen. Ook blijft het monitoren van het translocon en translocatiegebeurtenissen in levende systemen een grote uitdaging. Door het gebruik van cryo-elektronenmicroscopie kunnen verschillende toestanden van de translocatiereactie structureel worden opgehelderd om een volledig inzicht te krijgen in het translocatieproces op het moleculaire niveau.

Ringkasan dan Perspektif

-

Ringkasan dan Perspektif

-

Pengantar

Kehidupan bergantung pada adanya batasan yang memisahkan suatu entitas dari aktivitas di lingkungan sekitarnya. Sebagai contoh, bakteri menggunakan membran untuk memisahkan struktur dan bagian interiornya dari lingkungan eksternal. Bakteri telah mengembangkan berbagai sistem untuk berkomunikasi melewati batasan membran ini, dan melakukan berbagai proses seluler esensial untuk tumbuh dan berkembang. Batasan utama yang dapat ditemukan pada seluruh bentuk kehidupan di muka bumi ini adalah 'membran dalam' atau membran sitoplasma. Lapisan ini terdiri dari dua lapisan fosfolipid atau dikenal dengan *phospholipid bilayer*, dan juga menjadi tempat untuk berbagai mesin seluler yang membantu keseimbangan metabolik, mencegah hilangnya komponen intraseluler secara tidak disengaja, serta menyerap atau memasukkan nutrisi-nutrisi yang dibutuhkan untuk aktivitas sel. Membran ini tidak dapat ditembus oleh berbagai zat terlarut yang berukuran kecil, protein dan berbagai komponen sel lainnya, oleh karena itu protein-protein yang berperan di luar perlu ditranspor ke bagian luar sel secara aktif. Untuk keperluan tersebut, terdapat beberapa mesin translokasi pada membran yang memungkinkan protein untuk menembus membran dengan cara-cara yang sangat diatur. Proses pengeluaran atau sekresi protein telah dipelajari dengan cukup mendetil pada bakteri model *Escherichia coli*. Jalur utama dan paling terkonservasi untuk transport protein dari dalam sel untuk masuk ke atau menembus membran adalah jalur *Sec*. Sebagian protein yang disintesis oleh sel diarahkan untuk berfungsi di luar membran sitoplasma. Setelah disintesis di dalam sel, sekuen sinyal pada protein-protein tersebut akan dikenali oleh SecA, yang selanjutnya akan berasosiasi dengan kanal SecYEG yang berada pada membran. SecA yang merupakan protein motor akan mendorong protein yang belum terlipat untuk melewati kanal SecYEG.

Bab 1 membahas komponen-komponen utama *Sec tranlocase* dan mememberikan gambaran terkini terkait mekanisme translokasi. Kanal atau saluran umum untuk translokasi protein ini terdapat pada membrane dan terdiri dari tiga protein integral. Pada *E. coli*, ketiga protein ini dikenali sebagai SecY, SecE dan SecG. Dengan informasi dari stuktur *Sec translocase* SecYEG dan homolognya di archaea SecYEβ (Gambar 1), diketahui bahwa saluran tersebut dibangun oleh formasi SecY yang menyerupai 'kulit kerang' yang membentuk bangun jam pasir yang simetris secara semu. Setiap sisi dari 'kulit kerang' terdiri dari 5 segmen transmembrane, TMS1-5 dan TMS6-10, yang dihubungkan oleh daerah engsel. Dua heliks SecE melingkupi sebagian dari SecY, sementara Secβ

yang merupakan homolog SecG *E. coli* dalam posisi yang hampir perpendikular terhadap membran. SecY merupakan unit utama dari kanal, dengan bagian tengah yang menyempit, yang tersusun oleh enam residu asam amino hidrofobik yang berfungsi mencegah kebocoran ion. Pada sisi trans atau luar dari cincin sempit tersebut, terdapat α-heliks kecil yang menyerupai sumbat dan menghalangi jalur keluarnya ion atau polipeptida. Pada sisi cis membran atau sitoplasma, pada sisi yang berlawan dengan engsel, kedua sisi 'kulit kerang' bertemu pada sebuah bukaan yang disebut sebgai gerbang lateral. Gerbang lateral ini dibangun oleh empat segmen transmembran yaitu TM2b, TM3, TM7 dan TM8. Ketika gerbang lateral ini membuka, maka akan terbentuk bukaan jalur atau akses ke lapisan lipid membrane.

Berbagai konformasi yang berbeda dari struktur kompleks SecYEG/β prokariot, dan juga Sec61 yang merupakan homolog pada eukariot, menunjukkan kanal yang sangat dinamis (Gambar 1A-F). Berbagai konformasi ini sangat mungkin merepresentasikan berbagai tahapan dari mekanisme terbukanya kanal.

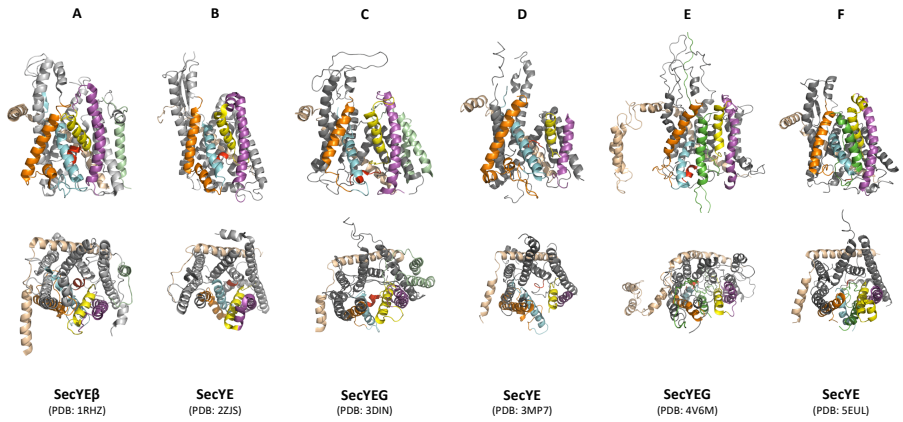

Gambar 1. Gambar kartun yang merepresentasikan berbagai struktur SecYE(G/β). SecY (abu), dengan struktur gerbang lateral yang dibangun oleh TMS 2b (kuning), TMS3 (magenta), TMS 7 (cyan) dan TMS8 (jingga), serta sumbat (merah); SecE (kuning muda); SecG (hijau pucat), polipeptida (hijau). **(A)** SecYEβ Methanocaldococcus jannaschii; **(B)** SecYE Thermus thermophilus; **(C)** SecYEG Thermotoga maritima; **(D)** SecYE Pyrococcus furiosus; **(E)** SecYEG Escherichia coli; **(F)** SecYE Geobacillus thermodenitrificans.

Pada saat istirahat (Gambar 1A), kerangka bangun kanal sangat kompak dan salurannya tertutup. Ketika terjadi penempelan SecA, gerbang lateral terbuka pada sisi *cis* (Gambar 1B) dan menyediakan ruang atau tempat bagi menempelnya sekuen sinyal. Perubahan konfigurasi ini juga mengakibatkan adanya bukaan menuju lapisan lipid membran. Gambar 1C merepresentasikan konfigurasi SecY yang menempel pada SecA pada saat intermediat proses hidrolisis ATP, yang menunjukkan adanya bukaan sekitar 5Å antara TM2 dan

TM7. Pada saat insersi polipetida, gerbang lateral akan terbuka lebih lebar serta mengakibatkan pelebaran cincin hidrofobik di bagian tengah kanal (Gambar 1D). Gambar 1E menunjukkan bukaan gerbang lateral yang lebih besar, dari sisi *cis* hingga *trans*, serta diikuti oleh berpindahnya struktur sumbat pada sisi trans. Gambar 1F menunjukkan susunan molekul yang mana sekuen sinyal polipeptida berada diantara bukaan gerbang lateral, dan menghasilkan bukaan yang jauh lebih besar, serta terbukanya bagian cincin hidrofobik di bagian tengah kanal.

Bab 2 mengkaji lebih jauh terkait dinamika bukaan gerbang lateral, secara khusus pada sisi *cis* dan sisi *trans*. Sepasang asam amino sistein diintroduksi pada masing-masing TM2-TM8 (bagian *cis*) dan TM3-TM7 (bagian *trans*). Reaksi oksidasi akan menghasilkan ikatan hidrogen pada gugus tiol dan mengakibatkan gerbang lateral tertutup secara permanen, dan tidak memungkinkan proses translokasi. Namun demikian, kondisi 'tertutup' ini masih memungkinkan penempelan SecA. Dinamika gerbang lateral ini dipelajari lebih lanjut dengan mengintroduksi beberapa *crosslinker* dengan kisaran panjang dari 5 hingga 13.3 Å pada sisi *cis* dan *trans*. Kecuali penggunaan molekul *crosslinker* terpanjang pada sisi trans, *crosslinking* gerbang lateral dengan berbagai *crosslinker* pada kedua sisi tersebut menyebabkan penghambatan proses translokasi. Hal ini menyiratkan bahwa translokasi dapat terjadi bila gerbang lateral terbuka secara penuh dari sisi *cis* hingga *trans*.

Pada **Bab 3**, kami menggunakan molekul *crosslinker* yang lebih panjang yaitu bismaleimidoazo-benzene, yang dapat diatur panjangnya secara optik dari ukuran 10 Å (cis) ke 19 Å (trans). Translokasi masih dapat terjadi walaupun dilakukan penambahan molekul ini pada sepasang gugus tiol di bagian trans gerbang lateral. Hal ini menunjukkan bahwa bagian periplasmik translokon cenderung lebih memungkinkan untuk terganggu dibandingkan bagian tengah atau *cis* gerbang lateral. Secara umum, seluruh data ini menunjukkan bahwa gerbang lateral membuka seperti pasak, dengan bukaan paling besar terjadi pada bagian *cis* dari membrane.

Pada **Bab 4**, kami mengkaji aktivitas satuan translokon dengan merekonstitusi SecYEG dalam nanodisc. Hasil eksperimen membuktikan bahwa translokasi dapat terjadi hanya dengan satu molekul atau monomer SecYEG. Translokon merupakan kompleks protein yang terdiri dari segmen transmembrane yang fleksibel. Menempelnya SecA sangat mungkin menyebabkan perubahan konformasi molekul, yang selanjutnya menyebabkan terbukanya gerbang lateral dan bagian tengah kanal, baik secara parsial maupun keseluruhan. Untuk mengamati bukaan kanal tersebut, kami melakukan eksperimen *Förster's resonance energy transfer* (FRET) intramolekuler dengan cara mengkonjugasikan fluorofor donor dan akspetor pada masing-masing sisi dinding gerbang lateral. Dan terbukti bahwa menempelnya SecA saja telah mengakibatkan bukaan gerbang lateral secara parsial.

Berbagai kajian sebelumnya menunjukkan bahwa langkah-langkah dalam proses translokasi terjadi secara bertahap, yang mana dalam dua tahap berurutan, polipeptida dalam ukuran tertentu akan melewati kanal akibat berikatannya SecA dan proses penempelan ATP pada SecA tersebut. Beberapa kajian menyiratkan bahwa *two-helix finger* (2HF) dari SecA memainkan peranan penting dalam proses tersebut. Namun, ada juga kajian lain yang menunjukkan bahwa bila 2HF tersebut diposisikan secara permanen (dengan *crosslinking*) pada bagian *loop* SecY, maka reaksi translokasi tidak banyak berubah.

Bab 5 mengkaji lebih jauh proses menempelnya SecA dan dinamika 2HF dalam translokasi protein. Pengamatan dinamika molekul dilakukan dengan mengkonjugasikan fluorofor donor pada berbagai asam amino dalam 2HF SecA dan fluorofor akseptor pada asam amino yang terdapat di bagian *cis* SecY TM2b, TM3 dan TM4. Selanjutnya uji FRET dilakukan untuk melihat dinamika molekul. Sinyal FRET yang signikan teramati saat terjadinya ikatan antara SecA SecY, namun tanpa diikuti oleh perubahan lebih lanjut. Hal ini menunjukkan bahwa setelah proses *binding*, penambahan nukleotida maupun substrat tidak mangakibatkan perubahan konformasi atau jarak yang signifikan antara 2HF dan daerah cis SecY pada TM2b, TM3 dan TM4. Hasil ini sejalan dengan temuan yang menunjukkan bahwa SecA lebih berperan dalam membuka kanal, daripada mendorong protein agar melewati kanal tersebut.

Perspektif

Seperti telah diperlihatkan pada gambar pertama pada bab pertama tesis ini, berbagai studi dengan memanfaatkan berbagai teknik dan teknologi telah dilakukan untuk menjelaskan interaksi yang rumit pada peristiwa transpor protein pada bakteri. Penelitian ini telah memberikan wawasan terkait bagaimana sub-unit dari *translocase* bekerja secara kooperatif untuk memandu polipeptida dalam melintasi membran. Namun demikian masih banyak pertanyaan yang tersisa. Kita masih perlu mengetahui mekanisme rinci terkait bagaimana SecA menggerakkan protein melalui saluran atau kanal. Dalam kaitannya dengan hal ini, penggunaan teknik *single molecule* akan sangat bermanfaat. Hal tersebut akan memberikan arahan terkait bagaimana masing-masing komponen bekerja sama, dan bagaimana dinamika proses interaksinya. Selain itu, pengamatan *translocase* ataupun tahapan proses translokasi pada sistem atau sel hidup tetap menjadi tantangan utama. Penggunaan *cryo-electronmicroscopy* kemungkinan besar dapat memberikan gambaran struktur molekul pada tahapan-tahapan reaksi translokasi, sehingga kita dapat memperoleh pemahaman yang lebih lengkap terakit proses translokasi pada tingkat molekuler.

Acknowledgements

-

Acknowledgements

-

Praise to Allah SWT who has provided me with this journey following the path to complete my PhD training. I could not have come so far to this end without many help and support from many people. At this moment, I would like to express my gratitude to some people who made this journey possible.

I would like to express my deepest gratitude to Prof. Arnold Driessen, foremost for providing me with the opportunity to join Molecular Microbiology group. Thank you for providing time, patience and endless encouragement throughout the laboratory work, and later during completing the thesis writing. I indebted for all the experience and discussions, and some reality check, that have come to my path. Thank you so much.

I would like to thank also Dr. Juke Lolkema and Prof. Dirk-Jan Scheffers for all the advice and suggestion during work discussion, and also checking up on me from time to time. I would also like to thank Prof. Ben Feringa for providing me with the cool optical switches. Bea and Manon for arranging administrative matters.

I would like to thank the Sec Group, first are my initial lab mates, Janny, Greetje, Andy and Jelger for teaching me how to conduct proper laboratory activities since the beginning of my stay. Francesco for providing me with initial materials for study. Alexej for letting me join his project. Ilja and Jeanine for many discussions. I would like also to thank Irfan, Anne-Bart, Amalina, Marten welcoming me back to the group. Amalina, thank you for all the help. Anne-Bart, thank you for translating the Dutch summary. I would also like to thank all other members of the Molmic for providing nice atmosphere. Thanks to Manfred, Stefan, Joeroen, Ali, Arsalan, Jan-Pieter, Oleksander, Olha, Reto, Loes, Sabrina, Yanping, and Yang. Yang, thank you for keeping me company many times.

Special thanks to my paranymphs, Jeroen and Marten.

I would like to thank my colleagues in SITH ITB, in particular expertise group of microbial biotechnology, especially to Prof. Pingkan Aditiawati who became a mother figure in campus. Prof. Nyoman P. Aryantha, Dr. Reni Sri Harjati, Dr. Gede Suantika dan Dr. Dea Indriani Astuti, my seniors who showed me how to 'work'. Dr. Ernawati A. Giri Rahman for many supports. I would like also to thank Prof. Intan Ahmad for his encouragements.

To my big alphabet family, Bapa dan Ibu, Aa, A'Budhy, T'Cenny, T'Dian, T'Effy, T'Fenty, T'Gati, T'Hanny. Mamah and Abah Cilember, Yayu-Andri, and Dimas-Uni. To all my nieces and nephew, and grandchildren.

To my dearest wife, I am incredibly thankful for being patience with me. Thank you for never stop encouraging me and believing in me. To my two children, Bianglala and Azzam, thank you. The three of you are the source for strength.